K. N. Toosi University of Technology
Faculty of Electrical and Computer Engineering
Department of power Systems

Power System Controlled Islanding Considering Transient Stability and Uncertainties

Thesis Submitted in Partial Fulfillment of the
Requirements for the Degree of Doctor of Philosophy (P.hd.)
in Electrical Engineering, Systems and Control.

By:
Sadegh kamali

Supervisor:
Turaj Amraee

Autumn 2019

Approved by:

Dr. Turaj Amraee,
Supervisor
School of Electrical Engineering.
K.N. Toosi University of Technology

Dr. Mahmoud-Reza Haghifam
Committee Member
School of Electrical Engineering.
Tarbiat Modares University

Dr. Seyed Mohammad Taghi Bathaee
Committee Member
School of Electrical Engineering.
K.N. Toosi University of Technology

Dr. Mostafa Parniani
Committee Member
School of Electrical Engineering.
Sharif University of Technology

Dr. Masoud Aliakbar Golkar
Committee Member
School of Electrical Engineering.
K.N. Toosi University of Technology

TABLE OF CONTENTS

LIST OF TABLES

LIST OF FIGURES

LIST OF SYMBOLS AND ABBREVIATIONS

Parameters:

A^+, A^-	**Accelerating and decelerating area**
α	**Threshold of the slow coherency criteria**
β_{ij}	**Factor to adjust the transfer impedance between generators i and j**
I	**Square identity matrix**
c	**Number of samples for rotor speed measurement**
ΔP_e^t	**Real time electrical power changes**
Bu_{ij}	**Auxiliary binary parameter**
$\frac{P_{ei}}{P_{mi}}$	**Electrical/Mechanical power of generator i**
e_{ij}	**Auxiliary binary parameter**
E_i	**Internal voltage of generator i**
E_k/E_p	**Kinetic/Potential energy**
h	**Large positive arbitrary constant**
M_i	**Inertia moment of generator $i(2H_i)$**
N_b	**Number of all nodes**
N_g	**Number of generating units**
N_g^K / N_g^{is}	**Number of generating units in island K**
N_{is}	**Number of electrical islands**
N_l^{is}	**Number of load buses at electrical islands**
N_l	**Number of load points**
n	**Number of measured samples**
H_T	**Equivalent inertia constant of entire system**
P_{l_i}/Q_{l_i}	**Active/reactive load powers at bus i**
$P_0^{initial}$	**Last normal condition electrical power**
P_{emin}	**Minimum tolerable active power of a generator**
P_{emax}	**Maximum tolerable active power of a generator**
P_{Gi}^0	**Initial active power generation at ith node**
P_{loss}	**Total network losses**
r/M	**Small/large positive arbitrary constants**
$\alpha_{lm}^{(k)}$	**Control factor to limit the transfer impedance between generators l and m**
γ	**Threshold of relative mechanical torque**
$\emptyset_{i,j}$	**Angle of transfer impedance between generators i and j**
ω_i	**Rotor speed of generator i**
$\omega_{i,j}^R$	**Real time estimated speed of generator i w.r.t. j**
$\omega_{COI_n}^k$	**n^{th} sample of the rotor speed in island k on the center-of-inertia (COI) reference**
Z_{ij}^c/Z_{ij}^{is}	**Transfer impedance between generator i and j in connected/islanded network**
$\delta_{i,j}^R$	**Real time rotor angle between generator i and j**
X_d'	**Transient reactance of a generator**
Y	**Admittance matrix**
δ_0	**Initial rotor angle of a generator**

Sets:

Ω^d	**Set of loads**
Ω^g	**Set of generation units**
Ω^l	**Set of transmission lines**

Variables:

$\delta_{i,j}$	**Rotor angle between generators i and j**
$\delta_{ij}^s/\delta_{ij}^{sep}$	**Rotor angle between generator i and j at the saddle point/ stable equilibrium point**
$\delta_{ij}^{s1}/\delta_{ij}^{s2}$	**Saddle point right before/after the topology change**
$GL_{i,j}/BL_{i,j}$	**Conductance /Susceptance between nodes i and j**
LF_{ij}	***Transmission line power flow***

P_{ij} **Power flow across the line between nodes *i* and *j***

P_{shed_j} ***Amount of load to be shed at bus j***

$\Delta P_{e_i}^{+}$ **Decelerating active power of generator *i***

$\Delta P_{e_i}^{-}$ **Accelerating active power of generator *i***

Q_{Gi} **Reactive power output of generator *i***

Q_{Li} ***Reactive power load at ith node***

θ_i **Voltage angle of bus *i***

θ_i^f ***Voltage angle in fictitious power flow***

U_{ij} **Open/close status of transmission line between nodes *i* and *j***

V_i **Voltage magnitude of bus *i***

ω_i **Rotor speed of generator *i***

$\omega_{i,j}$ **Speed of generator *i* w.r.t. generator *j***

$Z_{ij}\angle\emptyset_{i,j}$ **Transfer impedance between generators *i* and *j***

Z_{ij}^t **Transfer impedance between bus *i* and *j* at time of islanding**

Z_{ij}^0 **Transfer impedance between generators *i* and *j* after islanding by MIP-only method**

Z_{ij} **Transfer impedance between generator *i* and *j***

θ_i **Voltage angle of bus *i***

$\delta_{i,j}$ **Rotor angle between generator *i* and *j***

$\delta_{i,j}^{s(k)}$ **Saddle point between generator *i* and *j* at iteration *k***

δ **Rotor angle of a generator**

SUMMARY

The reliable, secure and stable operation of a power system is a top priority in modern societies. Power systems are exposed to different electric faults. Some severe electric faults can propagate throughout the power system and initiate a cascading outage. Widespread or regional blackouts are caused by propagating and uncontrolled cascading failures. Different emergency controls and system protection schemes (SPS) are utilized to stop the propagation of blackouts or cascading failures. During cascading outages, coherent groups of generators are formed and the harmful dynamics can propagate from one area to another one, due to their weak electrical conditions. In order to mitigate or minimize the effects of blackouts, the intentional splitting or controlled islanding is considered as a last resort.

The aim of controlled islanding is to split the whole interconnected power system into smaller electric islands, while the steady state and stability requirements in resulted islands are fulfilled with minimum load and generation changes. However, the mechanism of controlled islanding scheme including the time and location of the network splitting is a major challenge. There are mature and comprehensive islanding algorithms that address the preservation of steady state operational and topological constraints in islanding problems, however considering stability phenomenon in islanding models is still a major gap.

The most threatening phenomenon right after the network splitting is the transient instability of synchronous generators. The focus of this thesis is to determine the islanding boundary (i.e. where to island issue) under the transient stability constraint. While the steady-state operational constraints such as power balance in resulted islands are of great importance, a major prerequisite for the success of any controlled islanding scheme is the preservation of transient stability constraint. In this thesis, transient stability constrained network splitting is realized using two different approaches. First, a controlled islanding model, named by Method 1 in this thesis, is proposed to ensure and improve the transient stability of the islanded system. Linear transient stability constraints are derived off-line, based on the extended equal area criterion, to ensure the first swing transient stability of the synchronous machines, right after the controlled line switching. The islanding model with transient stability constraints is first developed as a

mixed-integer nonlinear programming (MINLP) optimization model. Further, the MINLP model is linearized, resulting in a computationally lighter mixed-integer linear programming (MILP) model. In the second part, based on the transient energy approach, two methods named by Method2 and Method3 in this thesis, are presented.

The transient stability constrained islanding models are perfected via two-stage models. First, the conventional controlled islanding problem is formulated as a MILP optimization model with considering operational, coherency and linear AC load flow constraints. The boundary of each island is determined using an optimization model aiming at minimizing the total power imbalance. To consider the transient stability, the network splitting plan obtained from the MIP model is then evaluated in the second stage using a proper transient stability assessment criteria based on the transient energy function method. In the second stage, to satisfy the transient stability constraint of the critical island, a linear constraint is constructed and added to the MILP formulation of a controlled islanding model.

Saddle or control unstable equilibrium points (CUEP) are determined using an optimization model. Finally, the proper islanding method is selected and then revised to consider the uncertainty of the controlled islanding problem. All the proposed network splitting models are simulated over the dynamic IEEE 118-bus system. In addition to the discussion given over the simulation results of each islanding method, a comprehensive comparative analysis is proposed to investigate the importance of each model.

CHAPTER 1. MOTIVATIONS AND BACKGROUND

1.1 Introduction

Large scale power systems play a vital role in nowadays societies. Access to electricity (% of populations) has increased from 71.39 % in 1990 to 87.38 % in 2016 [1]. In many developing and developed countries, access to electricity is now 100%. Also many industrial plants such as petroleum, refineries, water distribution, agriculture sector, electric traction and railways, and other plants and factories are supplied by electric energy. The demand for electric energy is increasing around the world, while there are major economic and environmental restrictions in power system expansion. Such dependency on electricity shows the great importance of security, stability, and continuity of modern power systems. Electric power systems are exposed to different electric faults. Under heavy loading conditions, stormy weather, or when some major equipment such as generating units or transmission lines are out for maintenance purposes, the power systems are vulnerable to electric faults. In these situations, a severe electric fault may initiate a cascading outage and without any automatic emergency actions, a local or system wide blackout is expected. In this regard, many emergency actions and system protection schemes have been implemented in power systems to stop the propagation of harmful cascading events. Controlled islanding is defined as the intentional splitting of an interconnected power system into isolated islands under cascading outages as the last resort. Transmission switching, load shedding and generation changes are common actions during the intentional power system islanding. In addition to the steady state operational requirements in each island the preservation of the stability of created island is a major prerequisite in any intentionally controlled islanding scheme.

1.1.1 Motivation and Problem Description

Over the past decades, several blackouts have occurred throughout the world, e.g., in the US and Canada [2], Europe [3], Iran [4], Turkey [5], and so on. Usually, such extreme events take place when the system is heavily loaded, and a few unplanned outages occur

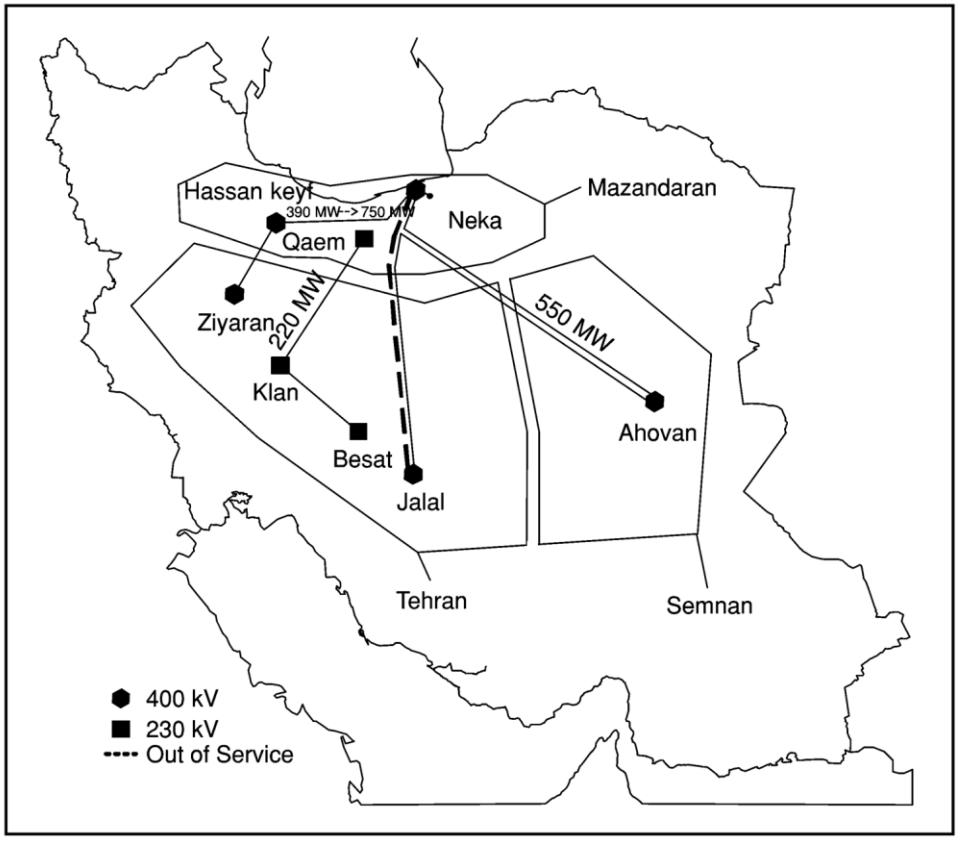

Fig 1-1: Schematic of North part of Iran grid

within short time intervals. One of the most important blackouts in the history of the Iranian national grid was experienced around 18 years ago [6]. In Iran grid blackout, as shown in Fig 1-1, a three-phase short circuit fault occurred on 400 kV transmission line connecting the northern part of the country to the central part of Iran. This line is one of the two 400 kV parallel transmission lines connecting a major power generation source in the northern region, Neka power plant to the central parts of the country including Iran capital, which is a major load center. Before fault occurrence, 550 MW power was being transferred from Neka to Ahovan. As this line was disconnected from the system by its protective relays, the power transfer on the other transmission lines connecting north to central regions was increased. Transferred power on Qaem to Klan and Neka to Hassan-keyf was increased to 220 MW and 750 MW, respectively. As a result these two lines were disconnected shortly after the removal of fault on the faulty 400 kV line. This way all the links connecting Neka power station to Tehran province were disconnected and these two regions became

isolated. Following this disturbance, although the interconnected transmission system tried to respond by redistributing of generations, system voltage- and frequency began to decline. Therefore, some of the system protective relays responded to declining voltage condition and operated automatically to disconnect some of the system's transmission lines. In addition, due to some protective device maloperation, parts of the grid including some major transmission lines were overloaded. The grid frequency declined due to the shortage of energy supply. False trips by some protective devices accompanied by inadequate load shedding by frequency relays resulted in a major grid collapse. More often than not, the power system blackout is caused by the malfunction of the Transmission system. [7]. Controlled islanding is a control strategy that aims at preventing the interconnected power systems from splitting in an uncontrolled manner so as to mitigate subsequent cascading outages.

1.1.2 Introduction to Islanding

Due to economic and environmental limitations in power system expansion in both generation and transmission sectors, nowadays, many power systems are operated near to their stability boundaries especially during peak load conditions. This issue increases the risk of instability phenomena such as rotor angle instability. Power system instability such as rotor angle instability, may cause a catastrophic cascading failure, especially in case of insufficient remedial control schemes. Many power systems around the world have experienced cascading failures with devastating results. The initiating event for blackouts is usually an unlikely contingency or a combination of series of implicated events [7]. During a cascading failure, due to resulted overloads and transmission outages, many synchronous machines become out-of-step. Several methods including practical out-of-step protective relays could be used to detect tripping generators (i.e. out-of-step conditions) and isolate them from the system [8, 9]. Unintentional islanding refers to the large electrical separation of generator rotor angles. Indeed, unplanned islanding causes large increasing oscillations between coherent groups of generators [10]. It is noted that the rotor angles of coherent generators have similar time variations. Therefore, the coherent groups of generators become unstable at the same time, approximately. In order

to give a clear definition of cascading failure phenomena and the unintentional islanding, a four-machine two-area test system as given in [11] is used. As shown in Fig 1-2, this system consists of two areas connected by two 230 kV transmission lines with 220 km length. Regardless of its small size, this test system mimics the behavior of a typical real-life test system. Each area has two generators rated 20 kV/900 MVA. Each generator has been equipped with a conventional power system stabilizer (PSS) and a standard IEEE DC1 excitation system[11]. In order to depict the trajectories of rotor angles during a cascading failure, a delayed three phase short circuit fault is applied at bus 9 at t= 1s with a duration of 0. 25s. As shown in Fig 1-3, the rotor angles of generators in Area1 become unstable at t=2.5sec. Indeed, in this situation, the Area1 is electrically separating from Area2, resulting in unintentional islanding. According to Fig 1-3, at t=2.5s, the difference between the rotor angle of Area1 and Area2 reaches 180, which confirms the occurrence of complete unintentional islanding. In this condition, the interconnected operation of the two areas is no possible any more. Without any remedial actions, after the few seconds all generators trip due to out-of-step conditions and the blackout is inevitable. This event highlighted the need for implementing remedial or system protection schemes to mitigate or minimize the effects of a blackout. Controlled islanding or intentional splitting refers to a system protection scheme to split the entire network into stable islands before the cascading outages.

1.2 Literature Review

Different researches have been done to develop a suitable controlled islanding scheme. In order to have a clear classification of previous research work, different aspects of controlled islanding scheme have been given in Fig 1-4. As shown Fig 1-4, two key aspects must be addressed in controlled islanding scheme including “where to island,” and “when to island,” issues. Based on these two issues, the previous researches are discussed.

1.2.1 When to Island Issue

The time of islanding or the “when to island” issue is critical for the success of any controlled islanding scheme, since an early recognition indicates if a disturbance will

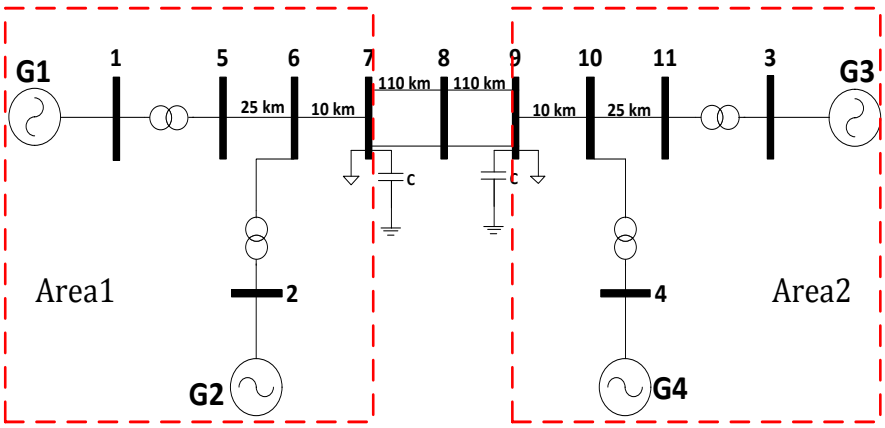

Fig 1-2. Single line diagram of two-area dynamic test system

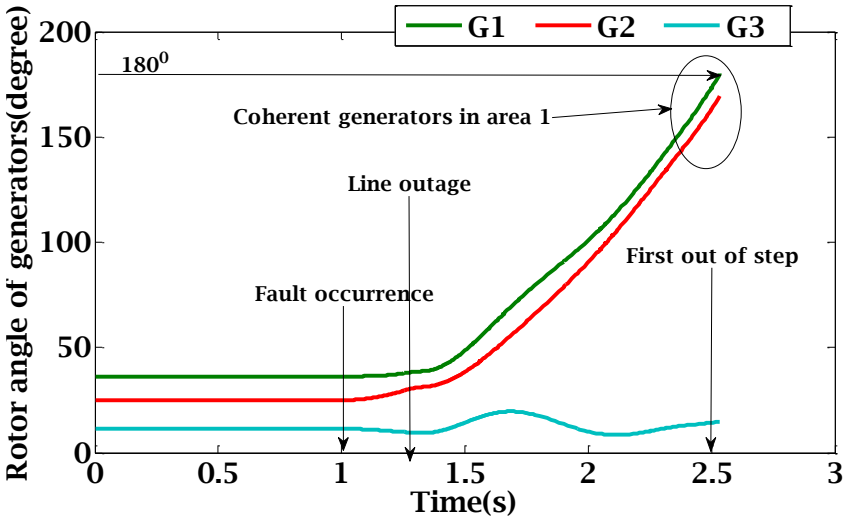

Fig 1-3. Rotor angle trajectories with reference to machine#4

evolve into a blackout or not. Based on the islanding prediction, proper action automatically or manually can be taken to mitigate or minimize the effect of possible blackouts. Possible consequences of false alarm and false dismissal have to be handled. A false alarm means the islanding condition predicted as a normal condition and a false dismissal means the non-islanding condition is predicted as an islanding condition. In the case of a false alarm, islanding is triggered too early, forcing a stable system to incorrectly be splatted into islands. In the case of false dismissal, islanding is triggered too late, allowing an unstable system to be operated, leading to an uncontrolled cascading blackout [12]. The when to island issue determines the proper time of controlled islanding based on the detection or prediction of the time of unintentional islanding. The proposed methods

addressing the when to island issue be categorized into two clusters including prediction of islanding and detection of islanding.

1.2.1.1 Prediction Methods

In islanding prediction, the possible occurrence of unintentional islanding in the near future is determined based on the conditions of the power system at the current moment. In most of the proposed methods for islanding prediction, first an islanding predictor is defined and then the threshold of this indicator is determined based on data mining techniques or the operator's experience.

In [13]a transient energy based index is proposed for power system islanding prediction. The total energy absorbed by the coherent synchronous generators during unplanned islanding conditions is formulated as an islanding predictor. Decision Tree (DT) data mining technique is utilized to extract the information gain of the proposed predictor over the input training samples. Authors in [10] have proposed a decision tree based tool to recognize the special conditions of the system that warrant the controlled islanding. In [14] an intelligently controlled islanding scheme based on wide area measurement systems has been proposed to avoid the wide area blackout. Authors in [15] describe and compare three possible ways to realize real-time decision-making of system splitting, and shows that online pre-analysis & real-time matching is a recommendable way under current technological condition. In[16], for predicting the size of a potential blackout, a three stages decision tree predictor is proposed for estimating the size of the possible blackout.

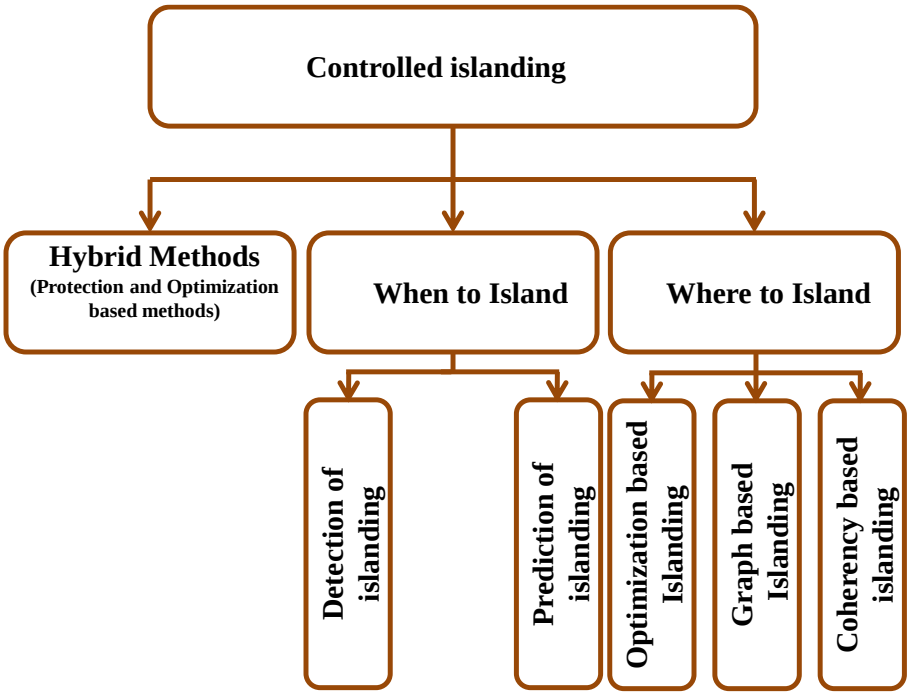

Fig 1-4: Controlled islanding concepts

1.2.1.2 Detection Methods

In islanding detection the cascading failure or unintentional islanding is detected near or during cascading failures. Authors in [12] use real-time information to estimate the rotor angles of generators, which, is used to define the number of coherent generators and the actual coherent groups. It then adopts the concept of area-based center of inertia (COI) rotor angle index to determine the actual time of unintentional islanding. In [17] The concept of feasible islanding time interval (FITI) is introduced as a time interval in which, if controlled islanding is performed for a given boundary, the island's generators will retain their synchronism.

1.2.2 Where to Island Issue

A major part of each controlled islanding plan is the procedure utilized to determine the boundary of the required islands. Indeed, after decision making about the execution of controlled islanding, as described in the previous section, the boundary of islands or splitting lines should be determined. Indeed by splitting the network, the system operator

is creating small power systems that must qualify all the steady state operational and stability requirements. In this regard, the "where to island" issue is one of the important aspects of the controlled islanding. Different methods have been proposed in the literature for determining the splitting point of islanding or simply island boundary. Most of the previously proposed schemes to determine the islanding boundaries, rely on the steady state conditions of power systems. The previously proposed algorithm can be categorized into three different clusters including slow coherency based techniques, graph-based methods, optimization techniques.

1.2.2.1 Coherency Based Islanding

The coherency-based approach has been successfully utilized for constructing power system dynamic equivalents. Two synchronous generators or groups of generators are assumed to be coherent if their rotor angle trajectories have similar variations under different faults. Indeed the coherent generators have similar dynamic characteristics. In coherency-based controlled islanding, the coherent generators are grouped on the same island. Indeed, the coherent generators shape the core of each island and then the boundary of islands is determined using a proper algorithm with considering operational and stability constraints. The key step in this approach is to identify the coherent groups of generators. Coherent generators can be determined based on comparing of generator responses (e.g. rotor angle or rotor speed trajectories) under different faults or disturbances. Different faults such as single-phase or three phase short circuit faults at different locations may give different sets of generator groupings. However, the following facts about the slow coherency method should be kept in mind.

- The sets of coherent generators are approximately independent of the size of the fault type and location. However to mitigate the small effects of occurred fault on the coherent set of generators different faults with various durations are applied at different locations. The coherency is then averaged over the simulated faults.
- The coherency between different pairs of generators is not affected by the model details of the system elements. As a result, it is acceptable to disregard controllers

such as governors and automatic voltage regulators in the generator dynamic model[18].

- Coherency can be used for detecting weak connections between different electric areas of the power system. For this reason, the coherency technique is used for the intentional islanding of the power system under emergency conditions [18]. In [19], the authors have presented a slow-coherency based network partitioning technique that groups generators and load buses simultaneously into several coherent areas. The technique uses the slow eigen-basis matrix which is extended to include load buses. [20] analysis of system dynamic response in the Manitoba Hydro network to split system based on coherent generators and coherent buses. The slow coherency method has been applied to the WECC system [21].

1.2.3 Graph Based Islanding

The network of the power system may be interpreted as a graph. The purpose of graph-based methods for controlled islanding is to reduce the structural complexity of large power systems. . In this method, buses and transmission lines are considered as vertices and edges, respectively.

In [22], an algorithm named mean field annealing (MFA), is applied to the graph-partitioning of the power system. The proposed MFA algorithm in [22] combines the simulated-annealing algorithm and the Hopfield neural network. Authors in [23] propose a two-phase method to find the proper splitting strategies by introducing the graph-model of the system. In [24-26] the Ordinary Binary Decision Diagram (OBDD) technique is proposed for proper splitting, considering the necessary steady-state operational constraints of the resulted islands. The authors in [27] propose an integrated algorithm to identify a cut set for a large power system for the application of a slow coherency based controlled islanding scheme. The large scale power system is then represented as a graph and a simplification algorithm is used to reduce the complexity of the system. This method has been applied in the WECC system [3]. [28] uses islanding to prevent the spread of the consequences of the fault to other areas and minimize the interaction of the two areas

during a fault. In this method, a disturbance is considered a decrease and an increase in the amount of load. In [29] controlled islanding has been considered as a self-healing approach using graph theory and considers the reactive power dissipation to improve the voltage profile on each island. Authors in [30] have formulated the controlled islanding problem as a graph-based model, and a MILP optimization model has been developed and solved to find boundaries of islanding. The difference between this research and other ones is to consider the connectivity of graph vertices in each sub graph (i.e. a sub-graph is an island).

1.2.3.1 Optimization Method

Recently the optimization methods have been utilized for determining the splitting points in controlled islanding problems. In optimization-based islanding methods, all the required operational constraints (e.g. power balance of resulted islands, transmission limits, and etc.) and structural constraints (e.g. connectivity of coherent generators on each island, dis-connectivity of non-coherent generators, and etc.) are integrated into an optimization model. Different objective functions are defined in the optimization model of controlled islanding problems such as minimization of power imbalance. The proposed model in [31] is able to maintain the voltage magnitudes within an acceptable range. Also the same approach considering the DC power flow has been presented in[32].

1.2.4 Hybrid methods

Hybrid MethodsIn hybrid methods, the splitting points of controlled islanding are determined using the combination of three mentioned approaches. The spectral partitioning algorithm is a two-step process using the spectral theory of graph theory where the coherent generators are determined using slow coherency technique[33]. In this algorithm, an optimization problem is defined that aims at minimizing the power imbalance of the resulted islands by considering the operation constraints. In this method, first, the entire network is modelled as a graph model. The weight of lines between generators is a synchronous coefficient that expresses the dynamic coupling between them and is weighted by the power transmission between the two generators. In the second step, all network

nodes are grouped according to the power balance and a criterion that minimizes the transmission overloads. This is done using the spectral classification algorithm of the graph theory. Smart protective relays can be used for controlled islanding. These relays are used in weak systems that are constantly exposed to the risk of unplanned islanding. The method proposed in [34], separates the network from designated locations if the synchronization of two generators is going to be lost. In this regard, the predictive methods are used to predict the rotor angles of generators. In this method, when the rotor angle difference between generators exceeds a predetermined threshold, the loss of the synchronization in the related generators is imminent and the network must be isolated to avoid the possible instability or blackout. In [35], the set of network elements that their outages may cause unplanned islanding is identified. In [36], the actions that must be taken to stabilize the system under the unintentional islanding conditions are investigated and analysed and the proper adaptive load curtailment is used for preserving the stability of each island.

1.3 Research Gap and Challenges

Most of the previously proposed method, especially those have been proposed for determining the islanding boundaries have focused on steady state conditions of power system after the islanding execution. Steady state operational constraints such as power balance, line limits, and topological requirements connectivity of coherent generators and dis-connectivity of non-coherent generators. However, a major requirement in each resulted island is the stability phenomenon such as transient stability. Indeed the most important stability which is heavily affected by the splitting actions is transient stability. This important aspect of controlled islanding is missing in previous researches. Also, in previously proposed methods less effort has been done to integrate linear AC power flow formulation as the power balance constraints. The main drawbacks and shortcomings of the previously controlled islanding schemes addressing the “where to island” issue are enumerated as follows:

1. Due to computational complexity, in most of the previous methods, the operational constraints have been considered using the DC network model. Using the DC network model there is no awareness about the voltage magnitudes and reactive power generation.

2. In controlled islanding methods, the islanding boundaries have been determined using the steady state model of the power system. Indeed, this is the propagation of harmful dynamics during the cascading failures that cause a regional or wide area blackout. Using the steady state model of machines and the network, there is no guarantee for the preservation of stability in resulted islands.

3. Since the network splitting is a major part of each controlled islanding plan, transient stability is the first phenomenon affected by network splitting, significantly. To the best of authors' knowledge the transient stability has not been considered in previous research works.

5. As the successfully controlled splitting of the network depends on the exact values of system parameters, any controlled islanding scheme in both static and dynamic regimes comes up with some degree of uncertainty. The uncertainties in the parameters such as system inertia have not been addressed before.

For better clarification, the research gap in the controlled islanding problem has been illustrated in Fig 1-5. Based on Fig 1-5, the major gap this thesis intends to fill, is the consideration of transient stability in controlled network splitting. Indeed, the major works done in this thesis, focuses on transient stability. In addition to the transient stability modeling, the objective functions, operational constraints (e.g. power balance, voltage magnitudes, and transmission limits) and topological requirements (e.g. locating the coherent generators in the same island and dis-connectivity of non-coherent generators) are improved to remove the major drawbacks of previous methods. Another gap addressed in this thesis, is the uncertainty of system parameters such as system inertia in controlled islanding problem.

Without considering the transient stability, the islanding strategy may fail to stop the propagation of harmful dynamics throughout the network. It is evident that during the intentional network splitting, there is a significant risk of transient instability. Indeed, although the previously proposed models determine the islanding boundaries considering power imbalance [10, 18, 20, 21, 27, 31, 37, 38] and/or frequency stability criterion[39],

the resulted splitting strategy might still be at the risk of transient instability. Therefore, the preservation of transient stability is a major prerequisite for the success of any controlled islanding problem.

1.4 Contributions

Different approaches for considering transient stability in controlled islanding problem are developed. Based on the characteristics of each method, the main contributions of this thesis are summarized as follows:

- The development of a transiently-stability constrained controlled islanding optimization named hereafter by Method 1 with the following highlights in both steady state and transient stability aspects:

  This method provides a benchmark mixed-integer nonlinear program (MINLP) model subject to full AC power flow constraints. The proposed method is then linearized to have a computationally lighter MILP approximation model.

  Coupling the steady state MIP model of controlled islanding with transient stability requirement. The extended equal area criterion (EEAC) is used in the optimization model to guarantee the first swing transient stability of the synchronous machines inside the created islands, after the controlled line switching. This model is extended and perfected in subsequent proposed models.
- The development of a transiently-stability constrained controlled islanding optimization model named hereafter by Method 2 with the following highlights in transient stability assessment method as well as the solution procedure:
  1) Method 2 presents a transient stability criterion as a function of the transfer impedances between coherent generators in each island. The network splitting is then carried out in a direction where the transient stability criterion is increased. Indeed, unlike the EEAC in Method 1, this method considers the impact of network splitting or topology changes on transient stability.
  2) A multi-objective MIP model is defined for the transient stability constrained controlled islanding (TSC-CI) model in order to consider the transient stability of islands and the minimum possible power imbalance goals in a single model. Based

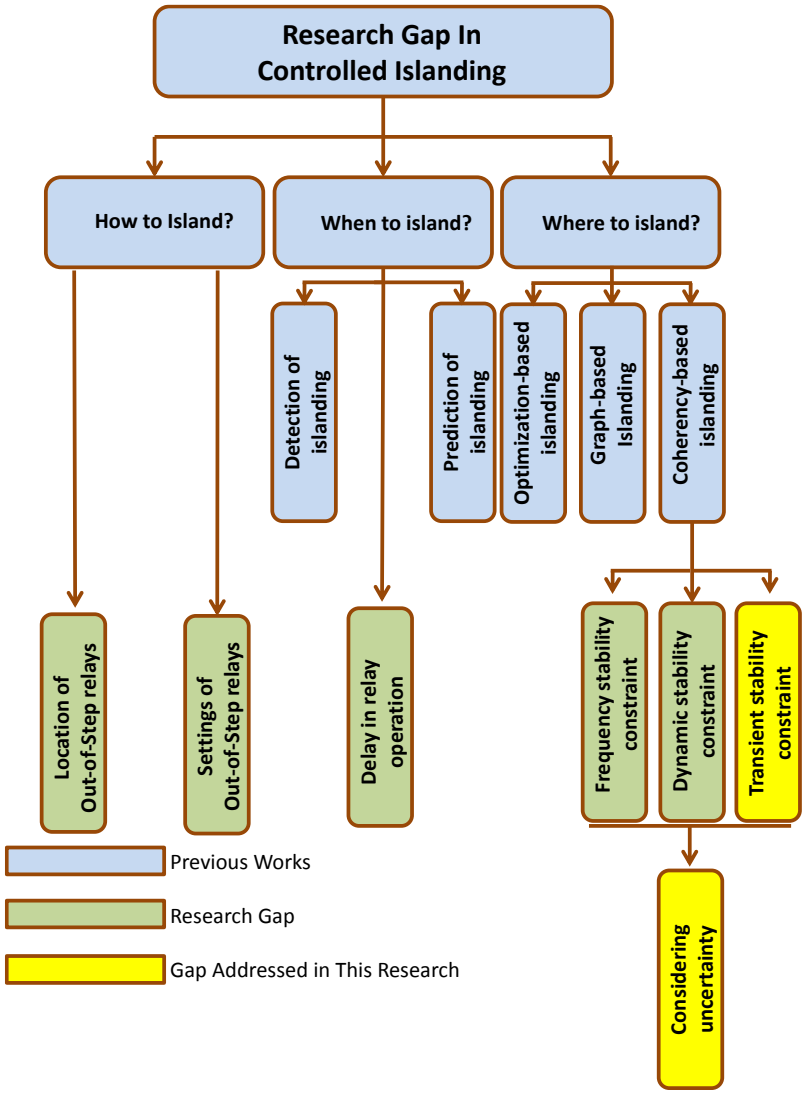

Fig 1-5: The research gap in controlled islanding problem

on wide-area measurements, a weighting procedure is developed to prioritize the critical islands and to avoid the unnecessary power imbalance in favor of transient stability.

- The development of a transiently-stability constrained controlled islanding model named hereafter by Method 3 with the following highlights :

  1) Proposing an analytical linear transient stability constraint using the transient energy function method without any need for further time domain simulation. The MIP optimization model developed in previous Methods 1 and 2 is used combined with a transient energy function approach to preserve the transient stability of resulted

islands.

2) Unlike, Method 1 and Method 2, the proposed transient energy function approach assure the transient stability of the resulted islands.
3) Developing an iterative procedure to converge the TSC-CI model to an optimal islanding strategy.
4) The development of a TSC-CI model named hereafter by Method 4 to consider the uncertainty of system inertia based on the framework proposed in Method 3.

1.5 Thesis Structure

The overall structure of this thesis is shown in Fig 1-6. It is noted that the proposed models for controlled islanding start with the basic models in beginning chapters and are extended and promoted in further chapters. . The background, motivation, literature review, and contribution have been already discussed in Chapter 1. The basics of power system islanding including the explanations of "where to island" and "When to island" issues are discussed in chapter 2. The formulation and simulation of Method 1 are presented in Chapter 3. Details of Methods 2 and 3 are given in chapters 4 and 5. The proposed formulation to address the uncertainty of system inertia is introduced in chapter 6. Also in this chapter a comprehensive comparison between the proposed methods is given. Finally, the findings of this thesis and the suggestions for future works are presented in chapter 7.

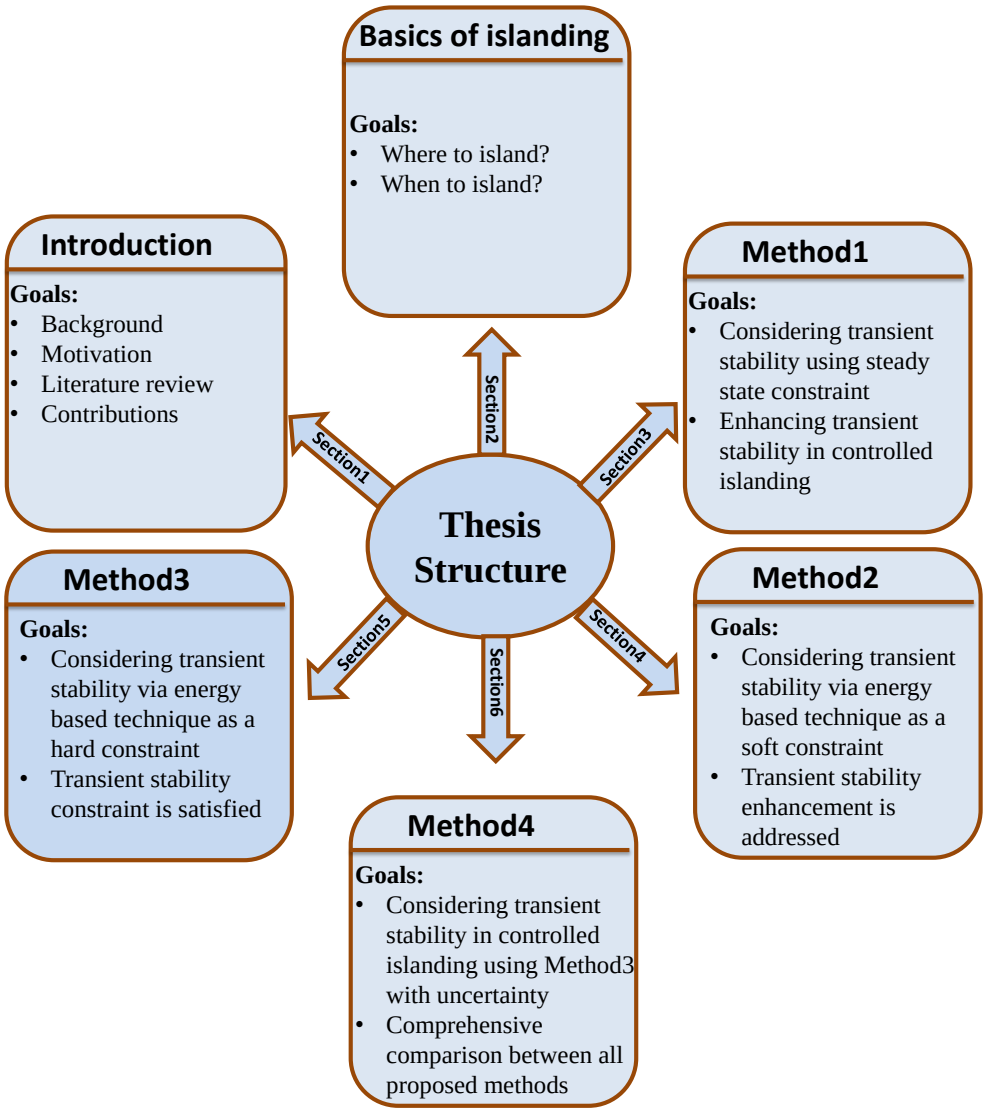

Fig 1-6: Overall Structure of Thesis

CHAPTER 2. FUNDAMENTALS OF POWER SYSTEM ISLANDIG

2.1 Introduction

Blackouts or cascading outages are costly events that menace the integrity of bulk electric energy systems around the world. Controlled splitting is executed as the last countermeasure to reduce the undesired economic and social consequences of a blackout. In this chapter, two main parts of each controlled islanding scheme including "where to island" and "when to island" issues are addressed. Details of both issues are discussed in the conventional islanding context. In the first part, the boundaries of electric islands are determined using a Mixed Integer Non-Linear Programming (MINLP) model with minimizing the cost of load curtailment over the resulted islands. In the second part, in order to give a better clarification of the "when to island" issue, a data mining technique is proposed to predict the risk of electric separation of an electric island from the rest of the network. To give a uniform and comprehensive description of the controlled islanding strategy, both parts are implemented in the same test case.

2.2 Basics of Conventional Controlled Islanding

The overall structure of the controlled islanding procedure has been shown in Fig 2-1. As shown in this figure, the conventional islanding method has three distinct parts including: determining coherent generators, where to island and when to island. The "when to island"

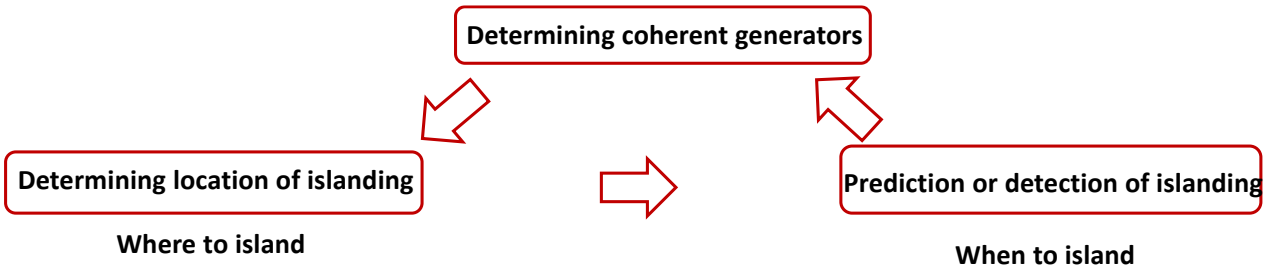

Fig 2-1: The overall structure of the controlled islanding method

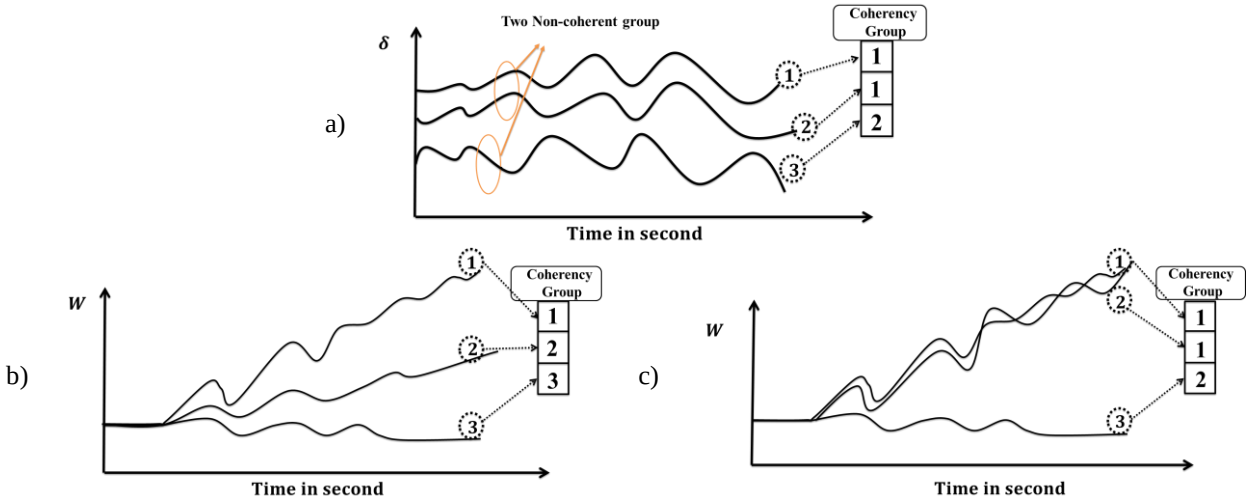

Fig 2-2: Responses of coherent groups

a) based on rotor angle trajectory, (Groups 1 and 2 are coherent and 3 is non-coherent

b) based on rotor speed trajectory, (groups 1 ,2 and 3 are non-coherent)

c) based on rotor speed (Group 1 and 2 are coherent and group 3 is non-coherent group)

issue or the time of islanding can be predicted using a data mining approach or other methods. It is noted that the aim of this two-stage algorithm is to clarify the basics of controlled islanding strategy, and in later chapters, the thesis is focused on the "where to island" issue.

2.3 Coherency and Where to Island Issue

Based on the power system topology and the operational conditions, synchronous generators can be classified into several electric coherent groups. In the first step, the coherent generators are determined using a slow coherency technique. In order to

determine the coherent generators, the correlation coefficients between the rotor angles of all pairs of generators are calculated under a single or given set of electric short circuit faults at different locations. The correlation ratio between two vectors of rotor angles is utilized as the coherency criterion. The correlation coefficient between the two machines is calculated as follows [40].

$$CR_{ij} = \frac{n\sum_{t=1}^{n}\left[\delta_i(t)\delta_j(t)\right] - \sum_{t=1}^{n}[\delta_i(t)] \times \sum_{t=1}^{n}[\delta_j(t)]}{\sqrt{\left[\ n\sum_{t=1}^{n}\left(\delta_i(t)\right)^2 - (\sum_{t=1}^{n}\delta_i(t))^2\ \right] \times \left[\ n\sum_{t=1}^{n}(\delta_j(t))^2 - (\sum_{t=1}^{n}\delta_j(t))^2\ \right]}} \quad (2\text{-}1)$$

where:

In order to minimize the dependency of coherency criteria to the input electric faults, the correlation ratio between two given generators can be averaged over their correlation ratios over a set of electric faults. Electric faults include three phase short circuit faults at different locations.

In the second step, the boundaries of islands are recognized such that the real power imbalance in each island is minimized, and the coherent generators are located in the same group. This issue promotes the stability of each island, indirectly. The boundaries of electric islands are determined using a Mixed Integer Non-Linear Programming (MINLP) formulation. It is noted that this MINLP model is presented only to describe the basics of the "where to island" issue and in later parts, all the optimization models are linearized. The objective function of the MINLP-based splitting strategy is defined as the minimization of the costs of generation re-dispatch and load curtailment under the islanding strategy as follows.

$$\min\ \ Cost = \sum_{i=1}^{N_g} \rho_i^+ . \Delta P_{G_i}^+ + \sum_{i=1}^{N_g} \rho_i^- . \Delta P_{G_i}^- + \sum_{i=1}^{N_l} \lambda_i . \Delta P_{L_i} \quad (2\text{-}2)$$

Practically, the cost of load curtailment is much more than the cost of generation re-dispatch. This issue is considered in simulation results by assigning a higher weighting factor (i.e. λ_i) for load shedding. The different costs can be considered for generation re-

dispatch in both increasing (i.e. ρ_i^+) and decreasing (i.e. ρ_i^-) directions. The set of equality and inequality constraints in MINLP-based islanding strategy are defined as follows.

- **Power balance constraint**

The active and reactive power balance constraint at each node of each island is expressed via AC load flow equations as follows.

$$[P_{Gi}^0 + \Delta P_{Gi}^+ - \Delta P_{Gi}^- - (P_{Li}^0 - \Delta P_{Li})] = U_{ij}V_i \sum_{n=1}^{N} U_{kj}V_k\, Y_{in}\, cos(\theta_i - \theta_k - \theta_{in}^z) \tag{2-3}$$

$$[Q_{Gi} - Q_{Li}] = U_{ij}V_i \sum_{n=1}^{N} U_{kj}V_k\, Y_{in}\, sin(\theta_i - \theta_n - \theta_{in}^z) \tag{2-4}$$

$$i = 1, \dots, N \quad and \quad j = 1, \dots, N_{is}$$

- **Operational Constraints**

The limits of transmission lines, the upper and lower limits of generation re-dispatch and the upper limit of load curtailment are expressed as follows.

$$-P_{ij}^{max} \le P_{ij} \le P_{ij}^{max} \qquad \forall\, ij \in \Omega^{l} \tag{2-5}$$

$$0 \le \Delta P_{Gi}^{+} \le \Delta P_{Gi}^{+\,max} \qquad \forall\, i \in \Omega^{g} \tag{2-6}$$

$$0 \le \Delta P_{Gi}^{-} \le \Delta P_{Gi}^{-\,max} \qquad \forall\, i \in \Omega^{g} \tag{2-7}$$

$$0 \le \Delta P_{L_i} \le \Delta P_{L_i}^{max} \qquad \forall\, i \in \Omega^{g} \tag{2-8}$$

$$Q_{Gi}^{min} \le Q_{Gi} \le Q_{Gi}^{max} \qquad \forall\, i \in \Omega^{g} \tag{2-9}$$

$$V_i^{min} \le V_i \le V_i^{max} \qquad \forall\, i \in \Omega^{d} \tag{2-10}$$

It is noted that the minimum and maximum amount of possible generation re-dispatch depends on the ramp rate capability of generators. For the sake of simplicity, it is assumed that the total amount of generation re-dispatch is known.

- **Grouping constraint**

Based on this constraint, each load point belongs to just one island.

$$\sum_{j=1}^{N_{is}} U_{ij} = 1 \qquad for \qquad i = 1,2, \dots, N_{is} \tag{2-11}$$

If the $\boldsymbol{i^{th}}$ load bus belongs to a $\boldsymbol{j^{th}}$ island then the binary variable $\boldsymbol{U_{ij}}$ will be equal to 1(i.e. $\boldsymbol{U_{ij}}$=1).

- **Connectivity constraint**

Based on this constraint, all nodes in each island must be connected. The graph of each island is connected if every node of the graph (e.g. node m_k) is reachable from every other node of that graph. The connectivity of each island is formulated as a non-linear constraint as follows.

$$Y_k^{-1}(i, m_k) \neq 0 \quad \forall\, i, m_k \quad \in \boldsymbol{\Omega_k^n} \tag{2-12}$$

where

$\boldsymbol{\Omega_k^n}$: The set of buses in island k

2.4 When to Island Issue

In this section, the procedure for the prediction of unplanned islanding is introduced. Although there are many protective relays throughout the network (e.g. out-of-step relays), the activation of protective relays is ignored. In other words, this algorithm is independent of the activation of OS relays. The set of the train and test scenarios including island and non-island events are constructed offline. In the online part, the prediction module determines the time of islanding. In other words, the online predictor decides about the activation of network splitting and in this regard the "where to island" module is mastered by the "where to island" module. The overall structure of the proposed prediction scheme is illustrated in Fig 2-3 Based on this figure, the islanding prediction is carried out via the following steps:

Step 1) Create the list of input scenarios (i.e. each scenario is a simulation event).

Step 2) Run a 15-second time domain simulation for each scenario using the transient stability simulator.

Step 3) Record the trajectories of rotor angles for all generators in each scenario.

Step 4) Assign a label to each scenario (i.e. island: 1 or non-island:0).

Step 5) Calculate the input feature for each scenario and create input-output pairs

Step 6) Construct the Decision Tree (DT) using input-output data (i.e. DT training and test) in a top-down fashion.

Step 7) Prune DTs using (7) and (8).

Step 8) Predict island conditions using online data.

Step 9) Update DTs

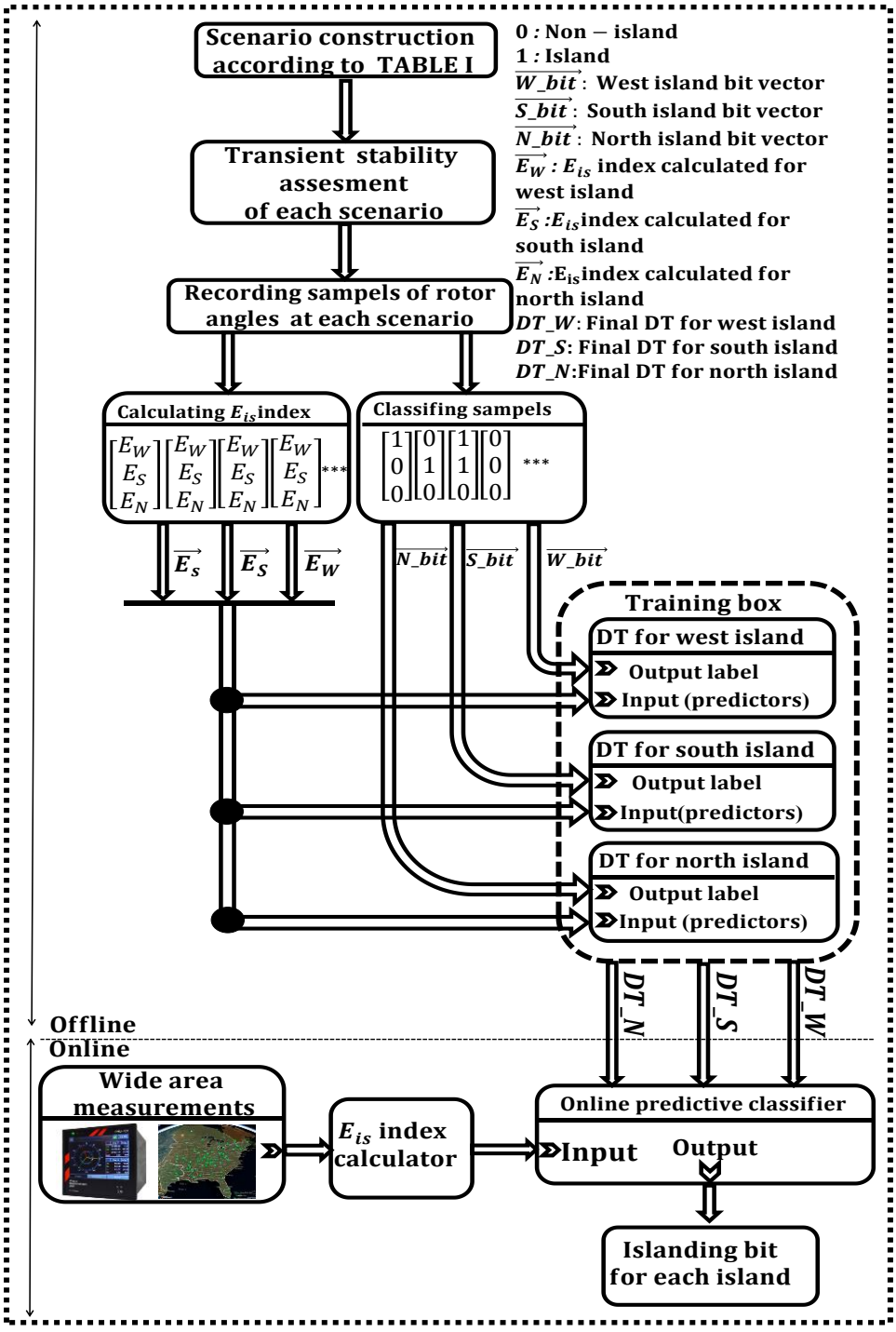

Fig 2-3: Overall structure of the power system unplanned islanding prediction

More details can be found in[13].

Table 2-1: Coherent generators in IEEE 39 bus test system

Island	Coherent Generators
North Island	30, 37, 38
West Island	31, 32, 39
South Island	33, 34, 35, 36

Table 2-2: Generation Re-dispatch and Load Curtailment of all nodes

Bus N0	Generation Re-dispatch and Load Curtailment		
	ΔP_G^+(MW)	ΔP_G^-(MW)	ΔP_D(MW)
30	0	66.9	0
31	106	0	0
32	0	50	0
34	0	32.9	0
Other nodes	0	0	0
Total Shed(MW)	106	149.8	0
Total Cost($/h)	15900	7490	0

2.5 Islanding Boundaries for IEEE 39-Bus System

In this section, the conventional controlled islanding scheme is applied to IEEE 39-bus test system. Based on the pairwise correlation coefficients, the coherent generators are determined as given in Table 2-1. For each coherent group of generators, an electric island is formed. Therefore, three different islands named by W (West), S (South), and N (North) are defined. Boundaries of these islands are determined using the proposed MINLP formulation. The proposed MINLP formulation is solved using SBB solver in GAMS. The costs of generation re-dispatch and load curtailments are assumed as $\rho_i^+ = 150 \frac{\$}{MWh}$, $\rho_i^- = 50 \frac{\$}{MWh}$ and $\lambda_i = 1500 \frac{\$}{\text{MWh}}$. It is noted that the cost of generation decrement can be interpreted as an opportunity cost. The obtained boundary for each island and the required generation re-dispatch and load curtailments have been given in Fig 2-4 and Table 2-2. Based on Table 2-2, due to the high penalties for load curtailments the splitting strategy tends to balance the islands using generation re-dispatch. In other words, the interconnected power system could be divided into three different islands with 255.8MW of generation re-dispatch without any load curtailment. In case of a blackout (i.e. without executing the

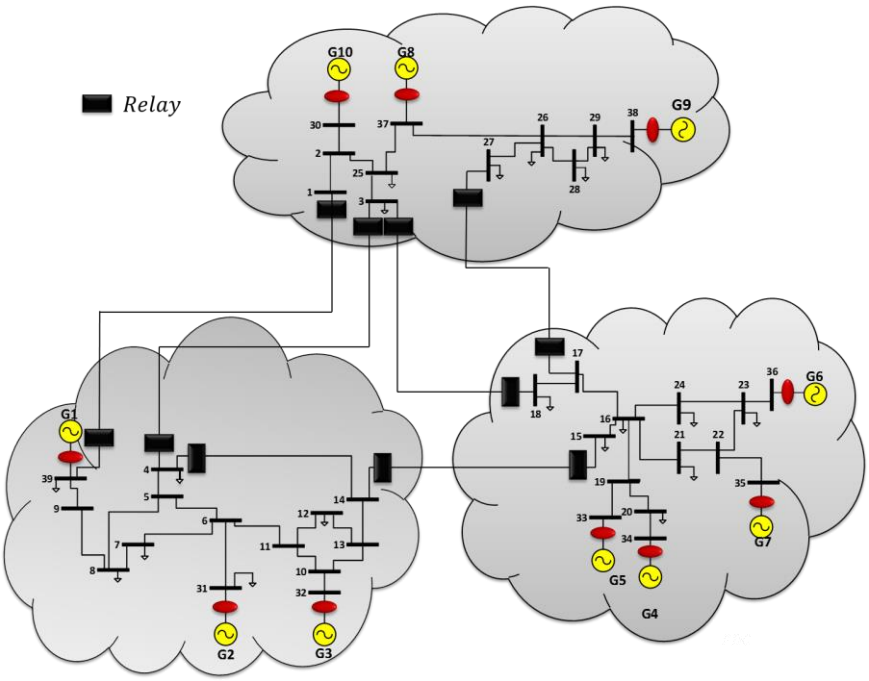

Fig 2-4: The obtained boundaries (i.e. islands) for IEEE-39 bus network using MINLP formulation

proposed scheme), a total load of 6254.2MW (i.e. the total base-case load) will be lost. The cost of this load curtailment is about 9381300 $/h(i.e. 6254.2MW *1500 $/MWh). The required measurements are provided by PMUs at generators' terminals. These data are then transmitted to a Phasor Data Concentrator (PDC) or Energy Management System to decide about the execution of the islanding strategy.

The performance of the conventional scheme is investigated following an SC fault (i.e. an unseen scenario) applied at $t = 0.1$ sec on bus 16 and cleared after $300ms$. Fig 2-5-a shows the rotor angle of each generator after the SC fault. As shown in this figure, 7 generators become unstable in less than 1.5 sec. Also, according to Fig 2-5-b, the speed trajectories of coherent generators in South island deviate from other generators. Therefore, without executing the controlled islanding strategy, the network will experience a blackout after about 2.5sec. Fig 2-6 shows the rotor angles of generators after the separation of

South island from the rest of the network after 0.52sec (i.e. including 0.1 sec for inherent delays). As shown in Fig 2-6, all generators have stable rotor angles.

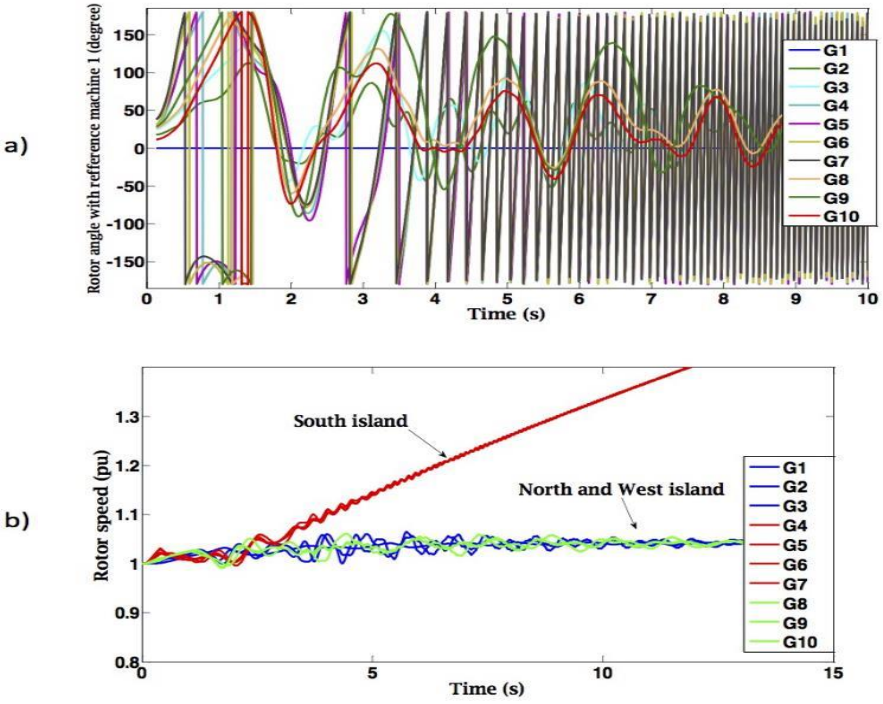

Fig 2-5: a) Variation of rotor angles w.r.t generator 1 following an SC fault at bus 16
b) Variation of rotor speeds w.r.t generator 1 following an SC fault at bus 16

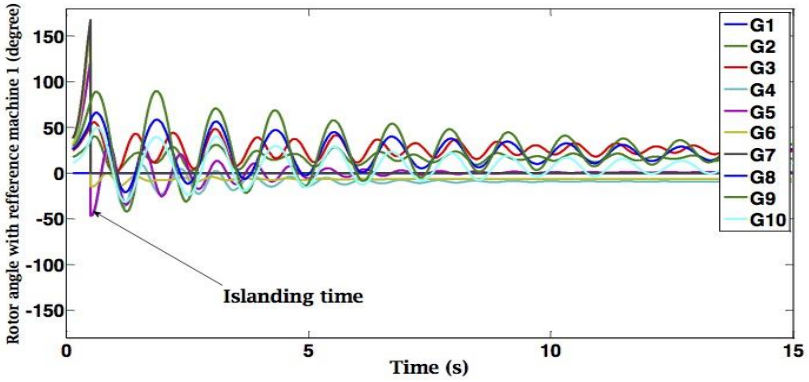

Fig 2-6: Trajectories of rotor angles w.r.t generator 1 when the south island is separated from the rest of the network at t=0.54sec

2.6 Conventional Islanding in Low Inertia System

The penetration of renewable resources including wind and solar power plants is increasing in many national and regional power systems. Renewable integration is fully compatible with the low carbon economy of power systems. The uncertainty of renewable generation is a major concern in power system operation. The penetration of non-synchronous renewable resources decreases the equivalent system inertia and affects the power system stability especially rotor angle and frequency stabilities. In this part, the challenges of the conventional islanding strategy under a low inertia scenario are shown using a simple case study. To this end, the value of system inertia is reduced to 50% in the IEEE 39-Bustest system. A time simulation is performed under a severe three phase short circuit fault in bus 16 and cleared after 300 ms. The conventional islanding scheme is applied at $t = 0.5sec$. The simulation results with and without implementing the conventional controlled islanding scheme are shown in Fig 2-7 to Fig 2-10. In such a condition (i.e. blackout due to instability of generators) the islanding scheme as the last resort is executed to reduce the damage caused by the possible blackout caused by the unintentional islanding. The results shown in Fig 2-8 and Fig 2-10 indicate the instability of some generators.

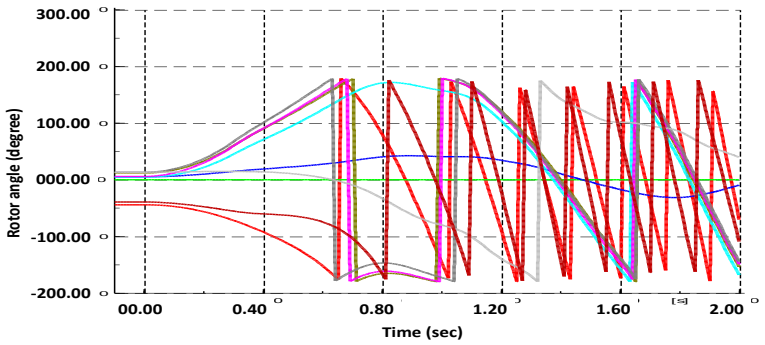

Fig 2-7: Rotor angle trajectories without applying conventional islanding in low inertia system

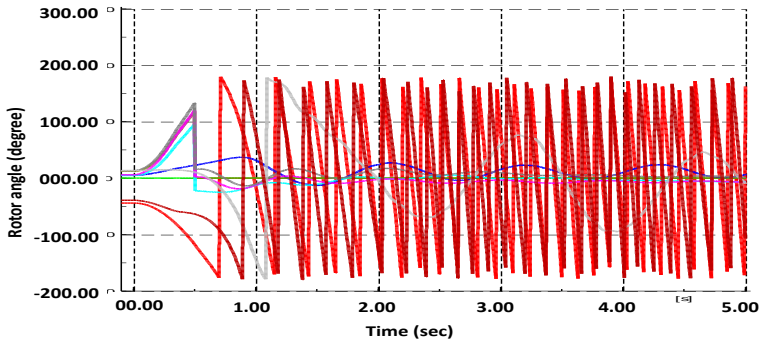

Fig 2-8: Rotor angle trajectories with applying conventional islanding in low inertia system.

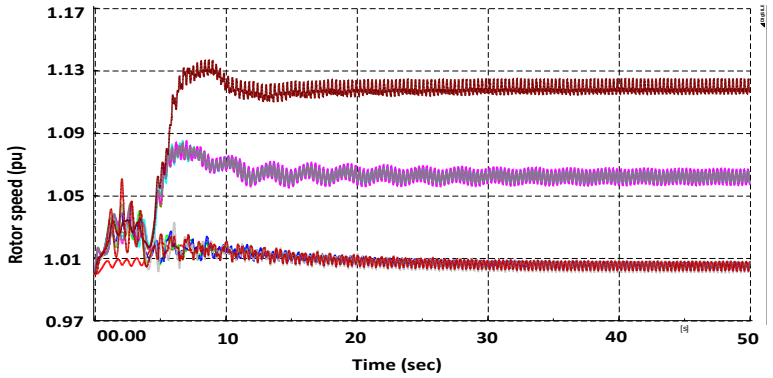

Fig 2-9: Rotor speed trajectories without applying conventional islanding in low inertia system

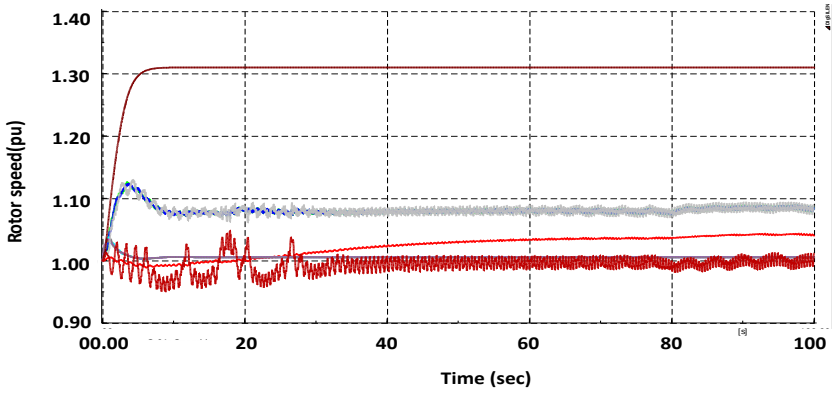

Fig 2-10: Rotor speed trajectories with applying conventional islanding in low inertia system.

2.7 Conclusion of the Chapter

In this chapter the fundamentals of conventional controlled islanding strategy including the "where to island" and "when to island" issues were briefly discussed. Based on the given results, it was shown that the success of any controlled islanding strategy is not guaranteed with just relying on steady state constraints. The conventional islanding strategy may fail to create stable islands. It was shown that the transient stability as the main requirement in controlled islanding scheme is not preserved using the conventional islanding strategy. Also this challenge is highlighted in modern low inertia power systems. Therefore it is concluded that transient stability is the major treat to the failure of controlled islanding strategy. To this end, a comprehensive transient stability constrained controlled islanding scheme is required to remove or minimize the risk of transient instability.

CHAPTER 3. EEAC BASED CONTROL ISLANDING WITH ENHANSING TRANSIENT STABILITY MARGIN

3.1 Introduction

Intentional islanding has been extensively studied recently as the last resort to prevent blackouts, mostly to restore the steady state power balance. However, as most previous studies on this topic do not address stability issues, the static controlled islanding plans might fail to ensure the stability of resulted islands, thereby delaying their acceptance and adoption by electric utilities. This chapter makes progress toward addressing stability issues, proposing a controlled islanding model that ensures and improves the transient stability of the islanded system. Linear transient stability constraints are derived off-line, based on the extended equal area criterion (EEAC), to ensure the first swing transient stability of the synchronous machines, just after the controlled line switching. The transient stability constrained controlled islanding model is first developed as a mixed-integer nonlinear programming (MINLP) optimization model. Further, the proposed MINLP model is linearized, resulting in a computationally lighter mixed-integer linear program (MILP). The objective function of the islanding model is to minimize the power imbalance and to increase the transient stability margin of the resulted islands. The obtained optimization results are then validated by doing the full scale time domain simulation. The proposed transient stability constrained islanding method in this chapter is named by Method1, throughout the thesis.

3.2 Overall Structure of the proposed model (Method1)

This section describes the overall structure of the proposed islanding algorithm. While the satisfaction of some operational constraints (e.g. power flows across transmission lines) does not incur significant computational burden, the transient rotor angle stability constraints are time-dependent and must be satisfied immediately after the network splitting. Two different goals are perused for efficient consideration of transient stability in controlled islanding strategy. First, the risk of transient stability of the synchronous

machines, immediately after the network splitting, is mitigated. Second, the transient stability margin, i.e., the minimum critical clearing time (CCT), at the steady-state operation of the created islands, is enhanced. These two requirements are described and formulated in the proposed islanding method. The first action of any controlled islanding scheme is to trip a few transmission lines to split the interconnected network into several isolated electrical islands. During the time delay between the controlled network splitting (i.e., transmission switching) and the execution of the required remedial actions (e.g., load shedding and generation changes), each island is exposed to an accelerating or decelerating power imbalance, which may result in the transient instability of synchronous machines. In addition to the electric power imbalance caused by the network splitting, another power imbalance caused by pre-islanding faults may be imposed on each generating unit. The summation of these two sources of electric power imbalance will drive the swing equation of each synchronous machine. The overall structure of the proposed method is illustrated in Fig 3-1. According to Fig 3-1, the phasor measurement data are required to calculate these two sources of electric power deviations. The procedure of calculating these deviations is described in the following. Transient stability constraints consist of minimum and maximum limits on generators' active power (corresponding to maximum allowable accelerating and decelerating powers) are calculated using the EEAC method [41]. The EEAC method has been extensively used for transient stability assessment in multi-machine power systems [42-45]. Typically, the transient stability of synchronous machines in power systems is assessed under short circuit faults. However, in controlled islanding the input disturbance is the network splitting, as a measure against a stability threatening event (e.g. anticipated cascading overload, fault, etc.). Synchronous generators will experience a given power imbalance (i.e. the change in electrical power at the generator terminal) due to network splitting. According to the EEAC criterion, it is assumed that the resulted electric power imbalance is imposed on a given generator while other ones do not contribute to compensating this electric power deviation. This condition can be assessed using the EEAC method. This is a conservative assumption in transient stability's point of view, justified by the emergency need to avoid the risk of instability.

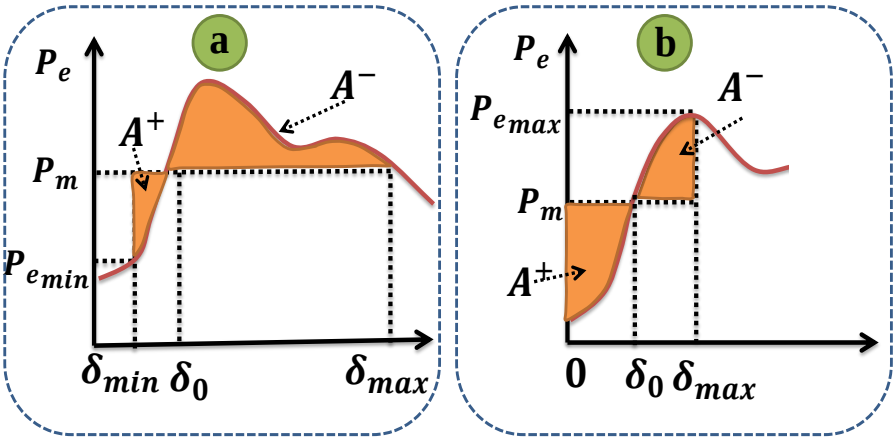

Fig 3-1: EEAC in the multi-machine system

3.3 Extended Equal Area Criterion

The EEAC for controlled islanding is described based on the equal area criterion. The classic model of synchronous generators can be defined in the center-of-inertia (COI) reference as follows:

$$2H_i \frac{d\omega_i}{dt} = P_m - P_{ei} - \frac{H_i}{H_T} P_{COA} \tag{3-1}$$

where

$$P_{ei} = \sum_{j=1}^{n} E_i E_j B_{ij} \sin \delta_{ij} + E_i E_j G_{ij} \cos \delta_{ij} \tag{3-2}$$

$$P_{COI} = P_T - 2 \sum_{k=1}^{n-1} \sum_{j=k+1}^{n} E_k E_j G_{kj} \cos \delta_{kj} \tag{3-3}$$

$$H_T = \sum_{j=1}^{n} H_j \qquad , P_T = \sum_{j=1}^{n} P_j \tag{3-4}$$

The accelerating power P_{Ai} is defined as:

$$P_{Ai} = a_i - \sum_{j=1}^{n} \left(b_{ij} \sin \delta_i + d_{ij} \sin \delta_i \right) \tag{3-5}$$

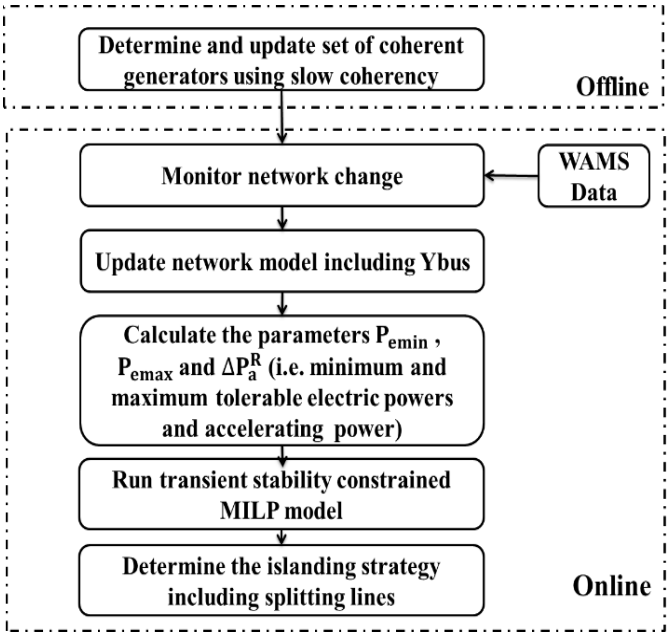

Fig 3-2: Overall structure of the proposed algorithm

where

$$a_i = P_i - \frac{H_i}{H_T} P_T + 2\frac{H_i}{H_T} \sum_{\substack{k=1 \\ k\neq i}}^{n-1} \sum_{\substack{j=k+1 \\ j\neq i}}^{n} E_k E_j G_{kj} \cos \delta_{kj} \tag{3-6}$$

$$b_{ij} = E_i E_j B_{ij} \cos \delta_j + E_i E_j G_{ij} \left(1 - \frac{2H_i}{H_T}\right) \sin \delta_j \tag{3-7}$$

$$d_{ij} = -E_i E_j B_{ij} \sin \delta_j + E_i E_j G_{ij} \left(1 - \frac{2H_i}{H_T}\right) \cos \delta_j \tag{3-8}$$

The amount of accelerating and decelerating powers caused by the network splitting are calculated as follows:

$$A^+ = \int_{\delta_i^{min}}^{\delta_i^0} [\, a_i - \sum_{j=1}^{n} \left(b_{ij} \sin \delta_i + d_{ij} \sin \delta_i\right)] \tag{3-9}$$

$$A^- = \int_{\delta_i^0}^{\delta_i^{max}=\delta_i^u} [\, a_i - \sum_{j=1}^{n} \left(b_{ij} \sin \delta_i + d_{ij} \sin \delta_i\right)] \tag{3-10}$$

For evaluating the transient stability of each machine, under the islanding disturbance, it is assumed that only one machine at the same time is severely disturbed, and the other

machines are not significantly affected by the disturbance. Hence, b_{ij} and d_{ij} are approximately constant. Therefore, (3-9) and (3-10) are obtained as follows:

$$A^{+} = a_i\left(\delta_i^0 - \delta_i^{min}\right) + \sum_{\substack{j=1 \\ j\neq i}}^{n} b_{ij}[(\cos\delta_i^0 - \cos\delta_i^{min}) - d_{ij}(\sin\delta_i^0 - \sin\delta_i^{min})] \quad (3\text{-}11)$$

$$A^{-} = a_i(\delta_i^{max} - \delta_i^0) + \sum_{\substack{j=1 \\ j\neq i}}^{n} b_{ij}((\cos\delta_i^{max} - \cos\delta_i^0) - d_{ij}(\sin\delta_i^{max} - \sin\delta_i^0)) \quad (3\text{-}12)$$

Finally, based on (3-11) and (3-12), the transient stability limits (i.e., P_{emax} and P_{emin}) are determined and included in the optimization model, to preserve the first swing transient stability of resulted islands.

- **Calculation of P_{emin}**

According to Fig 3-2(a), the minimum electrical power of each generator, i.e. P_{emin} , can be obtained by solving (3-13) as follows:

$$A^{-} = A^{+} \quad (3\text{-}13)$$

where δ_i^{max} is obtained from the equality of $P_{Ai} = 0$ assuming $\delta_i^0 < \delta_i^{max} < 180^0$. The value of the rotor angles of other generators is assumed to be constant. Therefore, the equality constraints given in (3-13) and (3-2) are solved to determine δ_i^{min} and P_{emin}.

- **Calculation of P_{emax}**

According to Fig 3-2 (b), δ_i^{max} can be obtained by solving (3-13), assuming $\delta_i^{min} = 0$. Therefore, the constraint given in (3-2) can be used to determine P_{emax}. Note that in (3-1)–(3-13), the values of E_1, E_2, and δ_0 are obtained from the last normal operating condition (i.e., before the fault occurrence). Unlike the short-circuit faults, during the islanding action or network splitting, the voltage magnitudes are not affected significantly.

- **Calculation of $\Delta\mathbf{P_a^R}$**

The second source of electric power deviations on each synchronous generator is incurred due to the fault conditions before executing the controlled islanding strategy. To this end,

this deviation must be measured and added to the total accelerating or decelerating power in swing equations. Without considering $\Delta \boldsymbol{P}_{\boldsymbol{a}}^{\boldsymbol{R}}$ the transient stability criterion may be underestimated. As shown in Fig 3-2, in real time application of this method and based on the phasor measurement unit (PMU) data, the value of $\Delta \boldsymbol{P}_{\boldsymbol{ai}}^{\boldsymbol{R}}$ is supposed to be equal to $\boldsymbol{P}_{\boldsymbol{m}_i} - \boldsymbol{P}_{\boldsymbol{e}_i}^{\boldsymbol{R}}$, where $\boldsymbol{P}_{\boldsymbol{e}_i}^{\boldsymbol{R}}$ is the real time electric power of unit *i* measured by PMU.

3.4 Transient Stability Enhancement Using UEP-SEP Concept

After ensuring that the resulting islands survive the risk of the first swing transient instability, it is desirable that the resulted stable equilibrium point (SEP) of each island has an acceptable stability margin against operational uncertainties and new possible disturbances. To this end, the secondary goal of the proposed method is to ensure that the final islanding boundaries not only maintain the transient stability, but also the transient stability margin of each island is enhanced. For this purpose, the concept of unstable equilibrium points (UEP) can be used indirectly to obtain the maximum transient stability margin based on the following principle. If the initial conditions of the resulted islands lie in the stability region of the desired SEP, the post-islanding system's condition will converge to that SEP [46]. For better clarification, it is assumed that under normal conditions, the power system is operated at the SEP. Due to the network splitting, the system moves away from the SEP and move toward its stability boundaries. Suppose that the pre-islanding SEP of an n-machine power system satisfies the following equilibrium equations:

$$P_{mi} - P_{ei} = 0 \quad i = 1, \dots, n \tag{3-14}$$

The islanding action changes the electrical power of the generators. Therefore, in an islanded system, (3-14) is rewritten for each island as follows:

$$\begin{cases} P_{mi} - P_{ei} + \Delta P_{ei}^{+} - \Delta P_{ei}^{-} + \Delta P_{mi} = 0 \quad \forall i \in \Omega_1^g \\ \dots\dots \\ P_{mi} - P_{ei} + \Delta P_{ei}^{+} - \Delta P_{ei}^{-} + \Delta P_{mi} = 0 \quad \forall i \in \Omega_{N_{is}}^g \end{cases} \tag{3-15}$$

According to (3-15), by minimizing the total electric power deviation caused by pre-islanding faults and the islanding action, i.e. ΔP_e, the post islanding SEP converges to the

pre-islanding SEP. Indeed by assuming $\Delta P_{ei}^{+} - \Delta P_{ei}^{-} \approx 0$, (3-15) and (3-16) will be the same. Therefore, the stability margin of each generator can be improved, by reducing the difference between its after-islanding operating point and the SEP. This issue is expressed as the minimization of the normalized deviation of a post-islanding operating point from the normal pre-islanding operating as follows:

$$min\ z = \sum_{i=1}^{N_g} (\Delta P_{e_i}^{+} + \Delta P_{e_i}^{-})/P_{m_i} \tag{3-16}$$

3.5 Formulation of the TSC-Constrained Controlled Islanding Model (Method 1)

This section presents the proposed MINLP controlled islanding model, including the objective function, and the operational (i.e. steady state) and the transient stability constraints.

3.5.1 The Objective Function

The islanding strategy should split the network in a manner that the overall power balance is met to the largest extent. Under the deviations of electric power due to network splitting, the power balance is expressed as follows:

$$\sum_{i=1}^{N_g} (\ P_{m_i} - \Delta P_{e_i}^{-} + \Delta P_{e_i}^{+}) = \sum_{j=1}^{N_l} P_{l_j} + P_{loss} \tag{3-17}$$

The islands with load excess can be balanced using either $\Delta P_{e_i}^{+}$ or P_{shed_j}, as given by (3-18) and (3-19), respectively.

$$\sum_{i=1}^{N_g^{is}} (\ P_{m_i} + \Delta P_{e_i}^{+}) = \sum_{j=1}^{N_l^{is}} P_{l_j} + P_{loss}^{new} \tag{3-18}$$

$$\sum_{i=1}^{N_g^{is}} P_{m_i} = \sum_{j=1}^{N_l^{is}} (P_{l_j} - P_{shed_j}) + P_{loss}^{new} \tag{3-19}$$

According to (3-18) and (3-19), by neglecting the small deviations of the power losses (i.e., $P_{loss}^{new} - P_{loss} = 0$), the equality constraint given in (3-19) may be approximated by (3-20).

$$\sum_{i=1}^{N_g^{is}} \Delta P_{e_i}^{+} = \sum_{j=1}^{N_l^{is}} P_{shed\,j} \tag{3-20}$$

By neglecting the changes of the power losses, and without any load shedding, the total increase and decrease in the electrical powers are equal:

$$\sum_{i=1}^{N_g} \Delta P_{e_i}^{+} = \sum_{i=1}^{N_g} \Delta P_{e_i}^{-} \tag{3-21}$$

According to (3-20) and (3-21), the following relation between the changes of load and generation is obtained:

$$\sum_{i=1}^{N_g} (\Delta P_{e_i}^{+} + \Delta P_{e_i}^{-}) \cong 2 \times \sum_{j=1}^{N_l} P_{shed\,j} \tag{3-22}$$

Therefore, minimizing the deviations of the electrical power of generators is approximately equivalent to the minimization of the load shed. Thus, the objective function of the proposed model can be written as given in (3-16).

3.5.2 Constraints

The operational and transient stability constraints of the proposed islanding model are presented below.

3.5.2.1 Power Balance

The AC active and reactive power balance equations in each island, considering the deviations of the electrical power are given in (3-23) and (3-24).

$$\left[P_{gi}^{0} + \Delta P_{ei}^{+} - \Delta P_{ei}^{-} - P_{Li}\right] = V_i \sum_{j=1}^{N_b} V_j (GL_{i,j}^{new} cos\left(\theta_i - \theta_j\right) + BL_{i,j}^{new} sin(\theta_i - \theta_j)) \tag{3-23}$$

$$[Q_{Gi} - Q_{Li}] = V_i \sum_{j=1}^{N_b} V_j (GL_{i,j}^{new} sin\left(\theta_i - \theta_j\right) - BL_{i,j}^{new} cos(\theta_i - \theta_j)) \tag{3-24}$$

The decision variables of the controlled islanding scheme are the transmission line

switching and the electric power deviations (i.e., $\Delta P_{e_i}^{-}$ and $\Delta P_{e_i}^{+}$). The binary variable U_{ij} is used to model the status of the transmission line between bus i and bus j. According to (3-25)-(3-28), the admittance matrix of the system is updated following the topological changes caused by the switching transmission lines (i.e., network splitting).

$$BL_{i,j}^{new} = BL_{i,j}U_{i,j} \quad for\ i \neq j \tag{3-25}$$

$$GL_{i,j}^{new} = GL_{i,j}U_{i,j} \quad for\ i \neq j \tag{3-26}$$

$$GL_{i,i}^{new} = GL_{i,i} + \sum_{\substack{j=1 \\ j\neq i}}^{N_b}(1 - U_{i,j})GL_{i,j} \tag{3-27}$$

$$BL_{i,i}^{new} = BL_{i,i} + \sum_{\substack{j=1 \\ j\neq i}}^{N_b}(1 - U_{i,j})BL_{i,j} \tag{3-28}$$

3.5.2.2 Operational Limits

The power flow limits across the transmission lines are modeled according to (3-29). The reactive power of the generators, the voltage magnitudes of the load buses, and the active power threshold of the generators (including transient stability limits) are constrained as given by (3-30)-(3-32).

$$-P_{ij}^{max} \leq P_{ij} \leq P_{ij}^{max} \qquad \forall ij \in \Omega^{l} \tag{3-29}$$

$$Q_{Gi}^{min} \leq Q_{Gi} \leq Q_{Gi}^{max} \qquad \forall i \in \Omega^{g} \tag{3-30}$$

$$V_i^{min} \leq V_i \leq V_i^{max} \qquad \forall i \in \Omega^{d} \tag{3-31}$$

$$P_{ei\ min} \leq P_{gi}^{0} + \Delta P_{ei}^{+} - \Delta P_{ei}^{-} + \Delta P_{a}^{R} \leq P_{ei\ max} \qquad \forall i \in \Omega^{g} \tag{3-32}$$

3.5.2.3 Connectivity and coherency constraints

In order to preserve the connectivity the equivalent graph of each island, a fictitious DC power flow (FPF) is used [47]. According to (3-33), this FPF is an artificial formulation to check only the connectivity of the resulting islands, without conflicting with (3-24)-(3-25).

$$LF_{ij} = y_{ij} \times \left(\theta_j^f - \theta_i^f\right)U_{i,j} \tag{3-33}$$

$$U_{i,j} = U_{j,i} \tag{3-34}$$

$$if\ y_{ij} = 0 \quad \rightarrow \ U_{i,j} = 0 \tag{3-35}$$

For each existing transmission line (i.e., $y_{ij} \neq 0$), the formulation given in (3-33) will guarantee the connectivity of the resulting islands under the following assumptions:

$$LF_{ij} = 0 \qquad \forall \text{ ij } \in \ \Omega^{l} \tag{3-36}$$

$$\theta_i^{fk} = CTE_k \qquad \forall \text{ i } \in \ \Omega^{g} \quad \text{k} = 1, \dots, \text{N}_{\text{is}} \tag{3-37}$$

$$CTE_1 \ \neq \ CTE_2 \neq \cdots \neq CTE_{N_{is}} \tag{3-38}$$

According to the first assumption given in (3-36), the power flows of all transmission lines in the FPF must be zero. Based on the second assumption, the voltage angles of the generators in the k^{th} island are fixed at the same value (e.g., CTE_k). Furthermore, the voltage angle assigned to each island is different from that of other islands (i.e., $\text{CTE}_\text{j} \neq \text{CTE}_\text{k}$). Regarding the proposed FPF, the following two conditions are possible. First, if $\text{U}_{\text{i,j}} = 1$, due to a zero-line flow, the two adjacent buses are on the same island (i.e., $\theta_\text{j}^\text{f} - \theta_\text{i}^\text{f} = 0$). Second, if $\text{U}_{\text{i,j}} = 0$, it means that nodes i and j are in two different islands. It is noted that in this condition, according to (3-38), the voltage angles of nodes *i* and *j* must be different. Therefore, the transmitted power flow across the line *ij* is zero, indicating that these two buses are in two different islands.

According to the coherency constraint, the coherent groups of generators must be on the same island. Note that the coherency of the generators is determined using the slow coherency technique [18]. According to [18], slow coherency is a network characteristic. Slow coherency among the groups of generators does not vary significantly by the change of initial conditions and input disturbance. The predetermined sets of coherent generators are then considered as the input of the islanding model. Also, the non-coherent groups must be separated from each other. This grouping constraint is satisfied via the proposed FPF under the assumptions given in (3-37)-(3-38). By assigning a different voltage angle for

each coherent group, the connectivity of the coherent generators and the separation of the non-coherent generators are guaranteed.

3.5.3 The Proposed MILP Model

Since the benchmark MINLP model may not comply with on-line requirements, it is approximated by a computationally lighter MILP model. To this end, the nonlinear constraints are given in (3-23), (3-24), (3-29) and (3-33) should be linearized, requiring the definition of some auxiliary variables, as given by (3-42)-(3-48):

$$\left[P_{gi}^{0} + \Delta P_{ei}^{+} - \Delta P_{ei}^{-} - P_{Li}\right] = \sum_{j=1}^{N_b} (A1_{ij} + A2_{ij}) \tag{3-39}$$

$$[Q_{Gi} - Q_{Li}] = \sum_{j=1}^{N_b} (A3_{ij} - A4_{ij}) \tag{3-40}$$

$$P_{ij} = A1_{ij} + A2_{ij} - A5_{ij}\, GL_{ij} \qquad i \neq j \tag{3-41}$$

where

$$A1_{ij} = V_i V_j GL_{i,j} U_{i,j} cos\left(\theta_i - \theta_j\right) \qquad i \neq j \tag{3-42}$$

$$A1_{ii} = V_i^2 (GL_{i,i} + \sum_{\substack{j=1 \\ j \neq i}}^{N_b} \left(1 - U_{i,j}\right) GL_{i,j}) \tag{3-43}$$

$$A2_{ij} = V_i V_j BL_{i,j} U_{i,j} sin(\theta_i - \theta_j) \tag{3-44}$$

$$A3_{ij} = V_i V_j GL_{i,j} U_{i,j} sin\left(\theta_i - \theta_j\right) \tag{3-45}$$

$$A4_{ij} = V_i V_j BL_{i,j} U_{i,j} cos(\theta_i - \theta_j) \qquad i \neq j \tag{3-46}$$

$$A4_{ii} = V_i^2 (BL_{i,i} + \sum_{\substack{j=1 \\ j \neq i}}^{N_b} \left(1 - U_{i,j}\right) BL_{i,j}) \tag{3-47}$$

$$A5_{ij} = V_{ii}^2 U_{ij} \tag{3-48}$$

The power balance equations given in (3-39) and (3-40) is linearized at a given operating point (assuming normal operating conditions, i.e., $V_i \approx 1\ pu$ and $(\theta_i - \theta_j) \approx 0$).

$$A1_{ij} \approx (V_i + V_j - 1)\, GL_{i,j} U_{i,j} \qquad i \neq j \tag{3-49}$$

Table 3-1: Linearized formulation of the nonlinear equations

Eq.	Linearized formulation
(3-33)	$-M \times (1-U_{i,j}) \le LF_{ij} - y_{ij} \times \left(\theta_j^f - \theta_i^f\right) \le M \times (1-U_{i,j})$ $-MU_{i,j} \le LF_{ij} \le M \times U_{i,j}$
(3-49)	$-M(1-U_{i,j}) \le A1_{ij} - \left(V_i + V_j - 1\right) GL_{i,j} \le M(1-U_{i,j}) \;\; i \ne j$ $-MU_{i,j} \le A1_{ij} \le MU_{i,j} \;\; i \ne j$
(3-51)	$-M(1-U_{i,j}) \le A2_{ij} - BL_{i,j}(\theta_i - \theta_j) \le M(1-U_{i,j})$ $-MU_{i,j} \le A2_{ij} \le MU_{i,j}$
(3-51)	$-M(1-U_{i,j}) \le A3_{ij} - GL_{i,j}\left(\theta_i - \theta_j\right) \le M(1-U_{i,j})$ $-MU_{i,j} \le A3_{ij} \le MU_{i,j}$
(3-53)	$-M(1-U_{i,j}) \le A4_{ij} - \left(V_i + V_j - 1\right) BL_{i,j} \le M(1-U_{i,j}) \;\; i \ne j$ $-MU_{i,j} \le A4_{ij} \le MU_{i,j}$
(3-55)	$-M(1-U_{i,j}) \le A5_{ij} - (2V_i - 1) \le M(1-U_{i,j}) \;\; i \ne j$ $-MU_{i,j} \le A5_{ij} \le MU_{i,j} \;\; i \ne j$

$$A1_{ii} \approx (2V_i - 1)GL_{i,i} + \sum_{\substack{j=1 \\ j \ne i}}^{N_b} \left((2V_i - 1) - A5_{ij}\right) GL_{ij} \tag{3-50}$$

$$A2_{ij} \approx BL_{i,j}U_{i,j}(\theta_i - \theta_j) \tag{3-51}$$

$$A3_{ij} \approx GL_{i,j}U_{i,j}\left(\theta_i - \theta_j\right) \tag{3-52}$$

$$A4_{ij} \approx (V_i + V_j - 1)\, BL_{i,j}U_{i,j} \qquad i \ne j \tag{3-53}$$

$$A4_{ii} \approx (2V_i - 1)BL_{i,i} + \sum_{\substack{j=1 \\ j \ne i}}^{N_b} \left((2V_i - 1) - A5_{ij}\right) BL_{ij} \tag{3-54}$$

$$A5_{ij} \approx (2V_i - 1)U_{i,j} \qquad i \ne j \tag{3-55}$$

in the nonlinear constraints given in (3-49)-(3-55), are linearized using the linear constraints given in Table 3-1.

3.6 Reducing Computational Burden

To further reduce the computational complexity of optimization models, an innovative technique is used to reduce the number of candidate splitting lines. During cascading failures, the transmission lines in a coherent area exhibit similar variations between the voltage angles of their ends. Therefore, the coherency between the two ends of each line, expressed by the correlation ratio (CRs) as in (3-56) can be used to decide about the suitability of transmission lines for network splitting. The transmission lines with a low

correlation between their ends (e.g. below a threshold of 0.25 in normalized values) constitute the set of weak connections between non-coherent areas and are then used as the input of the islanding model.

$$CR_{ij} = \frac{\mathrm{n}\sum_{\mathrm{t}=1}^{\mathrm{n}}[\theta_{\mathrm{i}}(\mathrm{t})\theta_{\mathrm{j}}(\mathrm{t})] - \sum_{\mathrm{t}=1}^{\mathrm{n}}[\theta_{\mathrm{i}}(\mathrm{t})] \times \sum_{\mathrm{t}=1}^{\mathrm{n}}[\theta_{\mathrm{j}}(\mathrm{t})]}{\sqrt{\mathrm{A} \times \mathrm{B}}} \quad (3\text{-}56)$$

where

$$A = \left[n\sum_{t=1}^{n}\left(\theta_i(t)\right)^2 - \left(\sum_{t=1}^{n}\theta_i(t)\right)^2 \right] \quad (3\text{-}57)$$

$$B = \left[n\sum_{t=1}^{n}\left(\theta_j(t)\right)^2 - \left(\sum_{t=1}^{n}\theta_j(t)\right)^2 \right] \quad (3\text{-}58)$$

The CR between each pair of rotor angles or rotor speeds may be considered as the strength or value of their coherency. The coherency value is normalized as a value inside [0, 1] in which the correlation of 1 indicates the full coherency. In other words, the coherency of 1 between two ends of each line means that this line is considered as an internal line and is not suitable for line switching. Therefore, the set of candidate lines may be reduced based on their coherency values. The lines with lower CR are good candidates for network splitting. Since the CR is a relative measure of coherency, its threshold may be selected considering some technical issues.

The following procedure is used to set the threshold value of the CR criterion. The CRs under different faults at different locations are calculated for all transmission lines. The transmission lines with the lowest CR (i.e. the CR between the voltage angles of their two ends) are selected as the candidate lines for network splitting. This procedure continues and stops when a line with the following characteristics is reached.

a) A line that causes the physical disconnection between the coherent group of generators

b) A line that disconnects a load or generator from the rest of the network.

3.7 Implementation of the Method1 for IEEE 118-bus Test System

In this section, the proposed method is applied to the IEEE 118-bus test system. Different scenarios are simulated to show the improvement of the first swing transient stability, as well as the transient stability margin of the created islands using the proposed islanding models. The proposed MINLP and MILP models are solved using standard branch-and-bound (SBB) and CPLEX solvers in GAMS, respectively. For a clear comparison, all the transient stability simulations are performed using the full-scale model of the network in the DIgSILENT transient stability simulator. It is noted that the DIgSILENT software is

Table 3-2: Coherent groups of generators and maximum and minimum values of tolerable electrical powers of generators

Coherent Group	**Gen**	$P_{0_e}^{\text{initial}}$ (MW)	$P_{e\,min}$ (MW)	$P_{e\,max}$ (MW)
1	G10	450	86	**750**
	G31	7	0	**19**
	G12	85	0	**131**
	G25	220	0	**402**
	G26	314	0	**581**
2	G69	516.4	115	**696**
	G46	19	0	**28**
	G49	204	0	**385**
	G59	155	0	**254**
	G61	160	0	**268**
	G65	391	0	**512**
	G66	392	0	**595**
	G54	48	0	**82**
	G80	477	0	**801**
3	G89	607	132	**902**
	G87	4	0	**6.5**
	G103	40	0	**69**
	G111	36	0	**75**
	G100	252	0	**463**

utilized just to verify the transient stability of the obtained islanding strategy and the DIgSILENT package is not a required part of the proposed MIP model. The proposed model was solved using a PC with Intel core i7, 4.2 GHz 7700 CPU, and 32 GB DDR4 RAM. The results of the proposed transient stability-constrained islanding (TSI) models

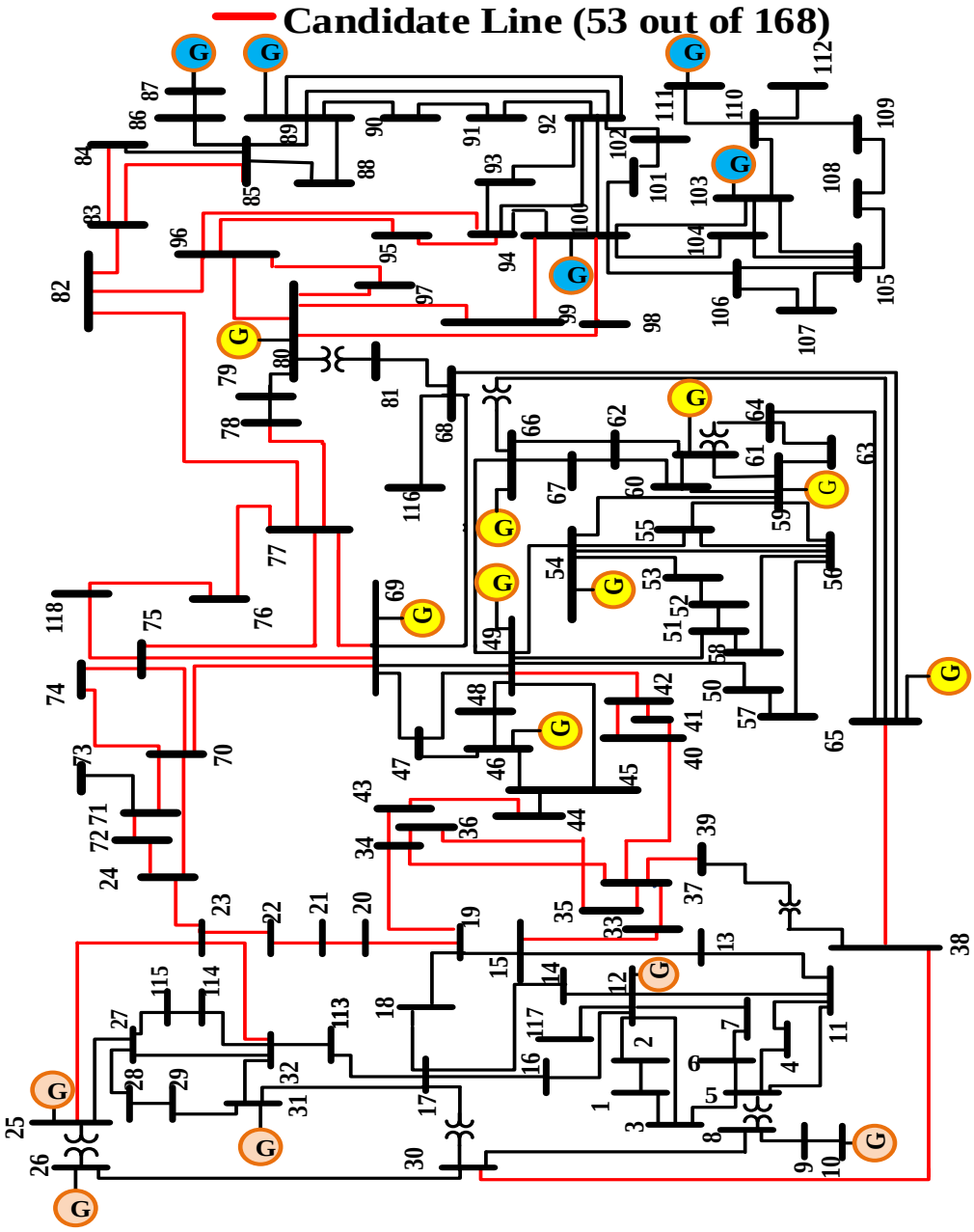

Fig 3-3: Candidate line location in the IEEE 118-bus test system.

are compared with the conventional islanding (CI) model proposed in [31]. Note that the CI model does not consider the transient stability constraint.

3.7.1 Determining the Inputs of the Model

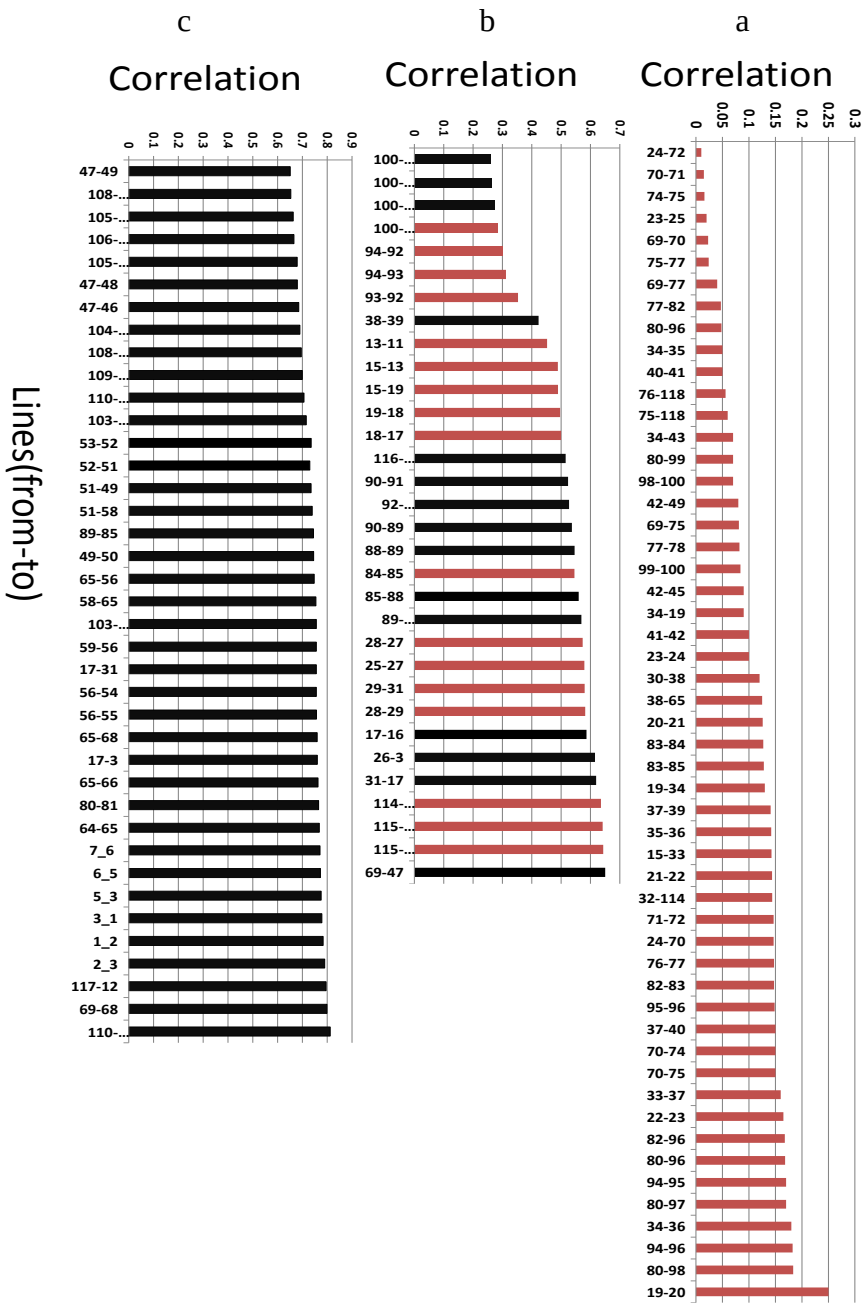

Fig 3-4: *a,b,c)* Average CR values for each line under different faults (lines with black bars are not selectable as splitting lines)

Both MINLP and MILP islanding models require the same inputs. First, the set of coherent groups of generators is determined using the slow coherency technique as proposed in [18]. The results of the coherent groups are reported in Table 3-2. According to the procedure given in section 3.6, the threshold of CR is obtained equal to 0.25 related to the

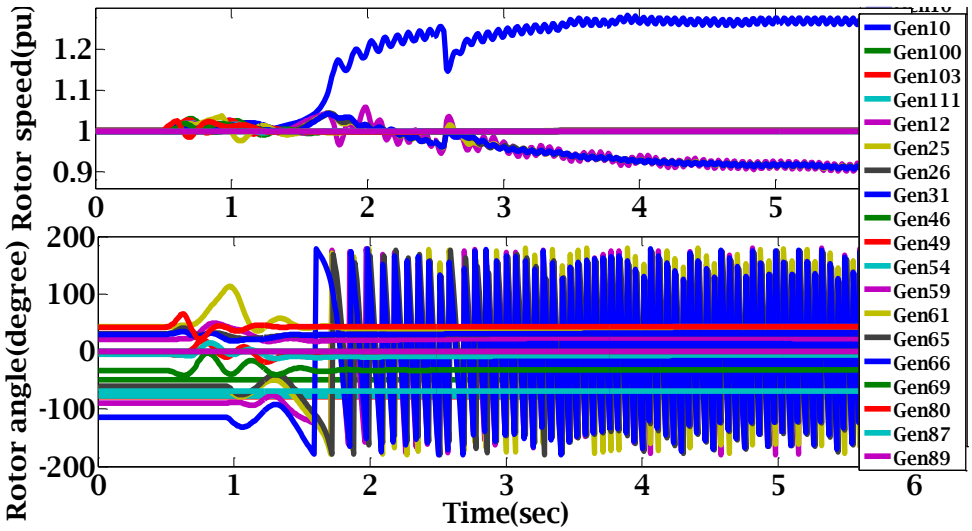

Fig 3-5: Evolutions of rotor speeds and angles during the cascading failure

transmission lines 19-20. The set of candidate lines has been illustrated in Fig 3-3 and Fig 3-4. To verify the efficacy of the proposed procedure, the results have been presented for another set consisting of 85 candidate lines (Fig 3-3-a, Fig 3-3-b and Fig 3-3.c). In this case, from lines 54(i.e. line 100-106) to line 85(i.e. line 69-47) some transmission lines have not violated the rules 1 and 2. Further, the maximum and minimum values of the tolerable electrical powers (i.e., P_{emin} and P_{emax}) to preserve the first swing transient stability of the created islands is obtained from the EEAC. The parameter $P_{0_e}^{\text{initial}}$ denotes the initial normal loading of the generators (i.e., the mechanical input power).

3.7.2 Cascading Scenario

A three-phase short-circuit fault occurs in bus 69 at t=0.5 sec. This fault is cleared at t=0.6 sec. Furthermore, another three-phase short-circuit fault occurs at bus 60 at t=0.73 sec, and is cleared at t=0.93 sec. According to the speed trajectories illustrated in Fig 3-5, four generators became unstable and to stop the propagation of the cascading failure and to avoid an imminent blackout, the controlled islanding must be executed.

3.7.3 Implementation of the Proposed Islanding Models

In this part, the results of the proposed TSI model are compared with the CI model. The results are presented for two sets of the pre-selected lines (i.e., 53 candidate lines with

Table 3-3: Boundaries of the IEEE 118-bus test system using the conventional and the proposed MINLP and MILP islanding models.

Method		Line NO	Splitting lines	Cost/ (MW Shed)	CPU time(sec)
TSI MINLP	Relative Gap(pu)=0	53	23-24, 38-65, 40-37, 77-82, 80-96 80-99 , 98-100, 43-44, 80-97,	1.4870/ (330MW)	4.12
		85	23-24, 43-44, 42-49, 38-65, 80-99 98-100, 80-97, 80-96, 77-82	1.3260/ (315MW)	45.22
	Relative Gap(pu)=0.05	53	23-24, 43-44, 42-49, 38-65, 95-96 98-100, 84-83, 100-99, 94-96, 83-85	1.5925/ (342MW)	3.12
		85			32.15
	Relative Gap(pu)=0.1	53	72-24, 43-34, 42-49, 38-65, 70-24 98-80, 80-97, 80-99, 80-96, 82-77	1.612/ (356MW)	2.34
		85	72-24, 43-34, 42-49, 38-65, 70-24 98-100, 80-97, 100-99, 80-96, 82-77	1.561/ (302MW)	27.74
TSI MILP	Relative Gap(pu)=0	53	23-24, 30-38, 19-34, 33-37, 80-99 80-98, 80-97, 80-96, 77-82	0.36/ (90MW)	0.91
		85			2.56
	Relative Gap(pu)=0.05	53	15-33, 19-34, 23-24, 30-38, 80-99 98-100, 80-97, 80-96, 77-82	0.47/ (113MW)	0.01
		85	19-34, 24-72, 30-38, 33-37, 70-24 77-82, 80-97, 98-100, 99-100, 96-80	0.407/ (97MW)	0.86
	Relative Gap(pu)=0.1	53	23-24, 19-34, 30-38, 33-37 34-19, 80-98, 82-83, 94-96, 95-96	0.7368/ (181MW)	0.01
		85			0.52
CI	Relative Gap(pu)=0	53	30-38, 15-33, 19-34, 23-24, 68-81 69-77, 75-77, 76-77	156MW/ (156MW)	3.01
		85			8.67
	Relative Gap(pu)=0.05	53	65-38, 42-49, 43-34, 23-24, 68-81 79-80, 80-77, 82-77	168MW/ (168MW)	1.56
		85			5.11
	Relative Gap(pu)=0.1	53	15-33, 19-34, 70-24, 30-38, 71-72 77-82, 80-97, 96-80, 98-100, 99-100	263MW/ (263MW)	1.13
		85	15-33, 19-34, 70-24, 65-38, 71-72 37-39, 77-82, 96-97, 96-80, 98-100 99-100	272MW/ (272MW)	3.48

correlation ratio lower than 0.25 and 85 candidate lines with correlation ratio lower than 0.65 according to the procedure given in section 3.6). Table 3-3 gives the sets of splitting lines obtained using the TSI and CI, the cost of the proposed model, and their associated computational times. For each method, the optimal solution(with a relative optimality gap of zero) and two sub-optimal solutions (with a relative optimality gap of 0.05 pu and 0.10 pu, respectively) have been reported.. These results show that the MILP solutions are obtained remarkably fast, compatible with the real-time requirements even without using powerful computing architecture. These scenarios can then be analyzed in detail to reach a

practical islanding solution using a full scale dynamic simulator. Note that without any remedial control actions the total load of the network (i.e., 4242 MW) is lost due to the complete blackout. However, using the TSI–MILP scheme, the network is splitted into three different stable islands and only 90 MW of load is shed (i.e, according to relative Gap=0 as given in Table 3-3), which clearly highlights the benefits of the proposed scheme. Although the optimal solution is obtained using the first set of candidate lines (i.e. 53 candidate lines), however the second set of input lines (i.e. 85 candidate lines) is a conservative selection to verify the efficacy of the proposed model.

3.7.4 First Swing Transient Stability Improvement

In this section, to verify the capability of the proposed method in ensuring the first swing transient stability of islands, both islanding strategies (i.e. the CI and TSI-MILP with zero relative optimality gap) reported in Table 3-3 are simulated. The trajectories of rotor angles resulted by implementing the CI and TSI-MILP schemes are illustrated in Fig 3-6-a and Fig 3-6-b. As shown in Fig 3-6-a, in case of using the CI model, the generator 31 became out-of-step at t=1.4 sec and generators 26, 25, and 12 became unstable at $t \approx$1.85 sec. However as shown in Fig 3-6-b, using the proposed islanding method, all of the generators maintain their transient stability. To justify the superiority of the proposed method compared to the conventional method, the amount of accelerating power and the changes in the equivalent impedance seen at the generator terminals are compared. The resulted accelerating powers are shown in Fig 3-7. Using the TSI-MILP scheme, the absolute amount of the accelerating power of all generators is limited without any considerable abrupt change. Additionally, the changes of the equivalent impedance seen at generator terminals (i.e., changes due to the network splitting) are reported in Table 3-4. According to Fig 3-8, which illustrates the impedance changes for generator G59, parameters D_{CI} and D_{TBI} are defined as follows:

$$D_{CI} = |Z_N - Z_1^{CI}| \quad , \quad D_{TSI} = |Z_N - Z_1^{TSI}| \tag{3-59}$$

where, Z_N is the equivalent impedance before the fault occurrence, Z_1^{CI} and Z_2^{TSI} refer to the first sample of equivalent impedance after executing the CI and TSI strategies, respectively. According to Table 3-4, the generators that experiencing out-of-step

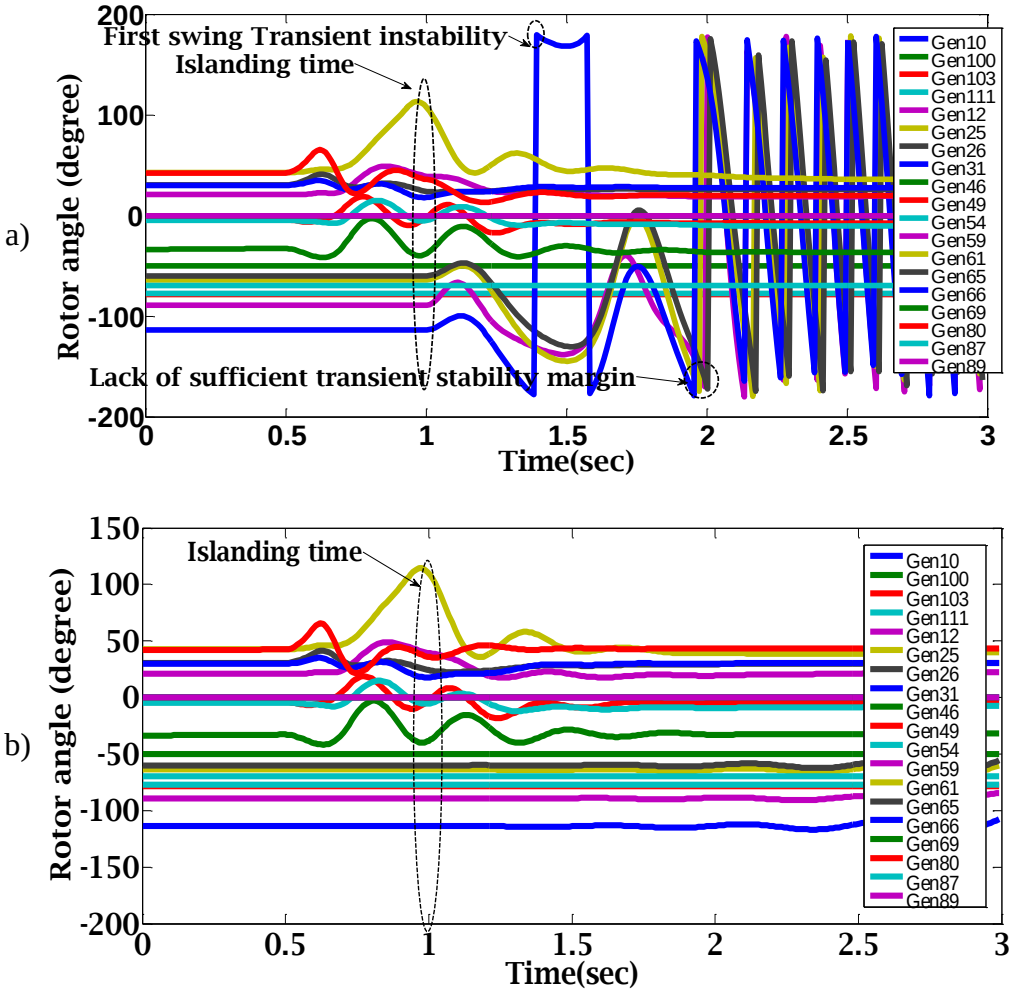

Fig 3-6: Rotor angle trajectories of the IEEE 118-bus system **a)** using the CI scheme **b)** using TSI scheme

condition using the conventional method (i.e., G12, G25, G26, and G31), will have significant changes in equivalent impedance seen at their terminals.

3.7.5 Improvement of Transient Stability Margin

In this section, the effectiveness of the TSI-MILP in enhancing the transient stability margin is investigated by considering the CCT as the transient stability criteria. The values of CCTs are presented in Table 3-5. The CCT is calculated using a 3-phases short circuit fault with duration beginning from 0.05sec toward the point of instability in steps of 0.001sec. Note that using the CI strategy, the four generators became unstable. In this

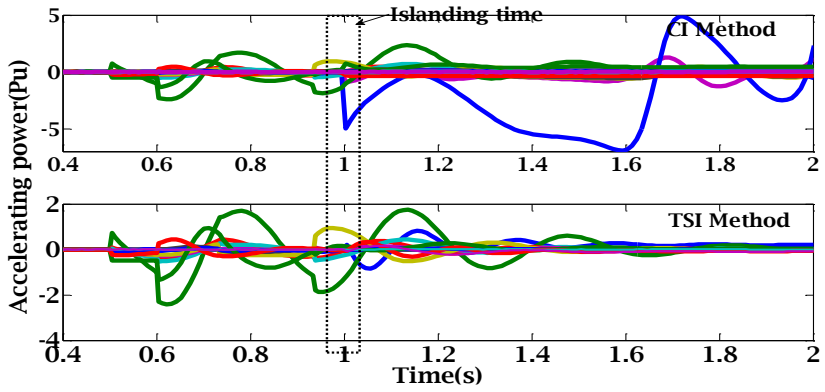

Fig 3-7: Accelerating power trajectories of the IEEE 118-bus test system using the CI and TSI schemes.

b)

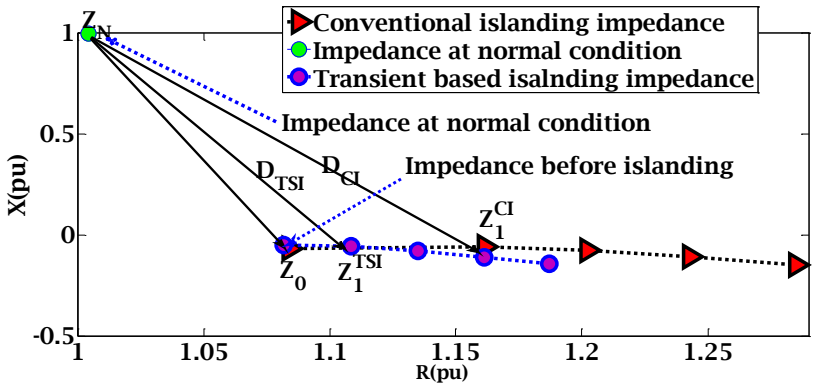

Fig 3-8: Resulted changes in the equivalent impedance using both the islanding methods for generator G59

situation, the transient stability is not preserved in resulted islands. Therefore, the CCT of

Table 3-4: Comparison between the D_{CI} and D_{TSI} parameters for the generators of the IEEE 118-bus system.

Gen NO	D_{CI}	$D_{TSI}(MINLP)$ $/D_{TSI}(MILP)$	Gen NO	D_{CI}	$D_{TSI}(MINLP)$ $/D_{TSI}(MILP)$
10	0.992	0.350/0.110	54	1.265	1.284/1.251
100	0.000	0.000/0.000	59	1.063	1.056/1.054
103	0.000	0.000/0.000	61	5.612	5.693/4.564
111	0.000	0.000/0.000	65	1.986	1.979/1.942
12	1.864	0.000/0.001	66	18.03	18.00/18.00
25	1.362	0.000/0.000	69	2.652	1.650/1.456
26	1.503	0.000/0.001	80	1.833	0.359/0.2954
31	10.00	0.000/0.000	87	0.000	0.000/0.000
46	2.102	2.336/2.004	89	0.201	0.071/0.059
49	0.361	0.358/0.357			

Table 3-5: CCTs of the islanded system using the CI and TSI schemes.

Gen	CCT(sec) CI	$\Delta \mathbf{P}_{\mathbf{ei}}^{+} - \Delta \mathbf{P}_{\mathbf{ei}}^{-}$ TSI		CCT(sec): TSI		$\Delta \boldsymbol{P}_{\boldsymbol{a}}^{\boldsymbol{R}}$
		MINLP	MILP	MINLP	MILP	
G10	0.117	273-0	0-85	0.136	0.146	**0.498**
G31	0.334	0-0	0-5	0.311	0.317	**12**
G12	0.650	0-0	0-0	0.471	0.436	**18**
G25	0.183	0-0	0-0	0.193	0.199	**42.5**
G26	0.202	0-0	0-0	0.212	0.213	**109.9**
G69	0.113	0-76.2	0-0	0.202	0.208	**173**
G46	0.452	0-0	0-0	0.542	0.545	**3.49**
G49	0.216	0-4.8	0-0	0.254	0.255	**20.39**
G59	0.242	0-0	0-0	0.283	0.298	**8.12**
G61	0.207	0-0	0-0	0.259	0.289	**81**
G65	0.221	0-76.2	0-0	0.268	0.274	**128**
G66	0.169	0-76.4	0-0	0.231	0.236	**198**
G54	0.334	0-0	0-0	0.410	0.421	**15**
G80	0.160	0-94.4	34-0	0.221	0.227	**53**
G89	0.122	60-0	56-0	0.139	0.146	**265.73**
G87(R)	----	0-0	0-0	----	----	
G103	0.433	0-0	0-0	0.570	0.563	**26**
G111	0.358	0-0	0-0	0.400	0.393	**20**
G100	0.141	0-0	0-0	0.198	0.208	**180**

the resulting islands using the CI method could not be calculated at steady state conditions. To present a fair comparison, let assume that the CI strategy would preserve transient stability using emergency control actions. It is noted that such actions are not the outputs of the CI method. The CCTs of generators in the islands created by the CI and TSI (MINLP and MILP) models are compared in Table 3-5. According to Table 3-5, the net sum of increase and decrease of electrical powers (i.e, $\Delta P_{ei}^{+} - \Delta P_{ei}^{-}$) is equal to 5 MW and zero for MINLP and MILP models, respectively. The non-zero summation of net changes in electrical powers is equal to the change of active power loss in the interconnected and the split network. It can be observed that the proposed method leads to a significant increase of all CCTs of critical generators, outperforming CI method results.

b)

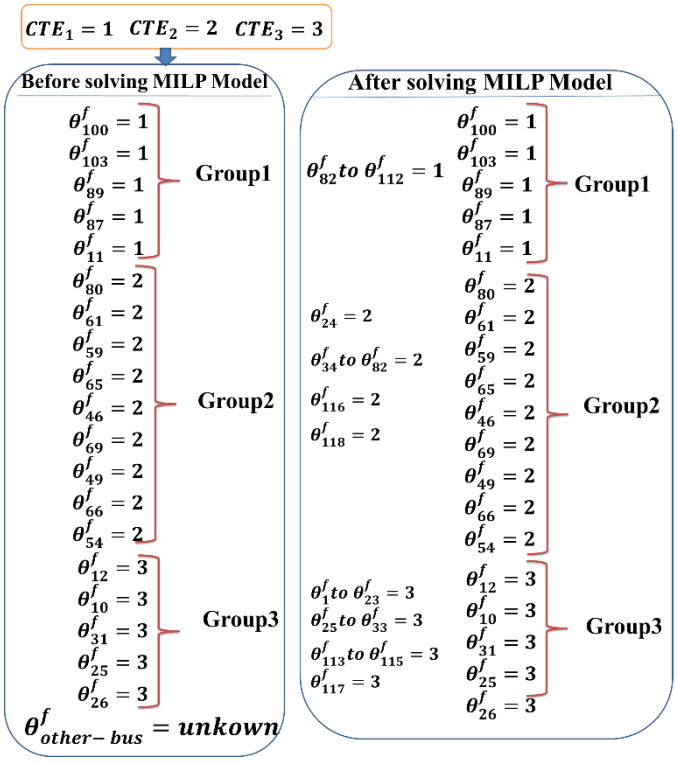

Fig 3-9: Fictitious voltage angles for generator buses and other buses to check the connectivity and dis-connectivity constraints in MILP model.

3.7.6 Connectivity and Dis-connectivity Check

The value of fictitious voltage angles in artificial power flow proposed for checking the connectivity and dis-connectivity constraints, before and after solving the MILP model is shown in Fig 3-9. These values are not unique and the connectivity of coherent generators and dis-connectivity of non-coherent generators can be fulfilled provided that the conditions given in (3-36)-(3-38) are satisfied. Here, the fictitious voltage angles are expressed in radian. As shown in Fig 3-9, the fictitious angle assigned to generators buses is fixed before MILP solving, however the fictitious angle of other buses (i.e. load buses) is determined by solving the MILP model. For example if a give load point (i.e. bus 23) belongs to the island 3, then the fictitious angle of that bus is obtained as $\theta^f_{23} = 3$.

3.8 Discussion and Analysis

The main advantages, disadvantages and novelty of Method1 are discussed as follows.

3.8.1 Novelties of Method1

The main contributions of this study are the development of two transiently-stability constrained controlled islanding optimization models: a benchmark mixed-integer nonlinear program (MINLP) model subject to full AC power flow constraints and a computationally efficient MILP model. The extended equal area criterion (EEAC) is used in the optimization models to guarantee the first swing transient stability of the synchronous machines, after the controlled line switching. The main advantages of Method1 include the preservation of transient stability using acceptable computational times. Other strengths of the proposed models are summarized as follows:

1) Enhancing the transient stability on each island by minimizing the accelerating and decelerating powers caused by network splitting.
2) Simultaneous improvement of the transient stability and minimizing load shedding or power imbalance.
3) Reducing the number of candidate splitting lines based on the coherency criteria and its suitability for large scale test systems.
4) Optimality of the obtained strategy using the approximated MIP model.

3.8.2 Disadvantages of Method-1:

The main disadvantages of the proposed controlled islanding scheme (Method1) are summarized as follows.

1) The EEAC method cannot estimate transient stability in case of the fault consequences is extremely propagated to other generators.
2) The enhancement of transient stability is not considered as a constraint. Indeed the transient stability is promoted indirectly.
3) The set of coherent groups of generators is determined offline.

3.9 The motivation for Developing the Next Method

. To remove the disadvantages of this method, a more comprehensive method is required to enhance the transient stability with a minimum power imbalance. Indeed the EEAC-based transient stability analysis can be replaced with a powerful transient stability assessment procedure. To this end, the transient energy based method can be used to design a sophisticated transient stability constrained islanding plan. .

3.10 Conclusion of the Chapter

In this chapter two controlled islanding optimization models including an MINLP for benchmarking purposes and a computationally efficient MILP, were proposed. In addition to satisfying the steady state operational and topological constraints, the proposed models are able to ensure and improve the first swing transient stability of the resulted islands. The numerical experiments for the IEEE 118-bus test system have shown that the computational effort of the MILP model is compatible with the real-time requirements. Furthermore, the performance of the proposed transient stability constrained MILP-based strategy has been validated by the full scale time dynamic simulation. The objective function used in this study determines the splitting points such that the generator's active

power remains close to its pre-fault normal conditions. Moreover, the proposed method minimizes the resulted accelerating or decelerating powers by minimizing the proposed objective function (i.e., the normalized deviations of electrical power at the generator terminals due to network splitting).

The computational complexity of the MILP model, which also takes advantage of the off-line identification of a subset of critical candidate lines for islanding, is suitable for the on-line applications. In order to promote the transient stability assessment of the islanding strategy, the energy-based controlled islanding method was identified for further improvement.

CHAPTER 4. REAL TIME CONTROLLED ISLANDING CONSIDERING CRITICAL ISALNDS

4.1 Introduction

In this chapter transient stability constrained controlled islanding (TSC-CI) model against cascading events in power systems is proposed. Using the wide area measurements, the proposed islanding algorithm considers the actual dynamic conditions of the power system. Since the main concern, right after the execution of controlled network splitting, is the transient stability of synchronous machines, a transient energy function is utilized for the proper network partitioning. The proposed transient stability criterion is expressed as a function of the transfer impedance between each pair of generators in the resulted islands. The transfer impedance between each pair of coherent generators determines the direction of network splitting for transient stability improvement. A multi-objective function is then introduced to provide transient stability with the least possible power imbalance over the created islands considering the operational and topological constraints. Based on the wide-area measurements, a proper weighting procedure is utilized to prioritize the critical islands, avoiding the unnecessary power imbalance in favor of transient stability improvement. The proposed TSC-CI model is formulated as a mixed integer linear programming (MILP) multi-objective model and is solved using CPLEX in GAMS. The obtained results are compared with the conventional islanding scheme using the IEEE 118-bus system. The proposed TSC-CI in this chapter is called Method-2 throughout the thesis.

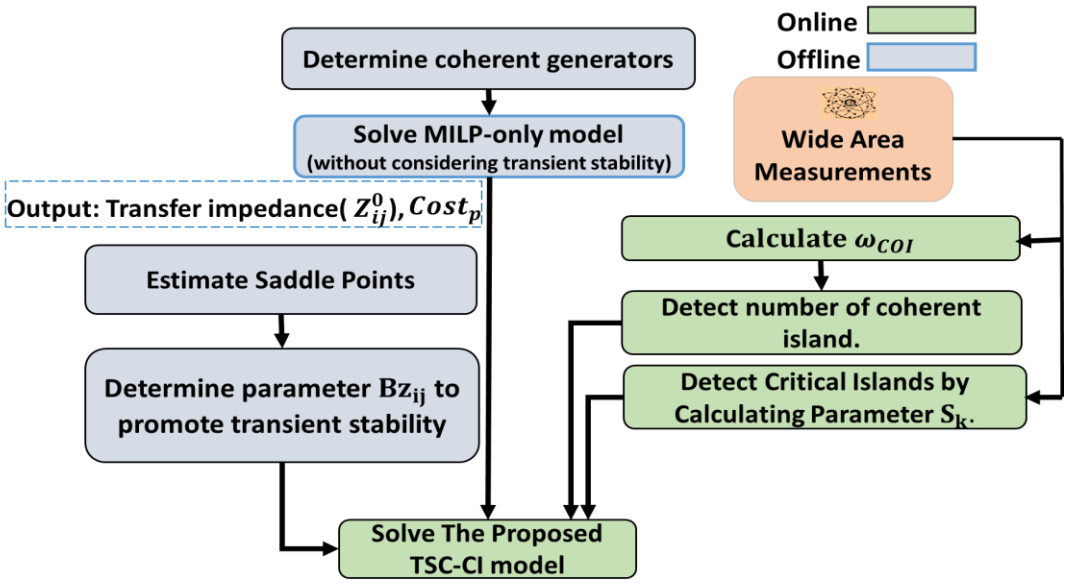

Fig. 4-1. Overall structure of the proposed TSC-CI model

4.2 Overall Structure of the Proposed TSC-CI Method

Fig. 4-1 shows the overall structure of the proposed TSC-CI model. The proposed islanding plan consists of two offline and online parts. In the offline part, the coherent generators are recognized and the MIP-only model is executed. In the online part, the rotor angles of generators are received by the wide area measurement system to update the set of coherent generators. Indeed, the set of coherent generators may change under different operational conditions. Wide area measurements are used to prioritize the critical islands that struggle with the transient instability problem. The output of the MIP-only model is used as the input of the TSC-CI model. Finally, the proposed TSC-CI model is solved. According to the flowchart given in Fig. 4-1, the MIP-only model refers to the steady state model of the controlled islanding without considering the transient stability constraint. The TSC-CI model refers to the optimization model by considering the transient stability constraint.

4.3 Derivation of Energy Function Based Criterion

The transient stability assessment of the constrained controlled islanding scheme is introduced in this section. To perfect the proposed islanding scheme, two issues including

the formulation of the transient energy function and estimation of saddle or Control UEPs(CUEPs) are introduced as follows.

4.3.1 The Proposed Transient Energy Function

Based on the rotor angles of synchronous generators a transient energy function is developed to evaluate the transient stability of the splitting strategy found in the first stage. It is assumed that the values of rotor angles before and right after the controlled islanding execution are the same (i.e. no abrupt changes in rotor angles). In this regard, the developed Transient Energy Function(TEF) is evaluated individually for each resulted island based on the rotor angles measured by the PMUs. The proposed TEF needs just one sample of rotor angles before the controlled islanding. To introduce the proposed TEF, the swing equation of each machine in a system with n_g synchronous machines are supposed to be as follows[46].

$$M_i\ddot{\delta}_i = P_{mi} - \frac{E_i^2}{Z_{ii}}\cos(\emptyset_{ii}) + \sum_{\substack{j=1 \\ j\neq i}}^{n_g} \frac{E_i E_j}{Z_{ij}}\cos(\delta_{ij} + \emptyset_{ij}) \tag{4-1}$$

Based on[48, 49], the relative swing equations for two synchronous machines is as follows:

$$\begin{aligned}
&[M_j(M_i\ddot{\delta}_i) - M_i(M_j\ddot{\delta}_j)]\dot{\delta}_{ij} = M_iM_j\ddot{\delta}_{ij}\,\dot{\delta}_{ij} = \\
&= M_j\left[P_{mi} - \frac{E_i^2}{Z_{ii}}\cos(\emptyset_{ii}) + \sum_{\substack{j=1 \\ j\neq j}}^{n_g} \frac{E_iE_j}{Z_{ij}}\cos\left(\delta_{ij} + \emptyset_{ij}\right)\right]\dot{\delta}_{ij} \\
&\quad - M_i\left[P_{mj} - \frac{E_j^2}{Z_{jj}}\cos\left(\emptyset_{jj}\right) + \sum_{\substack{i=1 \\ i\neq j}}^{n_g} \frac{E_jE_i}{Z_{ji}}\cos\left(\delta_{ji} + \emptyset_{ji}\right)\right]\dot{\delta}_{ij}
\end{aligned} \tag{4-2}$$

To extract a transient energy function, and for the sake of simplicity, the relative swing equations for a system with three synchronous machines are extracted as follows:

$$
\begin{aligned}
&M_1M_2\ddot{\delta}_{12}\dot{\delta}_{12} + M_1M_3\ddot{\delta}_{13}\dot{\delta}_{13} + M_2M_3\ddot{\delta}_{23}\dot{\delta}_{23} = \\
&+M_3\frac{E_1E_2}{Z_{12}}\left[\cos(\delta_{12}+\emptyset_{12})\,\dot{\delta}_{13} - \cos(\delta_{12}-\emptyset_{12})\,\dot{\delta}_{23}\right] \\
&+M_2\frac{E_1E_3}{Z_{13}}\left[\cos(\delta_{13}+\emptyset_{13})\,\dot{\delta}_{12} + \cos(\delta_{13}-\emptyset_{13})\,\dot{\delta}_{23}\right] \\
&+M_1\frac{E_2E_3}{Z_{23}}\left[\cos(\delta_{23}-\emptyset_{23})\,\dot{\delta}_{13} - \cos(\theta_{23}+\emptyset_{23})\,\dot{\delta}_{12}\right] \\
&+\left[M_2\frac{E_1E_2}{Z_{12}}\cos(\delta_{12}+\emptyset_{12}) + M_1\frac{E_1E_2}{Z_{12}}\cos(\delta_{12}-\emptyset_{12})\right]\dot{\delta}_{12} \\
&+\left[M_3\frac{E_2E_3}{Z_{23}}\cos(\delta_{23}+\emptyset_{23}) + M_2\frac{E_2E_3}{Z_{23}}\cos(\delta_{23}-\emptyset_{23})\right]\dot{\delta}_{23} \\
&+\left[M_3\frac{E_1E_3}{Z_{13}}\cos(\delta_{13}+\emptyset_{13}) + M_1\frac{E_1E_3}{Z_{13}}\cos(\delta_{13}-\emptyset_{13})\right]\dot{\delta}_{13} \\
&+\{M_2[P_{m1} - \frac{E_1^2}{Z_{11}}\cos(\emptyset_{11})] - M_1[P_{m2} - \frac{E_2^2}{Z_{22}}\cos(\emptyset_{22})]\}\dot{\delta}_{12} \\
&+\{M_3[P_{m1} - \frac{E_1^2}{Z_{11}}\cos(\emptyset_{11})] - M_1[P_{m3} - \frac{E_3^2}{Z_{33}}\cos(\emptyset_{33})]\}\dot{\delta}_{13} \\
&+\{M_3[P_{m2} - \frac{E_2^2}{Z_{22}}\cos(\emptyset_{22})] - M_2[P_{m3} - \frac{E_3^2}{Z_{33}}\cos(\emptyset_{33})]\}\,\dot{\delta}_{23}
\end{aligned}
\tag{4-3}
$$

To derive a suitable TEF it is required to integrate (4-3), over the interval $[\delta^s, \delta^R]$. However the first three terms located in the right hand side of (4-3) cannot be integrated due to the existence of dependent variables in each term (e.g. δ_{12} and $\dot{\delta}_{13}$ in $\cos(\delta_{12}+\emptyset_{12})\,\dot{\delta}_{13}$). Assuming a lossless network, each of the first three terms may be rewritten as follows:

$$
M_3\frac{E_1E_2}{Z_{12}}\sin(\delta_{12})\left[-\dot{\delta}_{13}+\dot{\delta}_{23}\right] = M_3\frac{E_1E_2}{Z_{12}}\sin(\delta_{12})[-\dot{\delta}_{12}] \tag{4-4}
$$

Therefore, the indefinite integral of (4-3) is obtained as follows:

$$
\begin{aligned}
&\frac{M_1M_2\ddot{\delta}_{12}{}^2}{2} + \frac{M_1M_3\ddot{\delta}_{13}{}^2}{2} + \frac{M_2M_3\ddot{\delta}_{23}{}^2}{2} = \\
&[\mathrm{M_2+M_1+M_3}]\{\frac{\mathrm{E_1E_2}}{\mathrm{Z_{12}}}\cos(\delta_{12}) + \frac{\mathrm{E_2E_3}}{\mathrm{Z_{23}}}\cos(\delta_{23})
\end{aligned}
\tag{4-5}
$$

$$+\frac{E_1 E_3}{Z_{13}}\cos(\delta_{13})\}T_{m_{12}}(\delta_{12}) + T_{m_{13}}(\delta_{23}) + T_{m_{23}}(\delta_{13})$$

where

$$T_{m_{ij}} = M_j[P_{mi}] - M_i[P_{mj}] \tag{4-6}$$

Now, to extend the TEF formulation to a n-machine system the expression given in (4-6), is integrated over the interval of $[\delta_s, \delta_R]$ as follows:

$$\frac{1}{\sum_{i=1}^{n} M_i}\sum_{i=1}^{n-1}\sum_{j=i+1}^{n}\frac{M_i M_j {\omega_{ij}^R}^2}{2} = \sum_{i=1}^{n_g-1}\sum_{j=i+1}^{n_g}\frac{E_i E_j}{Z_{ij}}[\cos(\delta_{ij}^R) - \cos(\delta_{ij}^s)] + \sum_{i=1}^{n_g-1}\sum_{j=i+1}^{n_g} P_{m_{ij}}(\delta_{ij}^R - \delta_{ij}^s) \tag{4-7}$$

It is noted that $\ddot{\delta}_{ij}$ at the saddle point (The Saddle point is the first UEP whose stable manifold has a nonempty intersection with the fault - on trajectory at the exit point) is zero. According to the general formulation of the potential energy given in (4-7) and the kinetic energy for a system consisting of n-machines are determined as follows:

$$En_p = \sum_{i=1}^{n_g-1}\sum_{j=i+1}^{n_g}\frac{E_i E_j}{Z_{ij}}[\cos(\delta_{ij}^R) - \cos(\delta_{ij}^s)] + \sum_{i=1}^{n_g-1}\sum_{j=i+1}^{n_g} T_{m_{ij}}(\delta_{ij}^R - \delta_{ij}^s) \tag{4-8}$$

$$En_k = \frac{1}{\sum_{i=1}^{n} M_i}\sum_{i=1}^{n_g-1}\sum_{j=i+1}^{n_g}\frac{M_i M_j \omega_{R\,ij}^2}{2} \tag{4-9}$$

4.3.2 Equilibrium and saddle points

Determination of the saddle point is a prerequisite in transient stability assessment using the TEF approach. Assuming a power system with n generators, the swing equation of the i^{th} generator can be represented by (4-10).

$$M_i\ddot{\delta}_i = P_{mi} - \frac{E_i^2}{Z_{ii}}\cos(\emptyset_{ii}) + \sum_{j=1,j\neq i}^{N_g^K} \frac{E_i E_j}{Z_{ij}}\cos(\delta_{ij} + \emptyset_{ij}) \quad (4\text{-}10)$$

The following steps are taken to estimate the saddle point of the power system at an operating condition[46].

Step 1. Find the SEP (i.e. δ_{ij}^{sep}) using the steady state power flow model.

Step 2. Find the set of equilibrium points (i.e. δ_{ij}^{eq}) using (4-11).

$$P_{mi} - \sum_{j=1,j\neq i}^{N_g^K} \frac{E_i E_j}{Z_{ij}} sin(\delta_{ij}) = 0 \qquad i \in \mathcal{M}_k^{\mathrm{g}} \quad (4\text{-}11)$$

Step 3. Identify those equilibrium points whose unstable manifolds contain trajectories approaching the SEP obtained in step 1.

All three steps could be integrated with the following optimization model:

$$\min\{E_p(E, \delta_{ij}^{sep}) - E_p(E, \delta_{ij}^{s})\} \quad (4\text{-}12)$$

subject to

$$P_{mi} - \sum_{j=1,j\neq i}^{N_g^K} \frac{E_i E_j}{Z_{ij}} sin(\delta_{ij}) = 0 \qquad i \in \mathcal{M}_k^{\mathrm{g}} \quad (4\text{-}13)$$

The aim of the objective function given in (4-12) is to minimize the difference between the potential energy at δ_{ij}^{sep} and δ_{ij}^{s}. The potential energy is calculated using (4-9). The mutual torque between two given generators is defined as follows:

$$P_{m_{ij}} = M_j[P_{mi} - \frac{\mathrm{V_i^2}}{\mathrm{Z_{ii}}}\cos\phi_{ii}] - M_i[P_{mj}\frac{\mathrm{V_i^2}}{\mathrm{Z_{ii}}}\cos\phi_{jj}] \quad (4\text{-}14)$$

Assuming a small positive or negative amount of $P_{m_{ij}}$, the saddle point is shown to be as $\delta_{ij}^{s} \approx 0$, otherwise the saddle point is approximated as $\delta_{ij}^{s} \approx \pi$.

4.3.3 Transient Stability Criterion

The transient stability margin is highly affected by the topological network changes such as transmission switching. As the network splitting is the main action in any controlled islanding scheme, here a criterion is proposed to improve the transient stability using the transmission switching. Based on the energy function method, the transient stability criterion can be expressed as given in (3-10). The more the criterion is negative, the more

the system is stable[46].

$$\Delta E = E_k - E_p \tag{4-15}$$

According to (4-15), since the kinetic energy is not affected by changing islanding boundaries, the transient stability of each island can be improved by increasing the potential energy of that island at the time of controlled islanding. Unlike the kinetic energy, the potential energy of the system changes by network splitting, immediately. In order to investigate the change of potential energy caused by the network splitting, variations of the saddle point are analyzed, first. Assume that the swing equation of a synchronous machine in a multi-machine power system is expressed as follows.

$$M_i\ddot{\delta}_i = P_{mi} - \frac{E_i^2}{Z_{ii}}\cos(\emptyset_{ii}) \sum_{j=1, j\neq i}^{N_g^K} \frac{E_i E_j}{Z_{ij}}\cos(\delta_{ij} + \emptyset_{ij}) \tag{4-16}$$

where, δ_{ij} is equal to $\delta_i - \delta_j$. The saddle points of the system represented by (4-16), are determined separately for each synchronous machine in each island as follows:

$$P_{mi} - \sum_{j=1, j\neq i}^{N_g^K} \frac{E_i E_j}{Z_{ij}} sin(\delta_{ij}) = 0 \tag{4-17}$$

For each island, the saddle points (i.e. δ_{ij}^s) are determined independently from other islands. Due to the network splitting, the equilibrium points of the resulted islands are changed. The new saddle points can be approximated according to (4-18) and (4-19). Indeed, the transfer impedance and the rotor angle difference between a given pair of generators are changed by network splitting from Z_{ij} to $\beta_{ij}Z_{ij}$ and δ_{ij}^{s1} to δ_{ij}^{s2}, respectively.

$$\frac{E_i E_j}{Z_{ij}} sin(\delta_{ij}^{s1}) = \frac{E_i E_j}{\beta_{ij} Z_{ij}} sin(\delta_{ij}^{s2}) \tag{4-18}$$

$$\beta_{ij} sin(\delta_{ij}^{s\,1}) = sin(\delta_{ij}^{s\,2}) \tag{4-19}$$

According to [48], the saddle point of the system occurs near the points of ($\delta_{ij}^{s1} \approx 0$) or ($\delta_{ij}^{s1} \approx \pi$). Therefore, the approximations given in (4-18)-(4-19), are simplified as follows:

$$\delta_{ij}^{s\,2} \approx \beta_{ij}\delta_{ij}^{s\,1} \qquad if \quad \delta_{ij}^{s1} \approx 0 \tag{4-20}$$

$$\delta_{ij}^{s\,2} - \pi \approx \beta_{ij}(\delta_{ij}^{s\,1} - \pi) \quad if \quad \delta_{ij}^{s1} \approx \pi \tag{4-21}$$

Now, based on (4-20)- (4-21), the change of potential energy, due to network splitting, is obtained as follows:

$$\Delta E_P = \frac{E_i E_j}{\beta_{ij} Z_{ij}}[cos(\delta_{ij}) - cos(\delta_{ij}^{s\,2})] - \frac{E_i E_j}{Z_{ij}} \times [cos(\delta_{ij}) - cos(\delta_{ij}^{s\,1})] - P_{m_{ij}}(\delta_{ij}^{s\,2}) + P_{m_{ij}}(\delta_{ij}^{s\,1}) \tag{4-22}$$

Finally, based on the location of the saddle point, the potential energy deviations are approximated as given in (4-23).

$$\begin{cases} \Delta E_{P_{ij}} \approx \dfrac{E_i E_j}{Z_{ij}}[cos(\delta_{ij}) - 1]\left(\dfrac{1}{\beta_{ij}} - 1\right) & if\ \delta_{ij}^{s\,1} \approx 0 \\ \Delta E_{P_{ij}} \approx \dfrac{E_i E_j}{Z_{ij}}[cos(\delta_{ij}) + 1]\left(\dfrac{1}{\beta_{ij}} - 1\right) & if\ \delta_{ij}^{s\,1} \approx \pi \end{cases} \tag{4-23}$$

According to (4-23), the network must be partitioned in a direction where the positive changes of potential energy (i.e. $\Delta E_P \geq 0$) is achieved. To this end, the direction of network splitting (i.e. the change of transfer impedance) is defined as follows:

$$\begin{cases} \Delta Z_{ij} \geq 0 \quad or \quad \beta_{ij} > 1 & if\ \delta_{ij}^{s\,1} \approx 0 \\ \Delta Z_{ij} \leq 0 \quad or \quad \beta_{ij} < 1 & if\ \delta_{ij}^{s\,1} \approx \pi \end{cases} \tag{4-24}$$

According to (13), if the saddle point is at $\delta_{ij}^{s1} \approx \pi$, the transfer impedance between the generator pair of ij must be decreased. Also, for the saddle point of $\delta_{ij}^{s1} \approx 0$, the related transfer impedance must be increased. In other words, in order to improve the transient stability of the resulted islands, the direction of network splitting should be selected based on (4-24)

4.3.4 Estimation of the Saddle Point

Determination of the saddle point is a prerequisite in transient stability assessment using the TEF approach. As the exact determination of the saddle point is challenging, the previously proposed methods make an approximation of saddle points. In this part, the

saddle point is estimated based on the method proposed in [48]. Assuming a lossless system, the mutual torque between two given generators is defined as follows:

$$P_{m_{ij}} = M_j[P_{mi} - \frac{V_i^2}{Z_{ii}} cos\,\phi_{ii}] - M_i[P_{mj}\frac{V_i^2}{Z_{ii}} cos\,\phi_{jj}] \quad (4\text{-}25)$$

Assuming a small positive or negative amount of $P_{m_{ij}}$, the saddle point is then selected as $\delta_{ij}^{s\,1} \approx 0$, otherwise the saddle point is approximated as $\delta_{ij}^{s\,1} \approx \pi$. This has been verified in [48] and is validated in our simulation section.

4.4 Introducing the TSA Method Using the Energy Function

The nonlinear and linear optimization models of the proposed TSC-CI algorithm including the objective function and constraints are presented below.

4.4.1 Multi-Objective Function and Weighting Procedure

The main goal of any controlled islanding scheme is to minimize the power imbalance in the resulted islands. Any controlled islanding plan must be able to assure the transient stability with the least possible power imbalance. To this end, the objective function given in (4-26) is introduced.

$$cost_p = \sum_{i=1}^{N_g} (\Delta P_{ei}^{+} + \Delta P_{ei}^{-}) \quad (4\text{-}26)$$

According to (4-26), by minimizing the deviation of the electric power of generators, the resulted power imbalance in each island is minimized. Also, based on the transient stability criterion proposed in Section 4.3.3, the objective function given in (4-27) is defined. The minimization of (4-27), will increase the potential energy which in turn promote transient stability of the resulted islands according to the criterion given in (4-24):

$$cost_S = \sum_{i\in\mathcal{M}_k^{\mathrm{g}}} \sum_{j\in\mathcal{M}_k^{\mathrm{g}}} (\Delta Z_{ij} \times Bz_{ij}) \quad (4\text{-}27)$$

where, the variable ΔZ_{ij} and the parameter Bz_{ij} are defined in (4-28) and (4-29), respectively:

$$\Delta Z_{ij} = Z_{ij}^{t} - Z_{ij}^{1} \tag{4-28}$$

$$\begin{cases} Bz_{ij} = -1 & if\ \delta_{ij}^{s\,1} \approx 0 \\ Bz_{ij} = +1 & if\ \delta_{ij}^{s\,1} \approx \pi \end{cases} \tag{4-29}$$

Parameter Z_{ij}^{1} is determined under the splitting strategy obtained by the MILP-only model. To prioritize the islands that struggle with the transient instability problem, the objective function given in (4-27) is modified as follows:

$$cost_s = \sum_{k=1}^{N_k} [S_k \sum_{i \in \mathcal{M}_k} \sum_{j \in \mathcal{M}_k} (\Delta Z_{ij} \times Bz_{ij})] \tag{4-30}$$

where, parameter S_k denotes the weight of each island based on the angle separation and is defined as follows:

$$S_k = \frac{1}{(\mathrm{N}_k^{\mathrm{g}} - 1)\mathrm{N}_k^{\mathrm{g}}} \sum_{i \in \mathcal{M}_k^{\mathrm{g}}} \sum_{j \in \mathcal{M}_k^{\mathrm{g}}} |\delta_i - \delta_j| \tag{4-31}$$

According to (4-31), island *k* with undesired transient stability conditions has more rotor angle differences among its generators and hence the parameter S_k gets a larger value for that island. Therefore, the islands with the transient instability problem get higher priority in the multi-objective function. This parameter is calculated right before the islanding time. Finally, the proposed multi-objective function is defined as follows:

$$\begin{aligned} cost_T = & \sum_{i=1}^{N_g} (\Delta P_{ei}^{+} + \Delta P_{ei}^{-}) \\ & + w_1 \sum_{k=1}^{N_k} S_k \sum_{j \in \mathcal{M}_k^{\mathrm{g}}} \sum_{j \in \mathcal{M}_k^{\mathrm{g}}} (\Delta Z_{ij} \times Bz_{ij}) \end{aligned} \tag{4-32}$$

It is required to weight both parts of the multi-objective function, properly. Here, an approach is proposed to make a trade-off between the active power imbalance amount and the transient stability criterion. The first part of the multi-objective function given in (4-32) tries to achieve the minimum power imbalance in the resulted islands. The second part of the objective function is devoted to the transient stability improvement of the resulted islands. Based on the proposed objective function, the desired solution is a controlled

islanding strategy that creates the transient stable islands with the least possible power imbalance. The maximum value of $cost_s$ (i.e. the function given in (4-30)) is zero (i.e. $\Delta Z_{ij} = 0$). The MIP-only model of the controlled islanding with the single objective of $cost_p$ is solved. This MIP-only model gives the least possible amount of power imbalance named $cost_p^{min}$. The multi-objective function of TSC-CI model given in (4-32) is solved and the maximum value of power imbalance is now enforced at a user-defined value (e.g. $(1+\varepsilon) \times cost_p^{min}$ as given in (4-33)). According to (4-33), the multi-objective function is allowed to preserve the transient stability of the resulted islands with a maximum ε % additional power imbalance. It is noted that the TSC-CI model tries to find the transient-stable islands under the minimum amount of ε. Since the constraint given in (4-33) adjusts the maximum value of additional power imbalance, it is required to set the weighting factor of w_1 in (4-32) at an arbitrarily large number (e.g. 10^5).

$$\sum_{i=1}^{N_g} (\Delta P_{ei}^{+} + \Delta P_{ei}^{-}) \leq (1+\varepsilon) \times cost_p^{min} \qquad (4\text{-}33)$$

4.4.2 Constraints

Different constraints, including power balance, operational limits (e.g. line flows, voltage magnitudes and reactive power generation limits), topological constraints (e.g. connectivity of coherent generators and dis-connectivity of non-coherent generators) are considered in the proposed TSC-CI model as described below.

4.4.2.1 Power balance and operational constraints

Power balance and steady state operational constraints are formulated and linearized as discussed in **Error! Reference source not found.**section 3.5.2.1and section 3.5.2.2.

4.4.2.2 Topological or Structural Constraints

Structural constraint assures the connectivity of coherent generators and the dis-connectivity of non-coherent generators. In order to fulfill the coherency criterion, the coherent generators must remain on the same island. Two coherent generators are on the same island if and only if the constraint given in (4-34) is satisfied.

$$Z_{ij} \neq 0 \qquad \forall\, i \text{ and } j \in \mathcal{M}_k^g \tag{4-34}$$

The inequality of (4-34) can be linearized as follows:

$$\frac{Z_{ij}}{h} < e_{ij} < \frac{Z_{ij}}{h} + 1 \qquad \forall\, i \text{ and } j \in \mathcal{M}_k^g \tag{4-35}$$

Based on (4-35), if $Z_{ij} = 0$ the binary variable e_{ij} is bounded as $0 < e_{ij} < 1$ (i.e. infeasible). Therefore, (4-35) enforces two coherent generators *i* and *j* to be on the same island. Also, to locate the non-coherent generators in different islands, the constraint given in (4-36) is introduced. According to (4-36), two non-coherent generators are in different islands if and only if the constraint given in (4-36) is fulfilled.

$$Z_{ij} = 0 \qquad \forall\, i \in \mathcal{M}_k^g \text{ and } j \notin \mathcal{M}_k^g \tag{4-36}$$

4.5 Linear Formulation for Calculating Impedance Matrix

The proposed TSC-CI model improves the transient stability in a direction where the transfer impedance between the generators of each island is increased or decreased based on the location of a saddle point. Therefore, the impedance matrix is needed to be calculated during the optimization process. To this end, the impedance matrix should be included in the TSC-CI model via a linear formulation. According to the nonlinear equality given in (4-37), multiplication of the impedance and admittance matrices gives an identity matrix.

$$I = Z.Y \tag{4-37}$$

In (4-37), *Z* and *Y* are assumed as variables. In a lossless system, assume that element *(k,j)* of the vector equation given in (4-38), as follows.

$$I\,(k,j) = \sum_{i=1}^{N_b} Z_{ki} \times B_{ij}^{new} \tag{4-38}$$

Using the auxiliary variable of $R_{kij} = Z_{ki} \times B_{ij}^{new}$ and according to (3-25)-(3-28), the constraints given in (4-39)-(4-44) are linear equivalents of (4-38).

$$I(k,j) = \sum_{i=1}^{N_b} R_{kij} \tag{4-39}$$

$$-M\left(1 - U_{ij}\right) \le R_{kij} - Z_{ki}B_{ij} \le M\left(1 - U_{ij}\right) \quad j \ne i \tag{4-40}$$

$$-MU_{ij} \le R_{kij} \le MU_{ij} \qquad j \ne i \tag{4-41}$$

$$R_{kii} = Z_{ki} \times B_{ii} + \sum_{j=1, i\ne j}^{N_b} R_{kij}^{A} \tag{4-42}$$

$$MU_{ij} \le R_{kij}^{A} - Z_{ki}B_{ij} \le MU_{ij} \tag{4-43}$$

$$M\left(1 - U_{ij}\right) \le R_{kij}^{A} \le M\left(1 - U_{ij}\right) \tag{4-44}$$

4.6 Online Identification of Coherent Generators

As the required islands are formed around the coherent generators, it is needed to determine the coherent group of generators. In order to have a reliable and updated set of coherent groups, the coherency is considered in offline and online steps as follows:

1- Offline step: In order to minimize the effect of fault characteristics on the set of coherent generators, different faults are applied on all buses. The correlation coefficients between rotor speeds of generators are considered as the coherency criterion. The average correlation ratios under different fault conditions are considered as the coherency criterion.

2- Online step: In the online step, the value of the rotor speed of each generator is estimated using PMUs data. Depends on the rotor speed trajectories, the set of islands is determined based on the speed of generators on the center of inertia reference (i.e.ω_{COI}). Based on (4-45), two adjacent islands are coherent in online mode, if and only if α is neglectable.

$$\omega_{COI}^{k1} - \omega_{COI}^{k2} \le \alpha \tag{4-45}$$

where, to have a robust grouping, the rotor speed is averaged over c subsequent samples as follows.

$$\omega_{COI_n}^{k} = \sum_{n=1}^{c} \frac{\left(\omega_{COI_n}^{k}\right)}{c} \tag{4-46}$$

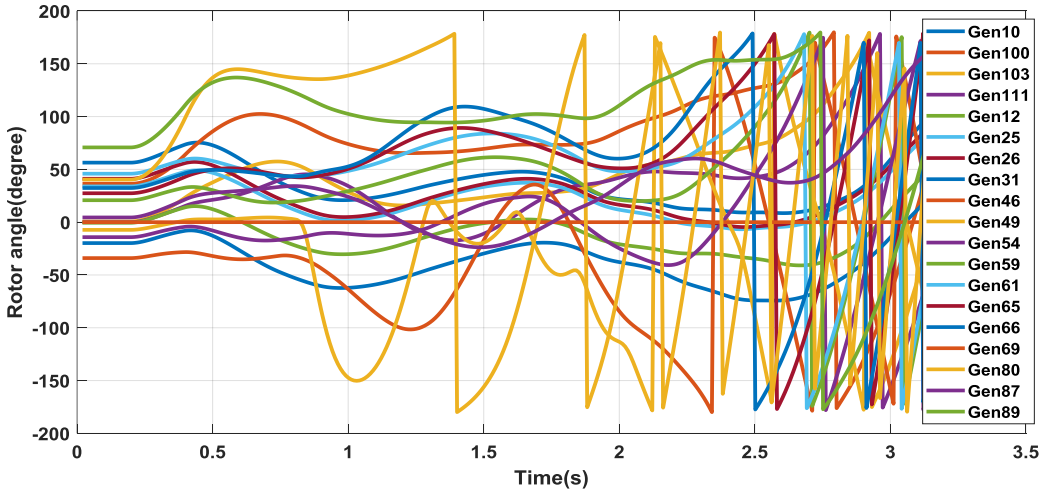

Fig. 4-2. Trajectories of rotor angles during blackout scenario

3- Physical path restriction: In some cases, disconnecting a given non-coherent island, may cause the physical disconnection of some other coherent islands. To this end, in case the force disconnected islands must be considered in connectivity and dis-connectivity constraint.

4.7 Implementation of the Method-2 for the IEEE 118-bus Test System

The proposed TSC-CI model is applied to the dynamic IEEE 118-bus test system. The effectiveness of the proposed method is compared with the conventional or MIP-only controlled islanding scheme under different case studies.

4.7.1 Cascading Outage Scenario

As shown in Fig. 4-2, a three-phase short circuit fault is applied on bus 77 at t=0.2sec and is cleared at t=0.4sec. Another short circuit fault is occurred on bus 47 at t=0.75sec and is cleared at t=0.90sec. Due to these subsequent faults, generator G80 goes out-of-step and trips at t=1.39sec. Due to the outage of G80, 477MW of power generation is lost. Within a short time, generator G49 trips at t=2.132sec due to the out-of-step condition. Finally, the entire network experiences a complete blackout in less than 4sec from the initiating event. The efficacy of the MIP-only and TSC-CI schemes in stopping such an event is investigated.

4.7.2 Predetermining the Coherent Generators

In order to minimize the dependency of coherency criteria on the fault characteristics, different short circuit faults are applied on all buses. The correlation coefficients between rotor angles of generators are calculated for each fault as the coherency criterion. The average correlation ratios under different faults are considered as the coherency criterion. For IEEE 118-bus test system, the set of predetermined coherent generators is obtained as given in Table 4-1.

4.7.3 Online Detection of Coherent Generators

The coherent groups of generators are determined based on PMUs data in online mode assuming $\alpha = 0.05$ and ten subsequent samples or $c = 10$ (i.e. the length of the data window is $10 \times 0.04 = 0.4sec$). The set of coherent groups has been reported in Table 4-3. Also, the value of ω_{COI} for each group is reported in Table 4-3. Based on Table 4-3, three coherent groups of generators are created. It is noted that the physical path (PR) restriction is considered in forming the final set of coherent groups. In Table 4-3, 0 and PR imply the non-connected islands and the value of 1 confirms the connection between islands. In other words, the disconnection of island2, enforces the disconnection of island1, island4 and island5.

4.7.4 Determining the inputs of TSC-CI Model

The saddle points can be calculated using the approximated method given in (4-19) or using the exact method given in (4-17)-(4-19). The exact values of saddle point using optimization model for each islanding strategy (i.e. strategy obtained by TSC-CI and MIP-only) are given in Fig. 4-3 and Table 4-4. For all three coherent groups, parameter BZ_{ij} is determined as given in

Table 4-5, Table 4-6, and Table 4-7. In order to improve the transient stability of each island, in case of positive BZ_{ij} (i.e. $Z_{ij} = +1$), it is required to decrease the transfer impedance between generators *i* and *j* and for negative values of BZ_{ij} (i.e. $BZ_{ij} = -1$), it is required to increase the transfer impedance between generators *i* and *j*. Increasing and decreasing the transfer impedances are realized by maximization and minimization of Z_{ij} , using the second term of the proposed multi-objective function, respectively. It is noted that $BZ_{ij} = BZ_{ji}$ for all pairs of coherent generators.

Table 4-1: Set of Coherent Generators in the IEEE 118-Bus System

Group NO	GEN NO
١	G10, G12, G25, G26, G31
٢	G46, G49, G59, G61, G65, G66, G54,
3	G69,G80
4	G89, G103, G111, G100
5	G87

Table 4-2: Set of Coherent Generators in IEEE 118-Bus System with $\alpha = 0.05$ in Online Mode Using PMU Data under the Blackout Scenario

Group NO	GEN NO
١	G10, G12, G25, G26, G31
٢	G46, G49, G59, G61, G65, G66, G54, G69,G80
3	G89, G103, G111, G100 G87

Table 4-3: Connectivity between Predetermined Islands Considering Physical Path Restriction

K/ω_{COI}	**1/1.08**	**2/1.15**	**3/1.17**	**4/1.09**	**5/1.06**
١/1.08	1	0	0	PR	**PR**
2/1.15	0	1	1	0	**0**
3/1.17	0	1	1	0	**0**
4/1.09	PR	0	0	1	**1**
5/1.06	PR	0	0	1	**1**

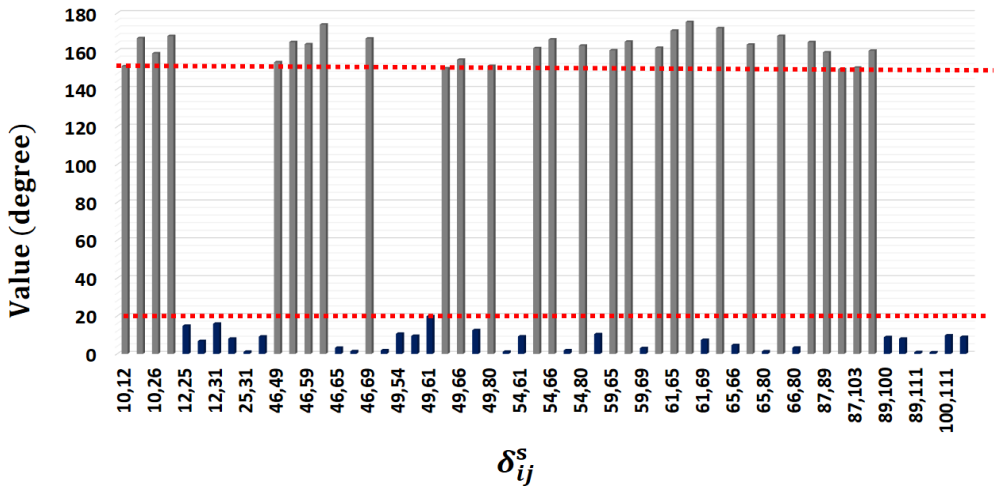

Fig. 4-3. Value of saddle points using an optimization model

Table 4-4: Saddle point of the islanded system using TSC-CI and MIP-only schemes

Group	Gen No.	M (**Inertia**)	Saddle point	
			MIP-only	TSC-CI
1	**10**	2.3	15.21	18.30
	12	4.8	171.80	170.28
	25	3.0	185.78	185.11
	26	3.7	179.20	177.07
	31	6.2	183.60	186.23
2	**46**	6.2	15.65	14.52
	49	3.0	169.71	168.59
	54	4.9	172.19	179.25
	59	4.1	178.13	178.10
	61	4.1	181.21	188.48
	65	2.6	17.91	17.74
	66	2.6	14.49	13.15
	69	2.3	189.53	181.12
	80	2.3	19.56	16.41
3	**87**	6.1	19.82	20.91
	89	2.6	181.93	180.17
	100	3.0	171.73	171.33
	103	5.0	175.22	172.14
	111	5.0	185.83	181.10

Table 4-5: Values of BZ_{ij} Parameter for Island 1(North)

GEN NO (Island1)	۱۰	۱۲	۲۵	۲۶	۳۱
۱۰		+1	+1	+1	+1
۱۲	+1		-1	-1	-1
۲۵	+1	-1		-1	-1
۲۶	+1	-1	-1		-1
۳۱	+1	-1	-1	-1	

Table 4-6: Values of BZ_{ij} Parameter for Island 2(West)

GEN NO (Island2)	۴۶	۴۹	۵۴	۵۹	۶۱	۶۵	۶۶	۶۹	۸۰
46		+1	+1	+1	+1	-1	-1	+1	-1
49	+1		-1	-1	-1	+1	+1	-1	+1
54	+1	-1		-1	-1	+1	+1	-1	+1
59	+1	-1	-1		-1	+1	+1	-1	+1
61	+1	-1	-1	-1		+1	+1	-1	+1
65	-1	+1	+1	+1	+1		-1	+1	-1
66	-1	+1	+1	+1	+1	-1		+1	-1
69	+1	-1	-1	-1	-1	+1	+1		+1
80	-1	+1	+1	+1	+1	-1	-1	+1	

Table 4-7: Values of BZ_{ij} Parameter for Island 3 (south)

GEN NO (Island3)	**87**	**89**	**100**	**103**	**111**
87		+1	+1	+1	+1
89	+1		-1	-1	-1
100	+1	-1		-1	-1
103	+1	-1	-1		-1
111	+1	-1	-1	-1	

Table 4-8: Results of Controlled Islanding with and without Considering Transient Stability Constraints

Gen NO	$P_{0_e}^{initial}$ (MW)	$\Delta P_i^+ - \Delta P_i^-$(MW)		Splitting lines		S_k (degree)
		TSC-CI	MIP-only	TSC-CI	MIP-only	
10	450	0-113	0-80	15-33 19-34 23-24 30-38	19-34 23-24 30-38 33-37	**402.8/20 =20.14**
31	7	0-0	0-0			
12	85	0-0	0-0			
25	220	0-0	0-10			
26	314	0-0	0-0			
69	516.4	0-0	0-0	15-33 19-34 23-24 30-38 80-96 96-97 77-82 100-98 100-99	19-34 23-24 30-38 33-37 77-82 80-97 80-96 98-100 99-100	**3291/72 =45.07**
46	19	0-0	0-0			
49	204	0-0	0-0			
59	155	0-0	0-0			
61	160	0-0	0-0			
65	391	0-0	0-0			
66	392	0-0	+20-0			
54	48	0-0	0-0			
80	477	+133-0	+90-0			
89	607	0-20	0-17	80-96 96-97 77-82 100-98 100-99	77-82 80-97 80-96 98-100 99-100	**403/20 =20.15**
87	4	0-0	0-0			
103	40	0-0	0-3			
111	36	0-0	0-0			
100	252	0-0	0-0			

4.7.5 MIP-only Model

The MIP-only model of controlled islanding is now solved for the test system under the cascading scenario. The obtained results have been reported in

Table 4-8. The obtained splitting strategy is applied to the full-scale model of the test system, and the results are illustrated in Fig. 4-4. According to Fig. 4-4, since the G80 trips at t=1.23sec, due to the out-of-step conditions, the conventional islanding strategy fails to create transient-stable islands. Before executing the TSC-CI model, some inputs, including

parameters BZ_{ij} and Z_{ij}^{0} are calculated based on the results of the MIP-only model. Also the value of $\boldsymbol{E_K - E_P}$ for island 1, island 2 and island 3 are -0.72 (i.e.12.60-13.32, or stable), 2.56 (i.e. 23.21-20.65, or unstable) and -2٢.81(i.e. ٥.17-27.98, or stable) respectively.

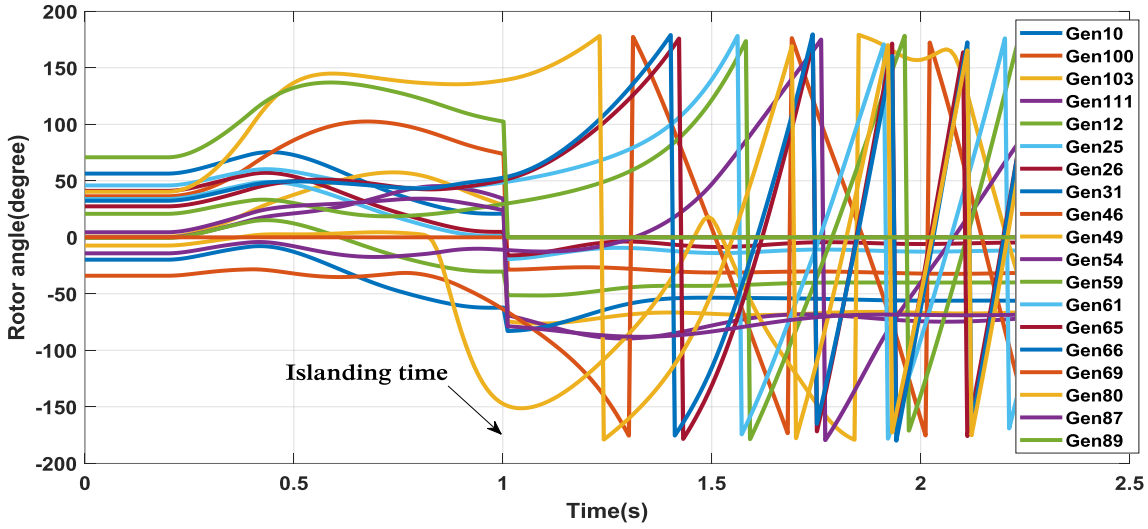

Fig. 4-4. Trajectories of rotor angles using conventional strategy

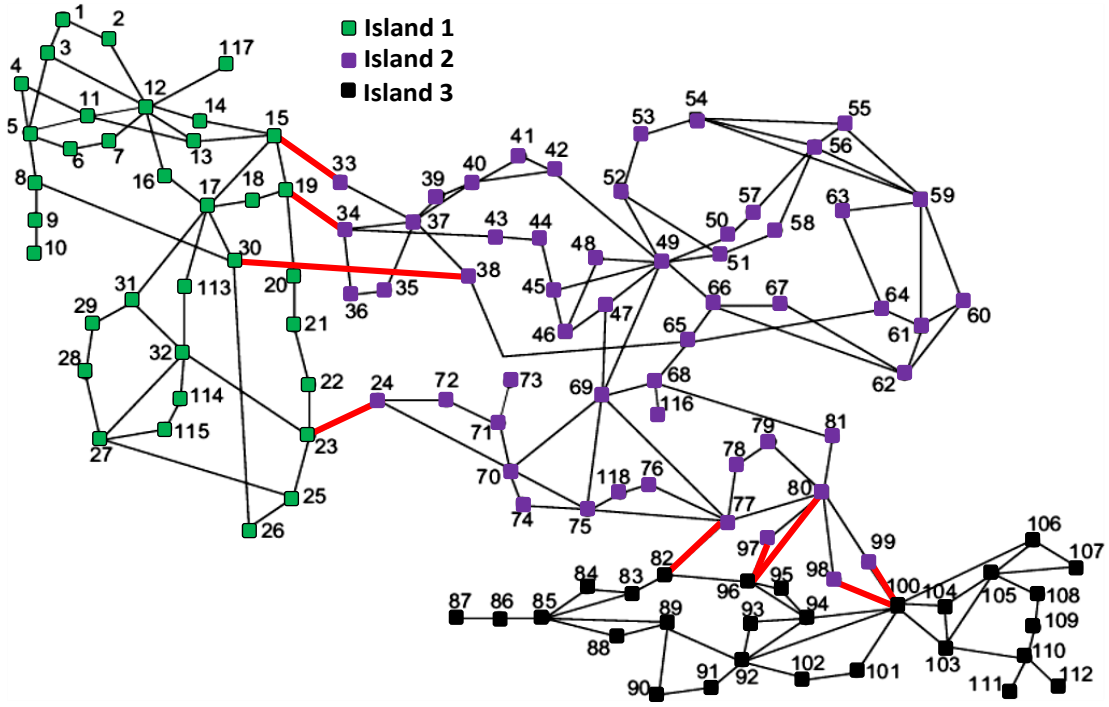

Fig. 4-5. Boundaries of islands using the proposed TSC-CI approach

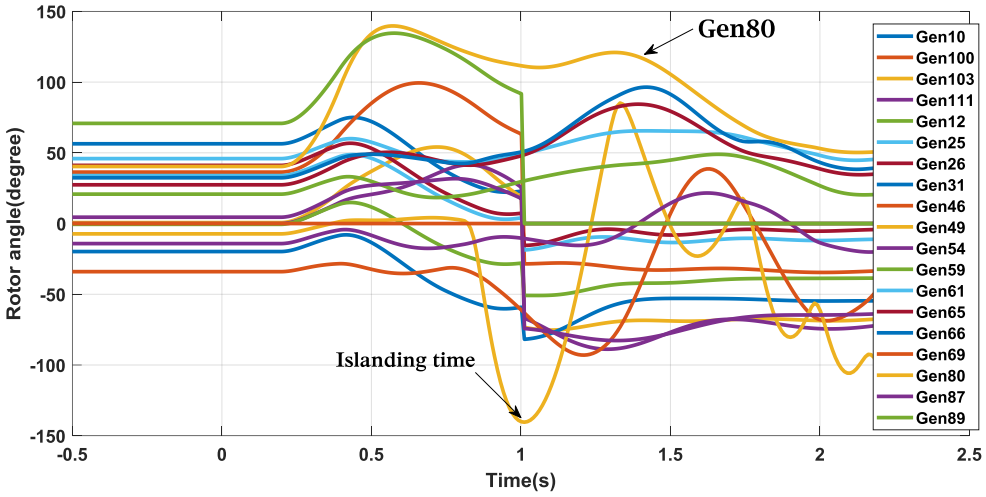

Fig. 4-6. Trajectories of rotor angles using the proposed TSC-CI approach

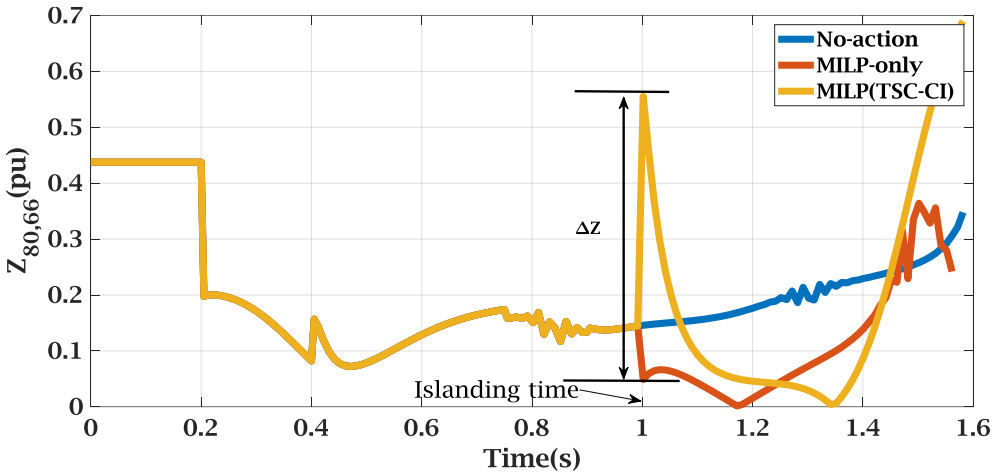

Fig. 4-7. Trajectories of transfer impedance $Z_{80,66}$ with and without the islanding strategies

4.7.6 TSC-CI Model

The TSC-CI model is now utilized to find the proper splitting strategy by considering the transient stability constraints. The parameter ε is assumed to be equal to 0.25. The results of the TSC-CI model, including the amount of power imbalance and the set of splitting lines have been reported in

Table 4-8. Also, the boundaries of islands using the TSC-CI model have been illustrated in Fig. 4-5. To verify the efficacy of the TSC-CI model, the obtained splitting strategy is applied to the full-scale dynamic model of the test system under the given cascading scenario, and the system responses are shown in Fig. 4-6. According to Fig. 4-6, the TSC-CI model has stabilized all the three islands, including generator G80 in island 2. Based on the results presented in

Table 4-8, the TSC-CI method results in an absolute power imbalance of 266MW (i.e.$(113 + 133 + 20)MW$), while the conventional islanding method results in a power imbalance of 220MW (i.e. $(80 + 10 + 20 + 90 + 17 + 3)MW$). In other words, the TSC-CI model gives a transient-stable islanding strategy with 46MW (i.e. 266MW-220MW) additional power imbalance. Although the upper bound of power imbalance was assumed as $\varepsilon = 0.25$, the obtained additional power imbalance using the TSC-CI model is equal to 0.209 (i.e.$46MW/220MW = 0.209$), which is lower than the initial threshold of $\varepsilon = 0.25$. Now, the variation of $Z_{80,66}$ is analyzed, note that G80 is unstable under the MIP-only islanding method. Variations of transfer impedance, $Z_{80,66}$ in the three cases, including without controlled islanding, with MIP-only and TSC-CI islanding methods have been depicted in Fig. 4-7. According to Table 4-6, the direction of transfer impedance change was obtained as $BZ_{80,66} = -1$, meaning that the transfer impedance of $Z_{80,66}$ must be increased. According to Fig. 4-7, under the TSC-CI islanding strategy, the value of $Z_{80,66}$ is increased right after the controlled islanding, significantly, while this change is in the opposite direction for the MIP-only strategy which in turn causes the transient

instability of G80. Also, the values of transfer impedances between G80 and other coherent generators in island 2, right

Table 4-9: Results of TSC-CI Model for Different Values of ε

	$Cost_s(pu.degree)$			$Cost_p(MW)$			
ε	Island 1	Island 2	Island 3	Island 1	Island 2	Island 3	stability
0.10	-60.8	-289.1	-28.5	109	121	12	u*
0.15	-81.9	-400.7	-32.1	112	126.5	14.5	u
0.20	-101.4	-647.1	-48.2	113	132	19	s
0.25	-160.6	-960.0	-88.3	113	133	20	s
0.30	-160.6	-960.0	-88.3	113	133	20	s

*u (unstable), s (stable)

after the network splitting using the MIP-only and TSC-CI plans have been shown in Fig. 4-7. In order to investigate the sensitivity of the proposed TSC-CI model with respect to the variations of ε, the results of the multi- objective TSC-CI model under different values of ε are given in Table 4-9. Indeed, for each value of ε a splitting strategy is obtained using the TSC-CI model. In Table 4-9, in addition to $Cost_s$ and $Cost_p$, the transient stability condition of the resulted splitting strategy have been reported. According to Table 4-9, it can be seen that for $\varepsilon \geq 0.20$, the TSC-CI model creates transient-stable islands with a similar amount of power imbalance. In other words, the proposed method creates the transient-stable islands with a 20 % additional power imbalance with respect to the conventional islanding approach. Also the value of $E_K - E_P$ for island 1, island 2 and island 3 are obtained as -1.51 (i.e. 12.60-14.11, or stable), -1.97 (i.e. 23.21-25.18, or stable) and -1٣.08(i.e. ٥.17-18.25, or stable) respectively. According to these results, it can be concluded that using the TSC-CI algorithm the potential energy is decreased in two areas (i.e. island 1 and island3) and increased in another island (i.e. island 2). Actually this decision is made based on the value of S_k in the TSC-CI model. The value of S_k for island 2 is 45.7o, however for island 1 and 3 are 30.14o and 15.15o respectively.

4.8 Discussion and Analysis

The novelties, advantages, and disadvantages of this method are discussed as follows.

4.8.1 Novelties of Method-2

1) A transient stability criterion is defined as a function of the transfer impedances between coherent generators in each island. The network splitting is then carried out in a direction where the transient stability criterion is increased. Using the wide area measurements, the coherent set of generators is updated. Also, based on the wide-area measurements, a weighting procedure is developed to prioritize the critical islands

2) A multi-objective MIP model is proposed for the TSC-CI model in order to provide the transient stability of islands with the least possible power imbalance.

4.8.2 Advantages of Method-2:

1) The CPU time of the proposed TSC-CI is acceptable and makes the proposed method suitable for real-time or online applications. Optimality of the obtained splitting strategy using the proposed linearization procedure
2) Enhancing the transient stability of each island using the transient energy function by considering the dynamic conditions of the power system.
3) Reducing the solution space in a large power system by reducing the number of candidate splitting lines.
4) Prioritizing the critical islands that struggle with transient instability based on online data. Updating the set of coherent generators to decide about the possible merging of coherent areas

4.8.3 Disadvantages of Method-2:

1) The uncertainty of the inputs is not considered in this method.
2) Setting the weighting factors of multi-objective function may be challenging in large scale power systems.

4.9 The motivation for Devolving the Next Method

Based on the aforementioned discussion, this method has some disadvantages which must be addressed in a more sophisticated model. The main disadvantage of Method-2 is that, the transient stability is formulated as a part of the multi-objective function. In addition to the difficulties in setting the weighting factors, this issue may result in more power imbalance on each island to provide the transient stability of islands. Although the additional power imbalance by this method is acceptable, however it is required to minimize such an additional power imbalance as much as possible.

4.10 Conclusion of the Chapter

In this chapter, the implementation of the controlled islanding under the transient stability consideration was addressed. Since the network splitting imposes a disturbance in terms of an electric power imbalance on each generator, the first and fast threatening phenomenon in the success of controlled islanding is the transient rotor angle instability. It was shown that without considering the transient stability constraints and relying just on the steady-state modeling of the power system, the controlled islanding may fail to create transient-stable islands. Major findings of this chapter are summarized as follows: 1) Each network splitting strategy has a unique impact on the potential energy (i.e. the transient stability criterion) of each island, 2) By changing the transfer impedances between the coherent generators in each island, in the proper direction, the transient stability is improved, indicating the truth that the transfer impedance between each pair of generators in each island is a useful criterion to improve the transient stability of that island, and 4) While the conventional objective function (MIP-only) of islanding tries to reach the minimum power balance in each island, the proposed TSC-CI finds the transient-stable islands with the least possible power imbalance. The online application of the TSC-CI model is possible provided that the solution space of candidate splitting lines is reduced and a fast WAMS infrastructure with powerful computational tools is utilized.

CHAPTER 5. CONTROLLED ISLANDING CONSIDERING TRANSIENT STABILTY CONSTRAINT

5.1 Introduction

In this chapter, based on the wide area measurements, transient stability constrained network splitting model (i.e. Method-3) is proposed using a proper transient energy function. The proposed TSC-CI model is perfected in two stages. The first stage is devoted to the conventional controlled islanding problem, formulated as a mixed integer linear programming (MILP) optimization model with considering operational, coherency and linear AC load flow constraints. In this stage, the boundary of each island is determined using an optimization model to achieve the minimum total power imbalance. To assess the transient stability, the network splitting plan obtained from the first stage is then evaluated in the second stage using a transient energy function. According to the transient stability criterion, in the second stage, a linear constraint is constructed and added to the MILP formulation of the controlled islanding model. As a major part of the second stage, the saddle or unstable equilibrium points (UEP) are determined using an optimization model. The proposed network splitting model is simulated over the dynamic IEEE 118-bus system. Unlike the transient stability based islanding methods proposed in Chapter 3 and Chapter 4, in current formulation the transient stability criterion is formulated as a hard constraint

of the optimization model. In other words, the transient stability constraint is fulfilled with a minimum power imbalance.

5.2 Transient Stability in Method3 Using the Energy Function Approach

The overall structure of the proposed transient stability constrained islanding model has been illustrated in Fig. 5-1. It is assumed that the issue of “when to island" is decided using an islanding prediction algorithm such as the method proposed in [10] and [13, 17]. This thesis addresses the "where to island” issue. The measurement data from the wide area measurement system (WAMS), including the network topology, are the inputs of the first stage (i.e. the MILP-only islanding model) of the proposed method. The proposed method might be used online or near to real-time provided that the required inputs or system states are known. Practically, the candidate splitting points are limited to inter-area transmission lines and the developed model may be run in a reasonable time (as discussed in 3.6). Also, using the slow coherency criteria as the correlation ratio between the voltage angles of both ends of transmission lines can be reduced. The requirements for online and offline applications of controlled islanding schemes can be found in [50]. The splitting strategy obtained from the MILP model of the first stage is then passed to the second stage where the TEF is defined to assess the transient stability of the network under the given islanding strategy. The proposed TEF needs the saddle points of each island. To this end, the saddle or control UEPs are determined in this stage. According to the developed TEF, if the transient stability criterion is met, the iterative process between the first and second stages is stopped, otherwise based on the most sensitive splitting lines a linear constraint is constructed and returned to the MILP model of the first stage. This iterative process continues until the stability criterion is ultimately satisfied.

5.2.1 Wide Area Measurement

The proposed controlled islanding is an offline scheme and can be performed near to real

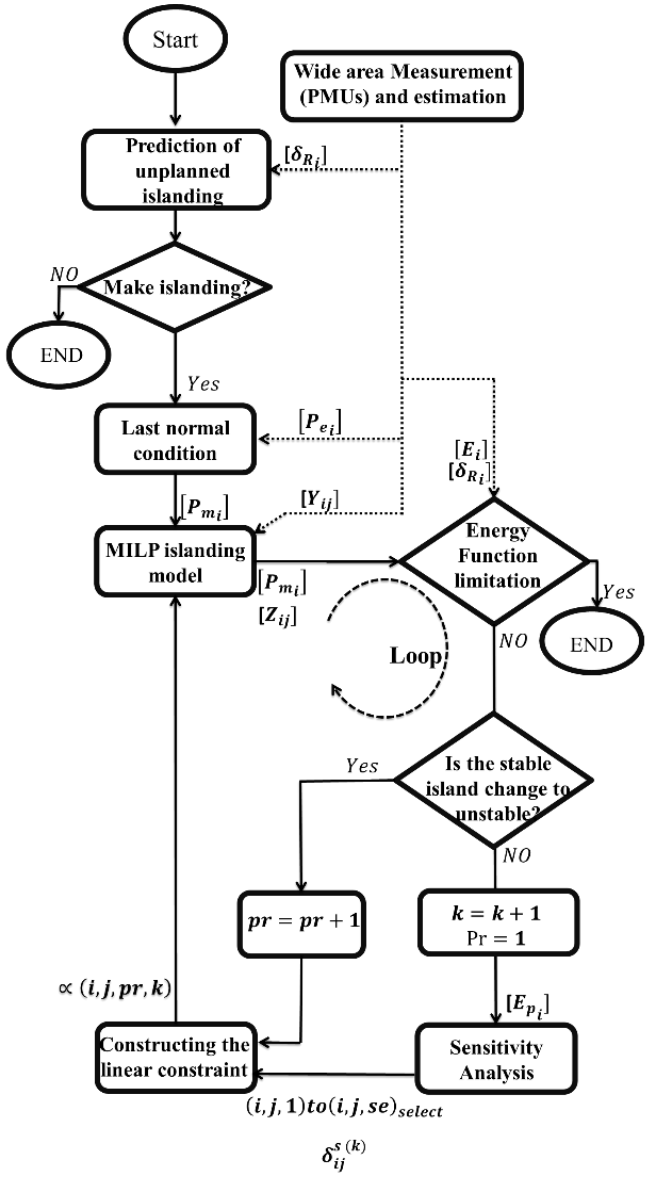

Fig. 5-1. Overall structure of the proposed TEF-based two-stage model

time using PMU measurements, i.e. active/reactive powers and voltage phasors at generators' terminals, that are transmitted to the energy management system (EMS) center

via the WAMS infrastructure. Alternatively, these variables can be estimated using the state estimation module in EMS centers. For the sake of simplicity, the measurement delay is assumed negligible. Also, the network topology for constructing the network admittance matrix (i.e.Y_{ij}) is assumed to be known from the topology processor. The developed TEF for the transient stability assessment of the islanding strategy needs the internal voltages of synchronous generators. To this end, the internal voltages of generators can be estimated based on (5-1).

$$E_i\angle\delta_i = V_i\angle\theta_i - Z_{gi} \times \frac{P_{ei} - jQ_{ei}}{V_i\angle-\theta_i} \tag{5-1}$$

5.2.2 Last Normal Condition of the Network

A major input parameter of the MILP-based controlled islanding plan is the input mechanical power of each generator that can be determined by measuring the electrical power output of that generator. During the transient regime, the input mechanical power of a given generator, is approximately constant. Due to various events or disturbances, the electrical power of a given generator may change before the controlled islanding. In such conditions, the input mechanical power of a given generator is assumed to be approximately equal to the last recorded amount of electrical power of that generator in normal conditions. Without loss of generality, in this thesis, it is assumed that the mechanical power of each generator is an input parameter and is known based on the measured electrical power output of that generator.

5.3 First Stage: The Proposed MILP Islanding Model

In the first stage, the set of splitting lines is determined without considering the transient stability constraint. In order to reduce the computational burden, the MINLP model of controlled islanding is converted to a MILP model. The objective function, operational constraints including the linear AC power balance model, the coherency-based grouping of generators and the connectivity constraint in each island are presented in the following.

5.3.1 The Objective Function

Conventionally, the islanding strategy should split the network such that the power balance in all resulted islands is fulfilled with minimum load and generation shedding. The objective function of the proposed model is defined to minimize the total power imbalance similar to the previous methods (i.e. Method-1 and Method-2) as follows:

$$PI = \sum_{i=1}^{N_g} (\Delta P_{e_i}^{-} + \Delta P_{e_i}^{+}) \quad (5\text{-}2)$$

5.3.2 Constraints

A variety of constraints including power balance, operational limits, a coherency-based grouping of generators and connectivity of each island must be considered in the optimization model of islanding in the first stage. All of these constraints are similar to the constrains given in Method-2 as given in section 4.4.2. They are not reported here, but are considered as part of the proposed Method-3.

5.4 Determination of the Saddle Point

In order to evaluate the transient stability of a given controlled islanding strategy using the proposed TEF, the saddle or UEP point (i.e. δ_{ij}^{s}) must be determined. Different methods have been developed for determining the control UEP [46]. As a part of the second

stage, a saddle point is determined using a Non-Linear Programming (NLP) optimization problem. At a given saddle point, the following issues are considered:

a) At the saddle point the following condition must be fulfilled (i.e. in saddle point $\ddot{\delta}_{ij} = 0$):

$$M_j\left[P_{mi} - \frac{E_i^2}{Z_{ii}}\cos(\emptyset_{ii}) + \sum_{j=1}^{N_g} \frac{E_i E_j}{Z_{ij}}\cos\left(\delta_{ij} + \emptyset_{ij}\right)\right] - M_i\left[P_{mj} - \frac{E_j^2}{Z_{jj}}\cos\left(\emptyset_{jj}\right) + \sum_{i=1}^{N_g} \frac{E_j E_i}{Z_{ji}}\cos\left(\delta_{ji} + \emptyset_{ji}\right)\right] = 0 \quad (5\text{-}3)$$

b) According to the mutual torque between two given generators i and j as given in (4-3), for small values of $T_{m_{ij}}$, the saddle point (i.e. δ_{ij}^{s}) should be selected as close to 0 as possible and otherwise the saddle point is selected close to 180^0[46]. These conditions are formulated as a simple NLP optimization model via the objective function given in (5-4) subject to the constraint expressed by (5-5).

$$SD = Min \sum_{i=1}^{N_g-1} \sum_{j=i+1}^{N_g} \left(\delta_i - \delta_j - \pi\, Bu_{ij}\right)^2 \quad (5\text{-}4)$$

$$\ddot{\delta}_{ij} = 0 \quad (5\text{-}5)$$

where the binary parameter Bu_{ij} is determined as follows:

$$\begin{cases} Bu_{ij} = 0 & if\ \ |T_{m_{ij}}| \le \gamma \\ Bu_{ij} = 1 & if\ |\,T_{m_{ij}}| \ge \gamma \end{cases} \quad (5\text{-}6)$$

This optimization model is solved separately for each island. It is noted that this simple NLP model is not included in the MILP model of the first stage. According to (5-4)-(5-6), when $T_{m_{ij}}$ is greater than γ, Bu_{ij} will be equal to 1 and the saddle point is selected close to180^0, otherwise (i.e. $|T_{m_{ij}}| \le \gamma$) the saddle point is selected close to zero.

5.5 Formulation of the TSC-Constrained Controlled Islanding (Method-3)

In the second stage, using the proposed TEF, the transient stability of the splitting strategy is evaluated. When the transient stability is met, the obtained solution is the final strategy, otherwise, a new constraint must be constructed to update the current splitting strategy. To this end, a sensitivity-based approach is introduced to update the transfer impedance between given pairs of generators with more impact on the TEF-based stability criterion. Indeed, by changing the splitting strategy, the potential energy of each island as well as the TEF-based stability criterion, is changed. In the second stage, the parameter $S_{i,j}$ is calculated as follows:

$$S_{ij}^{(k)} = \left| \frac{E_i E_j}{Z_{ij}} [cos(\delta_{i,j}^{R}) - cos(\delta_{ij}^{s})] \times \left[Z_{ij}^{c} - Z_{ij}^{is(k)} \right] \right| \quad (5\text{-}7)$$

Assume that the transfer impedance between two generators l and m is expressed as follows:

$$Z_{lm}^{(k+1)} = Z_{lm}^{(k)} \pm \Delta Z_{lm}^{(k)} \approx \alpha_{lm}^{(k)} Z_{lm}^{(k)} \quad 5\text{-}8)$$

where $\alpha_{lm}^{(k)}$ is a limiting factor. According to (5-7), the generator pair (l, m) with the highest value of $S_{i,j}$ in each unstable island is selected to construct a linear constraint to be added to the MILP model of the first stage. The sensitivity values are calculated for the generators of each island, separately. No optimization model is needed to calculate the sensitivity analysis. Also, the term $\left[Z_{ij}^{c} - Z_{ij}^{is(k)} \right]$ is considered in (5-10) to select the pair of (l, m) with higher sensitivity to the change in islanding boundary.

In order to meet the stability criterion (i.e. $En_k - En_p < 0$) it is needed to increase the amount of potential energy during the iterative process between the first and second stages. By changing the impedance Z_{lm} (i.e. by the splitting strategy) the location of the saddle point and the amount of potential energy in each resulted island are changed. It is noted that the kinetic energy is not changed by the line splitting at the instant of islanding. Indeed, to construct the linear constraint, the variation of potential energy and the related saddle point (i.e. the variations caused by the change of $Z_{l,m}$) are approximated. To fulfill the first

condition of saddle point given in (5-3), the following relation must be satisfied in two subsequent iterations between the first and second stages.

$$\frac{E_l E_m}{\alpha_{lm}^{(k)} Z_{lm}^{(k)}} \sin\left(\delta_{lm}^{s\,(k+1)}\right) \approx \frac{E_l E_m}{Z_{lm}^{(k)}} \sin\left(\delta_{lm}^{s\,(k)}\right) \tag{5-9}$$

Assuming constant values of E_l and E_m, the constraint given in (5-9), is simplified as follows:

$$\sin\left(\delta_{lm}^{s\,(k+1)}\right) \approx \alpha_{lm}^{(k)} \sin\left(\delta_{lm}^{s\,(k)}\right) \tag{5-10}$$

According to the second condition of the saddle point given in (5-4)-(5-6), the following approximations are valid.

$$\delta_{lm}^{s\,(k+1)} \approx \alpha_{lm}^{(k)} \delta_{lm}^{s\,(k)} \qquad if\ \delta_{lm}^{s\,(k)} \approx 0 \tag{5-11}$$

$$\delta_{lm}^{s\,(k+1)} - \pi \approx \alpha_{lm}^{(k)} (\delta_{lm}^{s\,(k)} - \pi) \quad if\ \delta_{lm}^{s\,(k)} \approx \pi \tag{5-12}$$

The variation of potential energy due to the change of $Z_{l,m}$ and saddle point is now determined using (5-13).

$$\Delta En_{Pij} \approx \frac{E_l E_m}{\alpha_{lm}^{(k)} Z_{lm}^{(k)}} [cos(\delta_{lm}^{R}) - cos\left(\delta_{lm}^{s\,(k+1)}\right)] - \frac{E_l E_m}{Z_{lm}^{(k)}} \times [cos(\delta_{lm}^{R}) - cos\left(\delta_{lm}^{s\,(k)}\right)] - P_{m_{l,m}}\left(\delta_{lm}^{s\,(k+1)}\right) P_{m_{ij}}\left(\delta_{lm}^{s\,(k)}\right) \tag{5-13}$$

According to (5-4)-(5-6), and (5-12), if $\delta_{lm}^{s\,(k)} \approx 0$ then (5-13) is expressed as follows:

$$\Delta En_{P_{ij}} = \frac{E_l E_m}{Z_{lm}^{(k)}} [cos(\delta_{lm}^{R}) - 1] \left[\frac{1}{\alpha_{lm}^{(k)}} - 1\right] \tag{5-14}$$

Based on the stability criterion (i.e. $E_K - E_P \leq 0$), to satisfy the transient stability constraint, the variation of potential energy must be positive (i.e. $\Delta En_P > 0$) during the iterative process. To this end, the limiting factor of $\alpha_{lm}^{(k)}$ must be selected greater than 1. According to (5-4)-(5-6), and (5-12), if $\delta_{lm}^{s\,(k)} \approx \pi$ then (5-13) is expressed as follows:

$$\Delta En_{P_{ij}} = \frac{E_l E_m}{Z_{lm}^{(k)}} [cos(\delta_{lm}^{R}) + 1] [\frac{1}{\alpha_{lm}^{(k)}} - 1] \quad (5\text{-}15)$$

In this case, to have a positive variation of potential energy (i.e. $\Delta E_P > 0$), the limiting factor of $\alpha_{lm}^{(k)}$ must be selected lower than 1.

Based on (5-14)- (5-15), if $\delta_{lm}^{s\,(k)} \approx \pi$, the constraint (5-16)and if $\delta_{lm}^{s\,(k)} \approx 0$ the constraint (5-17)is used as the linear constraint in MILP model.

$$Z_{lm}^{(k+1)} \leq \alpha_{lm}^{(k)} Z_{lm}^{(k)} \quad (5\text{-}16)$$

$$Z_{lm}^{(k+1)} \geq \alpha_{lm}^{(k)} Z_{lm}^{(k)} \quad (5\text{-}17)$$

5.6 Implementation of the Method-3 for IEEE 118-bus Test System

The proposed transient stability constrained controlled islanding model is implemented in a dynamic IEEE 118-bus test system. The required transient stability simulations have been done in the DIgSILENT transient stability simulator. All the optimization models

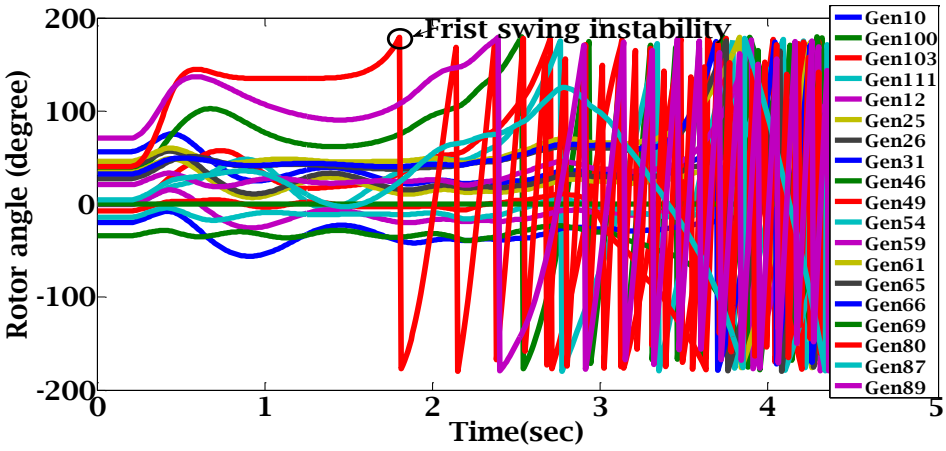

Fig. 5-2. The trajectories of rotor angles without any remedial actions

including the MILP model of the controlled islanding in the first stage are solved using CPLEX in GAMS. Also, the optimization model developed for determining saddle points, in the second stage, is solved by SBB in GAMS using a PC with Intel core i7, 4.2 GHz 7700 CPU, and 32 GB DDR4 RAM. Two different cases are simulated. In the first case, the MIP-only controlled islanding model proposed is simulated without considering the

transient stability criterion (i.e. the first iteration of the proposed algorithm). In the second case, the efficacy of the proposed transient stability constrained controlled islanding model (i.e. the iterative two-stage algorithm) is investigated. For both cases, it is assumed that a delayed three phases short circuit fault is occurred at $t = 0.2sec$ at node 77 and is cleared at $t = 0.4s$. According to Fig. 5-2, without any remedial action, the synchronous machine at node 80 goes out of step at $t = 1.8s$. After tripping G80, the generators G89, G100, G103, and G111 trip after 3sec due to out-of-step condition. Finally, without any remedial action the entire grid faces a complete blackout and the total load of the network (i.e.3668 MW) is lost. Two conventional and transient stability constrained islanding strategies are utilized to stop the propagation of the cascading failure as follows.

5.6.1 Case A. MILP-only Controlled Islanding Model

The MILP formulation of the controlled islanding without considering the transient stability constraint is solved and the obtained strategy is then executed. The optimal splitting strategy has been reported in Table 5-1(i.e. iteration 1 of the iterative process). The total simulation time of the optimization model is $0.01sec$ which makes it suitable to be implemented as a near real- time action. The obtained strategy is now applied to the network to verify its inefficacy in providing transient stability. According to Fig. 5-3, it can be seen that due to ignoring the transient stability in the MILP-only model, the second island is not stable and the G80 and a little later other generators experience transient instability. Indeed, the strategy obtained by the MILP-only islanding strategy is considered as the initial solution of the iterative transient stability constrained controlled islanding plan and hence the inefficacy of this solution in transient stability's point of view is investigated more in next simulation case.

5.6.2 Case B. Transient Stability Constrained Controlled Islanding

In this case, the iterative two-stage transient stability constrained controlled islanding scheme is simulated. The results of the first stage (i.e. the conventional MILP-only islanding) are reported in Table I. This solution is sent to the second stage to be evaluated in transient stability's point of view. As discussed before, using the MILP-only strategy the

second island does not fulfill the transient stability criterion. According to Table 5-1, it can be seen that the transient stability criterion is obtained as $En_k - En_p = 2.561 > 0$ which confirm the instability of the obtained splitting strategy on the second island. In the second iteration, the most important generators in each island are identified based on the sensitivity analysis proposed in (5-7). The impedance between these sensitive generators is then utilized to construct the linear constraint based on (5-16) and (5-17). According to (5-7), the generator pair of (G69, G80) is selected from the second island (i.e. unstable island). The impedance between this pair of generators is then selected to construct the linear constraint to be added to the MILP model of the first stage (i.e. the second iteration). The limiting factor is selected to adjust the impedance between the generator pairs of (G69, G80) to satisfy the transient stability criterion. To this end, the amount of limiting factor at

Table 5-1: The Result of Proposed Two Stage Algorithm in Each Iteration

Iteration (CPU Time)	**Splitting lines**	**Island No.**	$E_K - E_P$	**Stability check**		**Total imbalance**	**Selected** Z_{ij}/S_{ij}	$Z_{ij}^{c} - Z_{ij}^{is\,(k)}$	$\delta_{lm}^{s(k)}$	$\alpha_{lm}^{(k)}$
				TEF	**Full Simulation**					
1(0.01s)	**19-34, 24-72, 30-38, 33-37, 24-70,77-82, 80-98, 80-97,80-96, 99-100**	**1**	12.60-13.32	✓	✓	154 MW	---	---	---	---
		2	23.21-20.65	⊗	⊗		(69,80)/9.75	0.041-0.145	131	0.98
		3	5.17-27.98	✓	✓		---	---	---	---
2(0.03s)	**33-37,19-34,24-72, 30-38,24,70,77-82, 80-97,80-96,98-100, 99-100**	**1**	12.60-12.76	✓	✓	218MW	---	---	---	---
		2	23.21-21.29	⊗	⊗		(69,80)/9.68	0.041-0.141	132.2	0.98
		3	5.17-27.68	✓	✓		---	---	---	---
3(0.02s)	**33-37,19-34,23-24 30-38,77-82,80-97, 80-96,98-100,99-100**	**1**	12.60-12.76	✓	✓	220MW	---	---	---	---
		2	23.21-22.81	⊗	✓		(46,65)/9.51	0.052-0.151	131.7	0.98
		3	5.17-25.13	✓	✓		---	---	---	---
4(0.01s)	**15-33,19-34,23-24 30-38,77-82,80-97, 80-96,98-100,99-100**	**1**	12.60-12.76	✓	✓	259.8MW	---	---	---	---
		2	23.21-23.62	✓	✓		---	---	---	---
		3	5.17-23.95	✓	✓		---	---	---	---

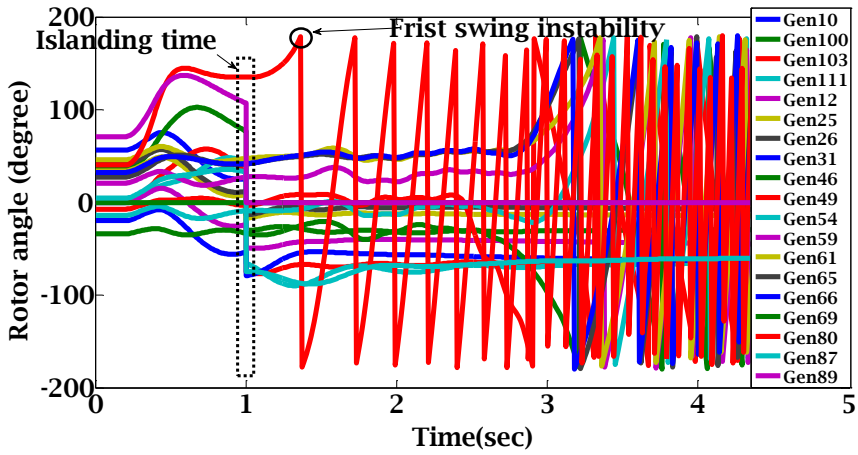

Fig. 5-3. Trajectories of rotor angles under the conventionally controlled islanding

the first iteration is set as $\alpha_{69,80}^{(1)} = 0.98$. It is noted that the normal or default value of limiting factor is 1 (i.e. $\alpha_{69,80}^{(0)} = 1$). By assigning a limiting factor very close to 1, the risk of slow convergence (i.e. the convergence between the first and second stage) is expected. Also by assigning a limit factor far from 1, the risk of divergence is increased. According to Table 5-1, this iterative process is converged at the fourth iteration. As shown in the first column of Table 5-1, the total CPU time of the proposed method is 0.07sec which makes the proposed method promising for online applications. In the fifth column of Table 5-1, the results of a stability check using the energy-based criterion and the full numerical transient simulation using the DIgSILENT package have been compared. It can be seen that, at the third iteration, the full numerical simulations confirm the stability of the obtained islanding strategy, however, the energy-based criterion will not confirm the stability. At the fourth iteration, both the energy-based criterion and the full numerical simulations confirm the transient stability. In this case, it can be concluded that the energy-based criterion is a bit conservative rather than the actual numerical simulations with 39.8 MW additional load shedding. Although the proposed method results in more shed in this test case, however using the proposed TEF method, the full time-consuming simulation is avoided. Unlike the TEF-based islanding method, the full numerical transient stability simulation is not able to govern the MIP model to select the proper splitting lines to improve the transient stability of unstable islands. The changes in islanding boundaries in each iteration are shown in Fig. 5-4. As shown in Fig. 5-4, the

change of islanding boundary in each iteration is very informative (i.e. The islanding boundaries of two consecutive iterations are close together). The trajectories of rotor angles under the splitting strategy obtained at the fourth iteration have been illustrated in Fig. 5-5. According to Table 5-1, it can be seen that during the iterative procedure, the potential energy of each island is changed. The amount of potential energy in each island is evolved such that the potential energy in each island is greater than the kinetic energy of that island and hence the stability criterion is fulfilled. Also, the variation of saddle points during the iterative process has been reported in Table 5-2. It can be seen that the maximum variation of the saddle point is related to the pair of $(G69, G80)$ in iteration 2 and 3 and the pair of $(G46, G65)$ in iteration 4.

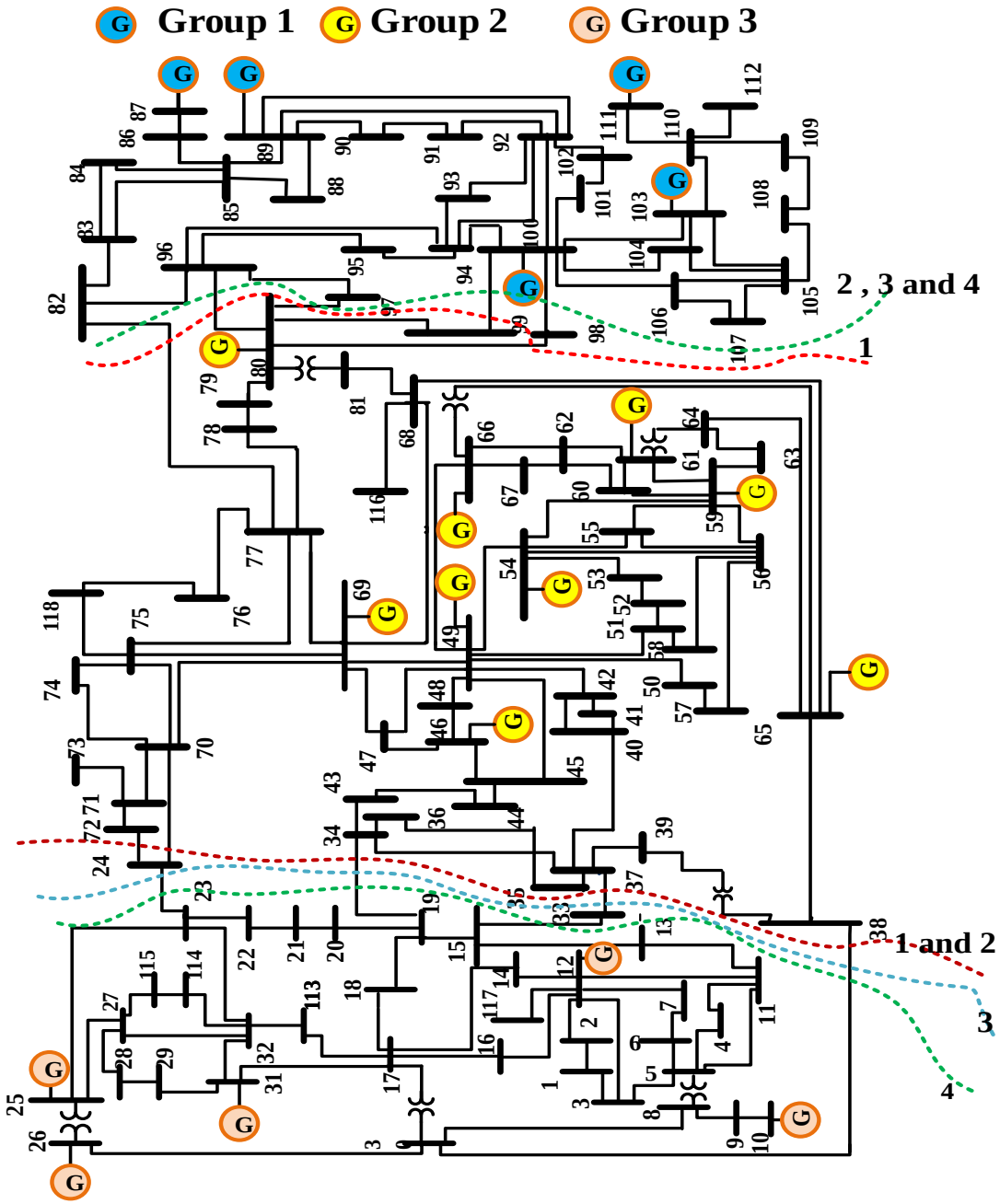

Fig. 5-4. Island boundaries in four iterations of the proposed islanding model

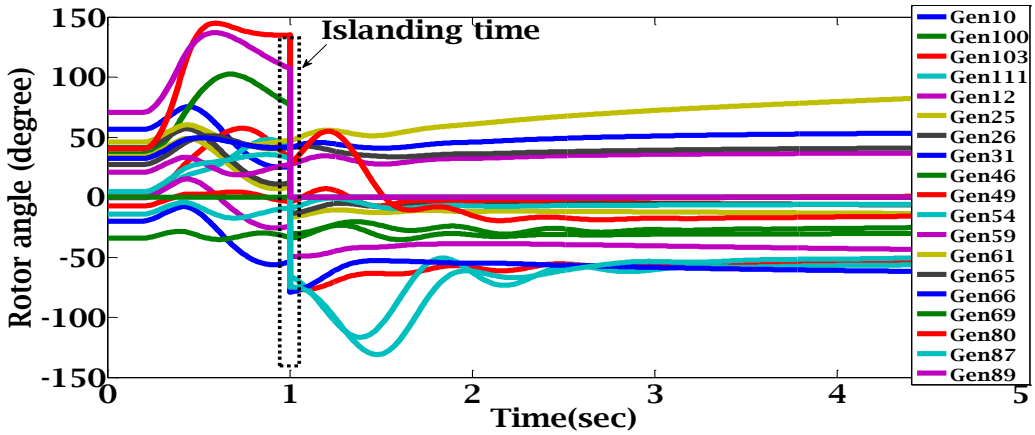

Fig. 5-5. Trajectories of rotor angles under the conventional controlled islanding strategy

Table 5-2: Saddle Points in Each Iteration of Proposed Algorithm

Group	Gen No.	Saddle Point			
		Iteration 1	Iteration 2	Iteration 3	Iteration 4
1	**10**	180	180	180	180
	12	161.80	161.40	160.18	160.28
	25	0	0	0.83	0.91
	26	163.20	163.89	167.07	167.07
	31	153.60	153.11	156.23	156.23
2	**46**	24.18	24.58	24.39	22.88
	49	35.18	35.32	35.12	34.96
	54	38.23	38.07	38.41	38.10
	59	31.36	31.23	30.04	28.96
	61	34.25	33.89	33.01	32.62
	65	158.53	158.18	156.13	156.24
	66	34.49	34.26	33.91	33.15
	69	150.53	151.12	152.31	143.12
	80	19.56	18.94	17.18	16.41
3	**87**	19.82	19.82	20.45	20.91
	89	105.93	105.93	108.17	113.17
	100	14.73	14.81	15.36	16.33
	103	24.22	24.11	24.27	24.14
	111	180	180	180	179.1

5.7 Discussion and Analysis

The main novelties, advantages, and disadvantages of Method-3 are discussed follow:

5.7.1 Novelties of Method-3

The novelties of Method-3 are summarized as follows:

1. Developing an iterative TEF-based two-stage model for transient stability constrained controlled islanding.
2. Determining the splitting lines with great impact on transient stability margin considering the post-islanding saddle or unstable equilibrium point (UEP).

5.7.2 Advantages of Method-3

1) Transient stability is considered as a constraint in the proposed optimization model for controlled islanding.
2) This method can be used in large scale power systems.
3) Like Method-2 and Method-3, to improve the computational efficiency for large scale power systems, the number of candidate splitting lines can be reduced based on the slow coherency criteria.
4) The proposed MILP model guarantee the optimality of the islanding strategy considering the related approximations.
5) Based on the wide area measurements, the set of coherent generators are determined online.

5.7.3 Disadvantages of Method-3:

1) The computational burden (CPU time) is a little more than the burden in Method-2
3) Like Method-1 and Method-2, the uncertainty of the inputs is not considered.

5.8 The motivation for Devolving the Next Method

Method-3 creates transient-stable islands with minimum power unbalance. However, the concern of uncertainty of input parameters is not considered in previously proposed islanding algorithms. Therefore, in the next chapter, the uncertainty of controlled islanding is addressed.

5.9 Conclusion of the Chapter

In this chapter, an iterative two-stage algorithm was proposed to consider the transient stability in a controlled islanding plan. The obtained results confirmed that the proposed TEF-based MIP islanding method preserves the transient stability of resulted islands by selecting the proper splitting lines. The proposed method considers the variations of saddle points of resulted islands. It was shown that the transient stability assessment by the proposed islanding method is comparable with the full dynamic simulation using a transient stability simulator. The presented iterative islanding method converges to the optimal solution in a few iterations between the first and second stages. By adjusting the potential energy of each island using the network splitting, the constructed linear constraint preserves the transient stability of created islands. Unlike the TEF-based islanding method, the full numerical transient stability simulation is not able to govern the MIP model to select the proper splitting lines to improve the transient stability of unstable islands. The real-time application of the proposed method can be realized by reducing the number of candidate transmission lines.

CHAPTER 6. UNCERTAINTY IN POWER SYSTEM ISLANDING

6.1 Introduction

Under severe cascading outages, the entire power system can be divided into isolated stable islands. The network splitting is a type of system protection schemes which is activated while other emergency and protection schemes fail to stop the harmful propagation of cascading events. Transient stability assessment of the resulted islands needs dynamic measurements about the actual conditions of the power system. Transient stability constrained controlled islanding like other power system studies comes up with uncertainties in parameters and system models. In all three presented islanding methods including Method-1 to Method-3, it is assumed that there is no uncertainty in parameters and related models. In this chapter, the transient stability constrained controlled islanding is extended to consider the uncertainties in transient stability criteria using an energy function method. While there is a vast range of uncertainties, in this chapter, the uncertainty of offline measured inputs is considered. First, the conventional network splitting model is prepared in the presence of operational, slow coherency, and linear AC load flow constraints to achieve the minimum amount of load and generation changes. In the second part, the transient stability criterion of the resulted islands is assessed using an energy function in the second stage. The uncertainty of the islanding strategy is directly considered in the utilized energy function. The point estimate method (PEM) is utilized to reduce the uncertain scenarios. The proposed uncertainty-driven islanding model is implemented in the dynamic IEEE 118-bus test system. Also a comprehensive comparison between all proposed islanding models is presented.

6.2 Introduction to Uncertainty Modeling

Monte-Carlo Simulation Method (MCSM) has been widely used in power system analysis to model different types of uncertainties. MCSM randomly generates values or

scenarios for uncertain input variables, and these values are taken into account to solve a deterministic problem [51]. The main drawback to the MCSM is the great number of simulations required to attain convergence.

Point Estimate Method (PEM) is a reasonably robust and satisfactory accurate scenario reduction technique with a low computational burden. PEM converts the continuous Probability Distribution Functions (PDFs) of uncertain parameters to two or more points (i.e. moments). In this thesis, the PEM is used to handle the uncertainties of the power system islanding scheme. The first PEM was developed for symmetric variables and was later revisited to consider asymmetric variables[52, 53].

Based on the PEM, the probability functions of stochastic variables are approximated using only their first few statistical moments (i.e., mean, variance, skewness, and kurtosis)[54]. The aim of any PEM is to compute the moments of a random variable, Z, that is a function of the stochastic input variables, x_i, i.e. $Z = f(x_1, x_2, \dots, x_n)$. PEM acts based on the concept of moments of uncertain input parameters. Indeed, PEM is used to calculate the statistical moments of a random quantity that is a function of one or several stochastic variables. Hong's PEM concentrates the statistical indices provided by the first few central moments of an input random variable on 3 points for each variable. Therefore, the function *f* has to be evaluated only three times for each input random variable, x_i . The k^{th} concentration of a random variable x_i can be defined as a pair of a location $x_{i,k}$ and a weight $w_{i,k}$, i.e. $(x_{i,k}, w_{i,k})$. The location $x_{i,k}$ is the k^{th} estimation of the variable x_i at which the function f is evaluated. The weighting factor $w_{i,k}$ accounts for the relative importance of input the variable x_i in the output random variables.

The location $x_{i,k}$ is determined as follows.

$$x_{i,k} = \mu_{x_i} + \xi_{i,k} . \sigma_{x_i} \qquad (6\text{-}1)$$

where $\xi_{i,k}$ is the standard location, μ_{x_i} and σ_{x_i} are the mean and standard deviation of the input random variable x_i , respectively.

Assuming *n* uncertain parameters, the standard location $\xi_{i,k}$ and the weighting factor $w_{i,k}$ are obtained by solving the nonlinear equations given by (6-2).

$$\begin{cases} \sum_{k=1}^{3} w_{i,k} = \dfrac{1}{n} \\ \sum_{k=1}^{3} w_{i,k} (\xi_{i,k})^{j} = \lambda_{i,j} \qquad j = 1,...,5 \end{cases} \tag{6-2}$$

where $\lambda_{i,j}$ denotes the j^{th} standard central moment of the random variable x_i with Probability Density Function of f_{x_i} and is determined as follows.

$$\lambda_{i,j} = \frac{M_j(x_i)}{(\sigma_{x_i})^j} \tag{6-3}$$

$$M_j(x_i) = \int_{-\infty}^{+\infty} (x_i - \mu_{x_i})^j . f_{x_i} \, dx_i \tag{6-4}$$

Once all the concentrations $(x_{i,k}, w_{i,k})$ are obtained, the function f is evaluated at the points $(\mu_{x_1}, \mu_{x_2}, \dots, x_{i,k}, \dots, \mu_{x_n})$ yielding $Z(l,k)$, where Z is the vector of output random variables. Finally, by using the weighting factors $w_{i,k}$ and the $Z(l,k)$ values, the j-order moment of the output variables are calculated as follows[54].

$$E(Z^j) \cong \sum_{i=1}^{n} \sum_{k=1}^{3} w_{i,k} \times (Z_m(i,k))^j \tag{6-5}$$

From a mathematical point of view, by solving (6-2), the standard locations and weights are determined using (6-6)-(6-7).

$$\xi_{i,k} = \begin{cases} \dfrac{\lambda_{i,3}}{2} + (-1)^{3-k} \sqrt{\lambda_{i,4} - \dfrac{3}{4}\lambda_{i,3}^2} & k = 1,2 \quad , i = 1,...,n \\ 0 & k = 3 \qquad , i = 1,...,n \end{cases} \tag{6-6}$$

$$w_{i,k} = \begin{cases} \dfrac{(-1)^{3-k}}{\xi_{i,k}(\xi_{i,1} - \xi_{i,2})} & k = 1,2 \quad , i = 1,...,n \\ \dfrac{1}{n} - \dfrac{1}{\lambda_{i,4} - \lambda_{i,3}^2} & k = 3 \qquad , i = 1,...,n \end{cases} \tag{6-7}$$

According to the rules of Hong's method, if the input random variable x_i has a normal PDF, then the standard locations and their weighting factors are determined as follows.

$$\xi_{i,k} = \left(\frac{(-1)^{k-1}(3-k)k}{2}\right)\sqrt{3} = \begin{cases} +\sqrt{3} & k = 1 \qquad , i = 1,...,n \\ -\sqrt{3} & k = 2 \qquad , i = 1,...,n \\ 0 & k = 3 \qquad , i = 1,...,n \end{cases} \tag{6-8}$$

$$w_{i,k} = \frac{1}{6n} \times \left(\frac{3-k}{(-1)^{k+1}(1+k.(-1)^{k+1})}\right) + \left(\frac{1}{n} - \frac{1}{3n}\right) \times \left(\frac{(k-1)(k-2)}{2}\right) = \begin{cases} \frac{1}{6n} & k = 1,2 \quad ,i = 1,\ldots,n \\ \frac{1}{n} - \frac{1}{3n} & k = 3 \quad ,i = 1,\ldots,n \end{cases} \tag{6-9}$$

The mean (i.e. μ_z) and the standard deviation (i.e. σ_z) of the random output variable Z can be calculated as follows.

$$\mu_z = E(Z) \tag{6-10}$$

$$\sigma_z = \sqrt{E(Z^2) - E^2(Z)} \tag{6-11}$$

In Hong's method, 2n+1 points or scenarios are generated for a problem with *n* uncertain input parameters. Each input variable x_i is represented by three points including$(x_i + \sqrt{3}\sigma)$, $(x_i - \sqrt{3}\sigma)$, and the average scenario as given in (6-12)-(6-14).

$$\begin{cases} x_{i,1} = (\mu_{x_1}, \mu_{x_2}, \ldots, \mu_{x_i} + \sqrt{3}\sigma, \ldots, \mu_{x_n}) & ,i = 1,\ldots,n \end{cases} \tag{6-12}$$

$$\begin{cases} x_{i,2} = (\mu_{x_1}, \mu_{x_2}, \ldots, \mu_{x_i} - \sqrt{3}\sigma, \ldots, \mu_{x_n}) & ,i = 1,\ldots,n \end{cases} \tag{6-13}$$

$$\begin{cases} x_{i,3} = (\mu_{x_1}, \mu_{x_2}, \ldots, \mu_{x_i}, \ldots, \mu_{x_n}) & ,i = 1,\ldots,n \end{cases} \tag{6-14}$$

6.3 Uncertainty Modeling in Power System Islanding

As discussed in section 4.3.1, the value of kinetic and potential energy is calculated as follows

$$En_p = \sum_{i=1}^{n-1} \sum_{j=i+1}^{n} \frac{E_i E_j}{Z_{ij}} [\cos(\delta_{ij}^R) - \cos(\delta_{ij}^s)] + \sum_{i=1}^{n-1} \sum_{j=i+1}^{n} T_{m_{ij}} (\delta_{ij}^R - \delta_{ij}^s) \tag{6-15}$$

$$En_k = \frac{1}{\sum_{i=1}^{n} M_i} \sum_{i=1}^{n-1} \sum_{j=i+1}^{n} \frac{M_i M_j \omega_{R\,ij}^2}{2} \tag{6-16}$$

The transient stability is preserved if $En_k - En_p < 0$ [46]. The proposed islanding scheme is executed near to online mode and all inputs are gathered in real time, except the equivalent inertia constant which is subject to uncertainty due to different reasons such as the penetration of non-synchronous renewable resources. Based on (6-16) and (6-15), the

system inertia impacts the value of En_k or the kinetic energy. The higher the inertia, the greater the kinetic energy. Therefore, the uncertainty of inertia could be interpreted as uncertainty in kinetic energy. It is noted that the value of potential energy is not

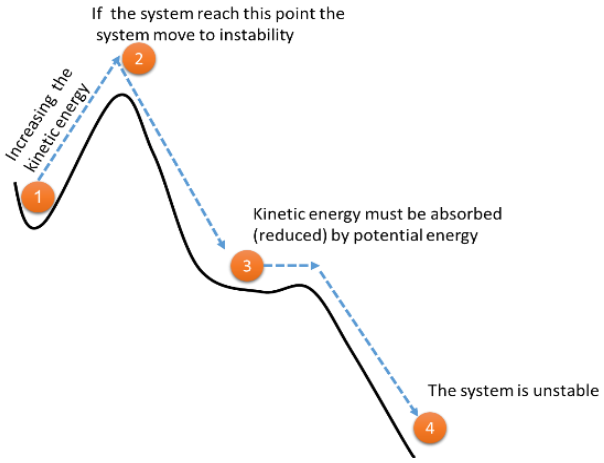

Fig. 6-1. Mechanical concept of kinetic energy level

affected by uncertain data). In this study, the penetration level of non-synchronous renewable resources is considered as $pe\%$(i.e. as a percentage of inertia). By considering (6-15)-(6-16), it can be concluded that under the uncertainty of inertia the maximum value of kinetic energy is changed by $pe\%$. It is noted that the worst case condition in transient stability's point of view coincides with the maximum amount of kinetic energy. To understand this, consider the mechanical equivalent problem shown in Fig. 6-1. The following points are valid about the conceptual system is shown in Fig. 6-1.

1) At operating point 1, the system is stable. There is not any disturbance and the kinetic energy deviation is zero.
2) At operating point 2, the system moves toward the instability
3) At operating point 3, the system is not stable and has non-zero kinetic energy($\Delta En_k \neq 0$). The higher the amount of system inertia, the greater the amount of kinetic energy.
4) At operating point 4, the system is unstable.

In order to show the impacts of the inertia uncertainty, it is assumed that the system is at the operating point 2 as shown in Fig. 6-1. Therefore as much as the kinetic energy is high, the controlling of system in point 2 is difficult (i.e. it needs more potential energy to

stabilize the system). Therefore, the worst-case scenario of transient stability occurs under the maximum value of kinetic energy. Therefore the proposed method acts based on the uncertainty of the kinetic energy. To this end, in the proposed model, the uncertainty level in kinetic energy is considered as $+pe\%$.(i.e. as a percentage of inertia). As the proposed method act in the near to real time regime, it is required to model the uncertainty of kinetic energy with the least possible number of scenarios. Therefore, the PEM is utilized. By considering the uncertainty of kinetic energy, there are $2n_{is}+1$ senarios where n_{is} is the number of resulted islands.

6.4 Simulation and Comparative Analysis of the Proposed Methods

The proposed transient stability constrained controlled islanding model is implemented in the dynamic IEEE 118-bus test system. The required transient stability simulations have been done in the DIgSILENT transient stability simulator. The proposed MIP optimization model is solved using CPLEX in GAMS. The nonlinear models of the second stage are solved using SBB in GAMS. In order to give a comprehensive overview, the results of the proposed uncertainty-driven islanding method are compared with the previous proposed methods. These methods are as follows:

Method-0: The details of this method have been given in Chapter 2.

Method-1: The details of this method have been given in Chapter 3.

Method 2: The details of this method have been given in chapter 4. This method acts based on a multi-objective function with considering the transfer impedance between coherent generators as the transient stability criteria.

Method-3: The details of this method have been given in Chapter 5. This method acts based on the minimization of power imbalance while transient stability is considered using an energy function approach.

Method-4: The details of this method are given in this chapter. This method acts based on the minimization of power imbalance while the uncertainty of system inertia is considered in the energy function based criterion. Indeed the deterministic part of this model is similar to Method-3.

Table 6-1: Set of coherent generators in IEEE 118-bus test system

Group NO	GEN NO
١	**G10, G31, G12, G25, G26**
٢	**G69, G46, G49, G59, G61, G65, G66, G54, G80**
٣	**G89, G87, G103, G111, G100**

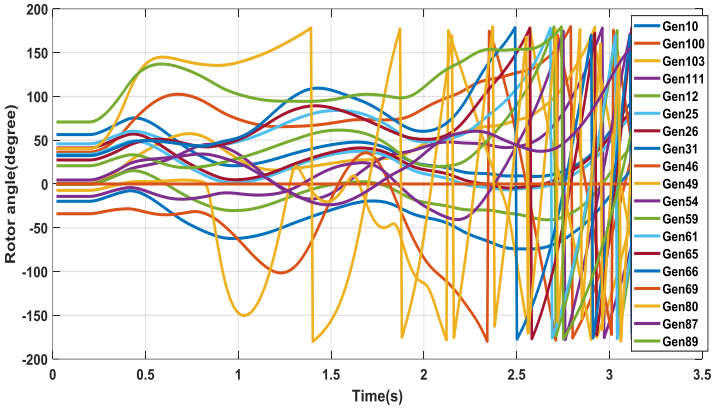

Fig. 6-2. Trajectories of rotor angles during blackout scenario

6.4.1 Generator Coherency

Under any islanding strategy, the coherent generators must be located on the same island. In this regard, it is required to determine the coherent groups of generators. Based on the correlation ratio as utilized in previous islanding methods, the set of coherent generators is determined as given in Table 6-1.

6.4.2 Cascading Outage Scenario

As shown in Fig. 6-2, a three-phase short circuit fault is applied on bus 77 at t=0.2sec and is cleared at t=0.4sec. Another short circuit fault is occurred in bus 47 at t=0.75sec and is cleared at t=0.90sec. Due to these subsequent faults, generator G80 goes out-of-step and it will trip at t=1.39sec. Due to the outage of G80, 477MW of power generation is lost. Within a short time, the generator G49 trips at t=2.132sec due to the out-of-step condition. Finally, the entire network experiences a complete blackout in less than 4sec from the initiating event. Under this cascading outage, the efficacy of all five mentioned methods is investigated below.

6.4.3 Method-0

In Method-0, the MIP optimization model of the controlled islanding plan is solved without considering the transient stability constraint. The obtained results are reported in Table 6-2. The rotor angles of generators under the execution of controlled islanding at t=1sec has been illustrated in Fig. 6-3. As shown in Fig. 6-3, generator G80 is unstable, making a decelerating power in island 2, which in turn make the G46 unstable at t=1.3sec. The outages of these two generators push the system towards a cascading outage. It is concluded that, unlike achieving the minimum power imbalance (i.e. 154MW), this method fails to preserve the transient stability of the resulted islands. Also, this fact was concluded in Chapter 2.

6.4.4 Method-1

In this method, based on the minimization of accelerating and decelerating powers imposed o generators terminal, the transient stability of created islands are improved. The results of this islanding method under the cascading scenario have been reported in Table 6-2. Also the rotor angle trajectories have been illustrated in Fig. 6-4. It can be seen that using this strategy, the generators G80 and G46 will be unstable. Indeed, in this method the transient stability is assessed using the EEAC method which is a local method and may fail to give stable islands under severe cascading outages. In chapter 3, it was shown that some cascading outages can be prevented using this method with satisfying transient stability criteria. The total amount of resulted power imbalance is 180MW which gives 26MW additional power imbalance w.r.t. the conventional islanding method (i.e. Method-0) for transient stability improvement.

Table 6-2: Boundaries of islands using different methods

Method NO	Description	Islanding boundaries	Stability CHECK	Total imbalance
0	**Conventional**	**15-33, 19-34, 23-24, 30-38, 68-81, 69-77, 75-77, 76-77**	NO	154MW
1	**Acceleration power minimization**	**19-34, 23-24, 30-38, 33-37, 77-82, 80-96, 80-97, 80-99, 80-98**	NO	180MW
2	**Z change direction in cost**	**15-33, 19-34, 23-24, 30-38, 77-82, 80-96, 96-97, 98-100, 99-100**	yes	۲۹۸,۸MW
3	**Z change in iteration**	**15-33, 19-34, 23-24, 30-38, 77-82, 80-96, 80-97, 98-100, 99-100**	yes	259.8MW
4	**Z change in iteration considering uncertainty**	**15-33, 19-34, 23-24, 30-38, 82-83, 80-96, 80-97, 82-96, 98-100, 99-100**	yes	284.8MW

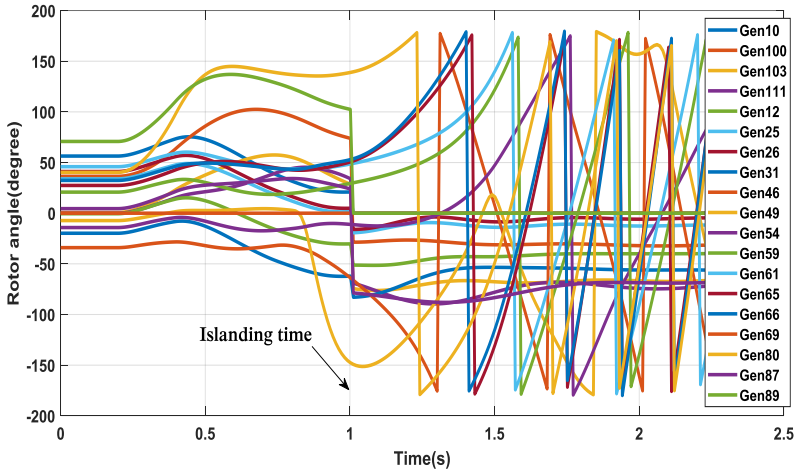

Fig. 6-3. Trajectories of rotor angles under the conventional controlled islanding

6.4.5 Method-2

In Method-2, to avoid the complexity of the islanding model, the transient stability is fulfilled by introducing a multi-objective function. This method, first, determines how the increase or decrease in transfer impedance affects the transient stability criterion using a transient energy function. The multi-objective function is then solved to minimize or maximize the related transfer impedance. Indeed, in this method, the transfer impedance is changed in a direction, where the transient stability is improved. The obtained islanding strategy using this method have been reported in Table 6-2. The system responses using this islanding strategy have been illustrated in Fig. 6-5. It can be seen that the created

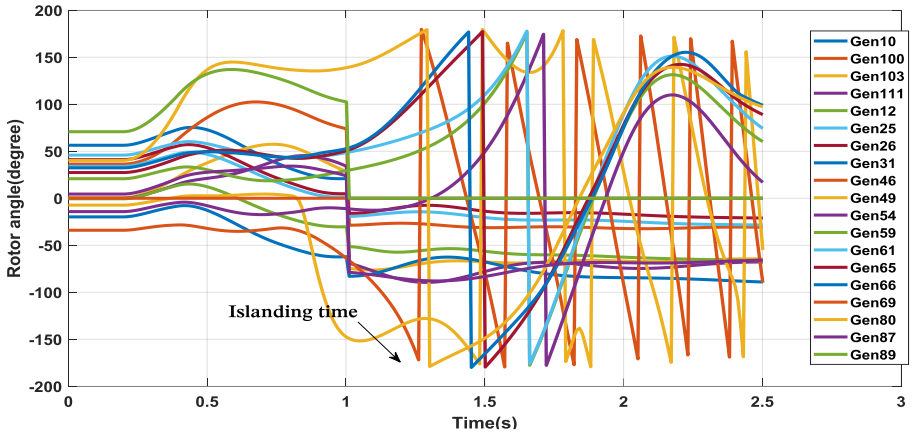

Fig. 6-4. Trajectories of rotor angles using the proposed islanding strategy (Method-1)

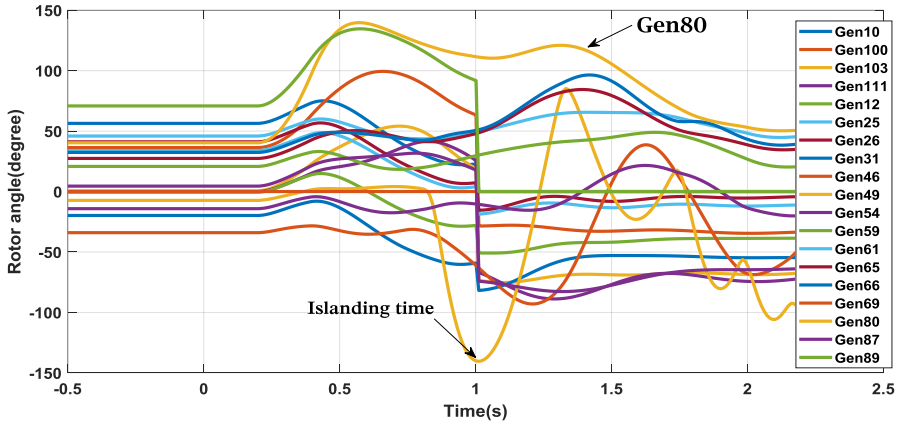

Fig. 6-5: Trajectories of rotor angles using the proposed islanding strategy (Method-2)

islands are transient-stable. This method gives 144.8MW additional power imbalance w.r.t the conventional islanding (i.e. Method-0) and 39 MW additional power imbalance w.r.t. Method-3. In this method, just transient stability improvement is considered. In other words, this method does not focus on preserving transient stability as a constraint.

6.4.6 Method-3

In this method, the transient stability criteria are considered using the energy function approach. The results of islanding using this method have been reported in Table 6-2. As

discussed in Chapter 5, this method is a two stages scheme. The first stage is the MIP-only model and the second stage is devoted to the transient stability criteria. The proposed method converges to a transient-stable strategy in five iterations. The obtained SEPs during iterations have been reported in Table 6-3. Using the sensitivity analysis, the transfer impedance between G80-G69 has the most impact on transient stability in island 2. The transfer impedance between G80-G69 is utilized for constructing the linear constraint which is then added to the MIP model of the first stage. This iterative process is continued until the islanding strategy creates stable islands. The total amount of power imbalance is increased to 259.8MW. The system responses under this islanding strategy have been illustrated in Fig. 6-6. It can be seen that the proposed method creates transient-stable islands. This method gives 105.8MW additional power imbalance w.r.t Method-0.

Table 6-3: The results of proposed algorithm (Method-4) in each iteration

Iteration (Time)	Splitting lines	Island NO	$E_K - E_P$	Stability check TEF	Stability check Full-S	Total imbalance	Selected Z_{ij}/ S_{ij}	$Z_{ij}^{c} - Z_{ij}^{is\,(k)}$	$\delta_{lm}^{s(k)}$	$\alpha_{lm}^{(k)}$
1	19-34, 24-72, 30-38,	1	12.٨١-1۴.۴١	✓	✓		---	---	---	---
(0.01s)	33-37, 24-70,77-82,	2	23.٣٢+2.٣٢-20.۵۴	⊗	⊗	154 MW	(69,80)/9.75	0.041-0.145	131	0.98
	80-98, 80-97,80-96, 99-100	3	5.٢۵-2۶.١۴	✓	✓		---	---	---	---
2	33-37,19-34,24-72,	1	12.٨١-1٣.۶٩	✓	✓		---	---	---	---
(0.03s)	30-38,24,70,77-82,	2	23.٣٢+2.٣٢-21.١٣	⊗	⊗	218MW	(69,80)/9.68	0.041-0.141	132.2	0.98
	80-97,80-96,98-100, 99-100	3	5.٢۵-2۵.٣٢	✓	✓		---	---	---	---
3	33-37,19-34,23-24	1	12.٨١-1٣.۶٩	✓	✓		---	---	---	---
(0.02s)	30-38,77-82,80-97,	2	23.٣٢+2.٣٢-22.۵۶١	⊗	✓	220MW	(46,65)/9.51	0.052-0.151	131.7	0.98
	80-96,98-100,99-100	3	5.٢۵-2٣.٧۵	✓	✓		---	---	---	---
4	15-33,19-34,23-24	1	12.٨١-1٣.۶٩	✓	✓		---	---	---	---
(0.01s)	30-38,77-82,80-97,	2	23.٣٢+2.٣٢.-23.٣٨	⊗	✓	259.8MW	(46,69)/8.16	0.081-0.171	120.2	0.98
	80-96,98-100,99-100	3	5.17-2٢.٨١	✓	✓		---	---	---	---
5	15-33, 19-34, 23-24, 30-38, 82-83, 80-96, 80-97, 82-96, 98-100, 99-100	1	12.٨١-1٣.۶٩	✓	✓		---	---	---	---
(0.03s)		2	23.٣٢+2.٣٢-25.82	✓	✓	284.8MW	---	---	---	---
		3	5.٢۵-2١.١٧	✓	✓		---	---	---	---

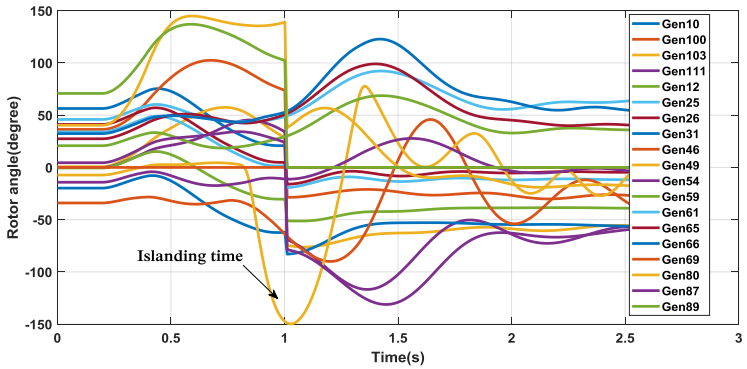

Fig. 6-6: Trajectories of rotor angles using the proposed controlled islanding strategy (Method-3)

6.4.7 Method-4

In all four previous islanding method the system parameters were considered without any uncertainty. In reality, system parameters, especially those affecting the transient stability

are subjected to some degree of uncertainty. Different system parameters including system inertia, renewable penetration, load damping, and load demand, have uncertainty. The uncertainty of these parameters may be considered in the energy function criterion. Therefore, the related uncertainties in islanding are interpreted as a given uncertainty in the energy function. Here, the uncertainty in kinetic energy is assumed as 10 %. Now the proposed uncertainty-driven controlled islanding scheme is implemented considering the transient stability constraints. According to Table 6-3, the proposed algorithm is converged in five iterations. It can be seen that the critical island is island 2, in which the difference between the kinetic and potential energy (i.e. 5.1 with considering 10% uncertainty in kinetic energy) confirms this criticality. Trajectories of rotor angles are shown in Fig. 6-7. The amount of kinetic and potential energy during the iterative process has been shown in Table 6-3. The amount of power imbalance is 284.8MW which is 130.8MW greater than the power imbalance obtained by the conventional islanding method (i.e. Method 1). Also the amount of power imbalance is 25 MW more than the power imbalance obtained using Method-4. The islanding boundary using all five methods have been illustrated in Fig. 6-8.

6.5 Discussion and Analysis

The main novelties, advantages, and disadvantages of the uncertainty-driven controlled islanding scheme are summarized as follows.

6.5.1 Novelties of Method-5

As the uncertainty in system parameters such as equivalent inertia may challenge the success of transient stability constrained controlled islanding, the proposed method in this chapter determine a splitting strategy that is robust against a pre-determined degree of uncertainty in kinetic energy of the system. Indeed the uncertainty in equivalent inertia is interpreted as the uncertainty in kinetic energy of the system at a given operating point.

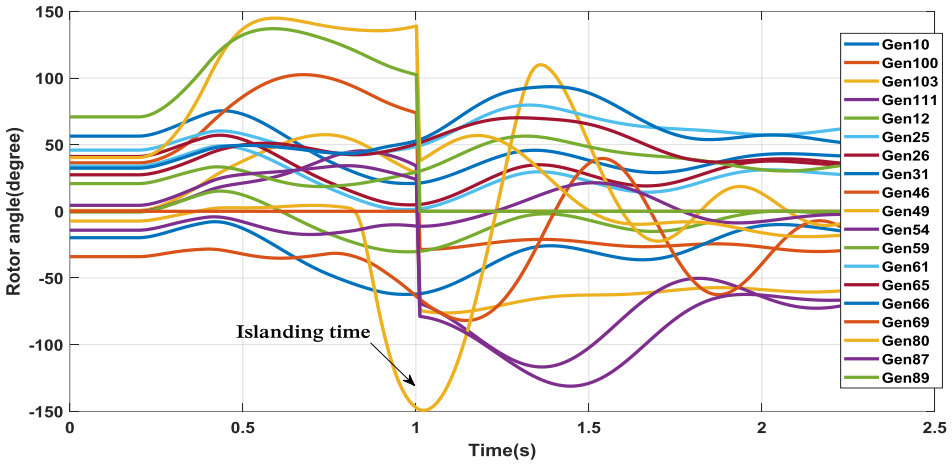

Fig. 6-7: Trajectories of rotor angles using the iteration based islanding strategy considering uncertainty(Method-4)

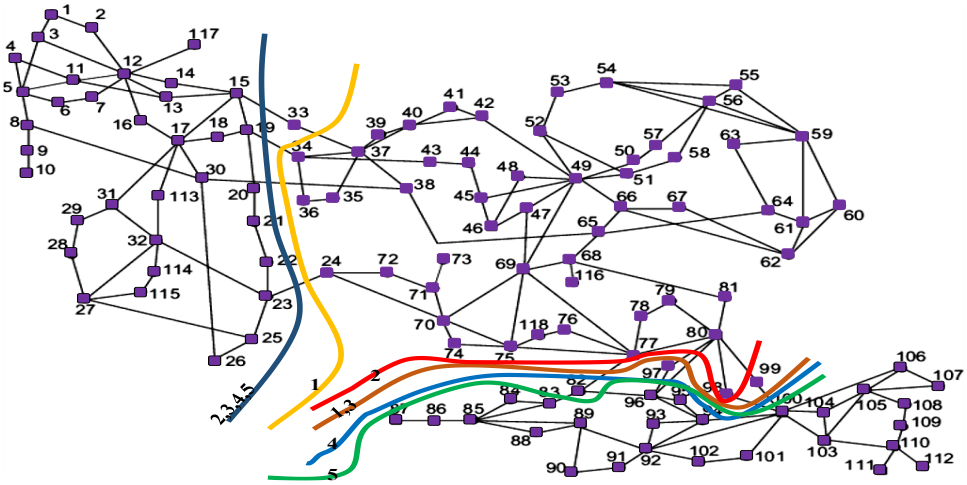

Fig. 6-8: Islanding boundaries using different islanding strategies

The integration of non-synchronous renewable resources in modern power systems is a real source of such uncertainty. Advantages of Method-5

1) Considering the transient stability in controlled islanding in presence of uncertainty in equivalent system inertia
2) Converting the uncertainty in system inertia into the uncertainty in kinetic energy of the operating point without adding computational complexities of stochastic scenarios

3) Simultaneous maximization of transient stability margin and minimizing the amount of load shedding.
4) Reducing the solution space by reducing the number of candidate lines.

6.5.2 Disadvantages:

1) Assuming the worst- case scenario of uncertainty in system inertia. More computational tools can be utilized to adapt the islanding scenario to the most credible scenario of uncertainty.
2) Ignoring the other sources of uncertainties such as uncertainty in load demand, generation level, load damping and system parameters.

6.6 Conclusion of Chapter

In this chapter, an iterative stochastic algorithm was proposed to design transient stability constrained controlled islanding plan in the presence of uncertainty in transient stability criterion. It was shown that by considering the uncertainty of system inertia, the amount of total power imbalance is increased. However, due to the penetration of inertia-free generating units, the utilized transient stability criteria come up with some degree of uncertainty. A comprehensive comparison was presented. The major findings of the presented comparative study are: 1) The conventional controlled islanding method fails to give transient-stable islands and it may worsen the system conditions, 2) The EEAC method is an efficient and approximated method to consider the transient stability. However, under some severe cascading outages, this method fails to give stable islands. 3) The transfer impedance between critical generators is an effective criterion which can be utilized to consider the transient stability in controlled islanding. 4) If the aim of controlled islanding is to just promote the transient stability, the proposed multi-objective function (i.e. Method-2) gives the proper islanding strategy with lower computational complexities. 5) The uncertainty of system parameters during the execution of controlled islanding is a real challenge that may affect the islanding strategy. The uncertainty of system inertia can be included in the kinetic energy. This will change the islanding strategy including the amount of power imbalance and the set of splitting lines.

CHAPTER 7. CONCLUSION AND FUTURE WORKS

7.1 Conclusions

Cascading failures or blackouts are major threats to the interconnected operation of a power system. Different remedial actions can be utilized to limit the propagation of cascaded failure in the system which could lead to a total blackout in the power system. Power system islanding is the last resort to avoid propagation of cascading failures. In addition to steady state operational and topological constraints, transient stability is a major concern that may challenge the success of the controlled islanding strategy.

This thesis proposed transient stability constrained islanding models as the last resort against cascading failures.

Based on the obtained results, the major findings of this thesis are summarized as follows:

1) Without considering the transient stability constraint, the conventional islanding model with just relying on steady state operational constraints fails to give transient-stable islands and in some cases it may worsen the system conditions in transient stability's point of view.

2) The EEAC method is an efficient method to consider the transient stability. This method defines the maximum allowable change of electrical power at the generator terminal. However, under some severe cascading outages, this method fails to give transient-stable islands.

3) The transfer impedance between the critical pairs of generators is an effective criterion which can be utilized to define the transient stability criteria in controlled islanding problem (i.e. method 3). The proper change of transfer impedances results in transient stability improvement of created islands.

4) If the aim of controlled islanding is to just promote the transient stability, the proposed multi-objective function (i.e. Method-2 as given in Chapter 4) gives the proper islanding strategy with lower complexities. However, the proposed multi-objective function does not

allow to define transient stability criteria as a hard constraint inside the optimization model of controlled islanding.

5) An iterative two-stage algorithm was proposed to consider the transient stability in a controlled islanding plan in method4. The obtained results confirmed that the proposed TEF-based MIP islanding method preserves the transient stability of resulted islands by selecting the proper splitting lines. The proposed method considers the variations of saddle points of resulted islands. It was shown that the transient stability assessment by the proposed islanding method is comparable with the full dynamic simulation using a transient stability simulator.

6) The uncertainty of system parameters during the execution of controlled islanding is a real challenge that may affect the success of the controlled islanding strategy. The uncertainty of system inertia can be included in the kinetic energy. This will change the islanding strategy in both the amount of power imbalance and the set of splitting lines.

7.2 Future Works

Controlled islanding is a complicated remedial action involving various steady state and dynamic phenomena. Also, new generation technologies and devices are integrated into modern power systems, bringing about new challenges in power system control, operation and protection. In order to further improve the efficacy of the controlled islanding strategy, the following challenges are recommended to be addressed in future works:

1) In slow coherency based controlled islanding the number of islands is assumed to be equal to the number of coherent groups of generators. However, the greater the number of islands, the more complicated the network restoration. Therefore, the implementation of a controlled islanding plan based on the disconnection of the faulted area is an open question for future researches.
2) The transient energy function is widely used to define proper transient stability criteria. In this thesis, the impacts of changing transfer impedances between

coherent generators were utilized in the proposed transient stability constrained controlled islanding plan. However, the value of potential energy can be changed by the amount of load demand on each island. Therefore, the distribution of load points in created islands based on the potential energy can be addressed as a useful approach for transient stability improvement of the controlled islanding scheme.

3) There are different sources of uncertainty in controlled islanding problem. In this thesis the uncertainty of system inertia in a controlled islanding scheme was addressed. The uncertainty of load demand, generation amount, load damping can be addressed in future works.
4) The activation of some protective relays such as distance and UFLS relays are not addressed in this thesis. Considering the impacts of protective relays on the boundary of controlled islanding is an open question for future research works.

REFERENCES

[1] [Online]: https://data.worldbank.org/indicator/EG.ELC.ACCS.ZS.

[2] N. Senroy and G. T. Heydt, "A conceptual framework for the controlled islanding of interconnected power systems," *IEEE transactions on power systems,* vol. 21, no. 2, pp. 1005-1006, 2006.

[3] G. Xu, V. Vittal, A. Meklin, and J. E. Thalman, "Controlled islanding demonstrations on the WECC system," *IEEE Transactions on Power Systems,* vol. 26, no. 1, pp. 334-343, 2011.

[4] M. R. Aghamohammadi and A. Shahmohammadi, "Intentional islanding using a new algorithm based on ant search mechanism," *International Journal of Electrical Power & Energy Systems,* vol. 35, no. 1, pp. 138-147, 2012.

[5] O. P. Veloza and F. Santamaria, "Analysis of major blackouts from 2003 to 2015: Classification of incidents and review of main causes," *The Electricity Journal,* vol. 29, no. 7, pp. 42-49, 2016.

[6] M. Sanaye-Pasand and M. R. Dadashzadeh, "Iran national grid blackout, power system protection point of view," 2004.

[7] B. Yang, V. Vittal, G. T. Heydt, and A. Sen, "A novel slow coherency based graph theoretic islanding strategy," in *Power Engineering Society General Meeting, 2007. IEEE,* 2007: IEEE, pp. 1-7.

[8] E. De Tuglie, S. M. Iannone, and F. Torelli, "A coherency recognition based on structural decomposition procedure," *IEEE Transactions on Power Systems,* vol. 23, no. 2, pp. 555-563, 2008.

[9] F. Jabari, H. Seyedi, and S. N. Ravadanegh, "Large-scale power system controlled islanding based on backward elimination method and primary maximum expansion areas considering static voltage stability," *International Journal of Electrical Power & Energy Systems,* vol. 67, pp. 368-380, 2015.

[10] N. Senroy, G. T. Heydt, and V. Vittal, "Decision tree assisted controlled islanding," *IEEE Transactions on Power Systems,* vol. 21, no. 4, pp. 1790-1797, 2006.

[11] P. Kundur, N. J. Balu, and M. G. Lauby, *Power system stability and control*. McGraw-hill New York, 1994.

[12] P. Demetriou, J. Quirós-Tortós, and E. Kyriakides, "When to Island for Blackout Prevention," *IEEE Systems Journal,* no. 99, pp. 1-12, 2018.

[13] S. Kamali, T. Amraee, and S. M. T. Bathaee, "Prediction of unplanned islanding using an energy based strategy," *IET Generation, Transmission & Distribution,* vol. 10, no. 1, pp. 183-191, 2016.

[14] G. Isazadeh, A. Khodabakhshian, and E. Gholipour, "New intelligent controlled islanding scheme in large interconnected power systems," *IET Generation, Transmission & Distribution,* vol. 9, no. 16, pp. 2686-2696, 2015.

[15] K. Sun, T. S. Sidhu, and M. Jin, "Online pre-analysis and real-time matching for controlled splitting of large-scale power networks," in *2005 International Conference on Future Power Systems,* 2005: IEEE, pp. 6 pp.-6.

[16] M. R. Salimian and M. R. Aghamohammadi, "A Three Stages Decision Tree-Based Intelligent Blackout Predictor for Power Systems Using Brittleness Indices," *IEEE Transactions on Smart Grid,* vol. 9, no. 5, pp. 5123-5131, 2018.

[17] L. Ding, Y. Guo, P. Wall, K. Sun, and V. Terzija, "Identifying the Timing of Controlled Islanding Using a Controlling UEP Based Method," *IEEE Transactions on Power Systems,* vol. 33, no. 6, pp. 5913-5922, 2018.

[18] H. You, V. Vittal, and X. Wang, "Slow coherency-based islanding," *IEEE Transactions on Power Systems,* vol. 19, no. 1, pp. 483-491, 2004.

[19] S. Yusof, G. Rogers, and R. Alden, "Slow coherency based network partitioning including load buses," *IEEE Transactions on Power Systems,* vol. 8, no. 3, pp. 1375-1382, 1993.

[20] V. Vittal, W. Kliemann, Y.-X. Ni, D. Chapman, A. Silk, and D. Sobajic, "Determination of generator groupings for an islanding scheme in the Manitoba hydro system using the method of normal forms," *IEEE transactions on power systems,* vol. 13, no. 4, pp. 1345-1351, 1998.

[21] B. Yang, V. Vittal, and G. T. Heydt, "Slow-coherency-based controlled islanding—a demonstration of the approach on the August 14, 2003 blackout scenario," *IEEE Transactions on Power Systems,* vol. 21, no. 4, pp. 1840-1847, 2006.

[22] D. E. Van Den Bout and T. K. Miller, "Graph partitioning using annealed neural networks," *IEEE Transactions on neural networks,* vol. 1, no. 2, pp. 192-203, 1990.

[23] K. Sun, Q. Zhao, D.-Z. Zheng, J. Ma, and Q. Lu, "A two-phase method based on OBDD for searching for splitting strategies of large-scale power systems," in *Power System Technology, 2002. Proceedings. PowerCon 2002. International Conference on*, 2002, vol. 2: IEEE, pp. 834-838.

[24] Q. Zhao, K. Sun, D.-Z. Zheng, J. Ma, and Q. Lu, "A study of system splitting strategies for island operation of power system: A two-phase method based on OBDDs," *IEEE Transactions on Power Systems,* vol. 18, no. 4, pp. 1556-1565, 2003.

[25] K. Sun, D.-Z. Zheng, and Q. Lu, "Splitting strategies for islanding operation of large-scale power systems using OBDD-based methods," *IEEE transactions on Power Systems,* vol. 18, no. 2, pp. 912-923, 2003.

[26] K. Sun, D.-Z. Zheng, and Q. Lu, "A simulation study of OBDD-based proper splitting strategies for power systems under consideration of transient stability," *IEEE Transactions on Power Systems,* vol. 20, no. 1, pp. 389-399, 2005.

[27] G. Xu and V. Vittal, "Slow coherency based cutset determination algorithm for large power systems," *IEEE Transactions on Power Systems,* vol. 25, no. 2, pp. 877-884, 2010.

[28] H. Mehrjerdi, S. Lefebvre, M. Saad, and D. Asber, "A decentralized control of partitioned power networks for voltage regulation and prevention against disturbance propagation," *IEEE Transactions on Power Systems,* vol. 28, no. 2, pp. 1461-1469, 2013.

[29] J. Li, C.-C. Liu, and K. P. Schneider, "Controlled partitioning of a power network considering real and reactive power balance," *IEEE Transactions on Smart grid,* vol. 1, no. 3, pp. 261-269, 2010.

[30] T. Ding, K. Sun, C. Huang, Z. Bie, and F. Li, "Mixed-integer linear programming-based splitting strategies for power system islanding operation considering network connectivity," *IEEE Systems Journal,* vol. 12, no. 1, pp. 350-359, 2018.

[31] P. A. Trodden, W. A. Bukhsh, A. Grothey, and K. I. McKinnon, "Optimization-based islanding of power networks using piecewise linear AC power flow," *IEEE Transactions on Power Systems,* vol. 29, no. 3, pp. 1212-1220, 2014.

[32] P. Trodden, W. Bukhsh, A. Grothey, and K. McKinnon, "MILP islanding of power networks by bus splitting," in *Power and Energy Society General Meeting, 2012 IEEE,* 2012: IEEE, pp. 1-8.

[33] L. Ding, F. M. Gonzalez-Longatt, P. Wall, and V. Terzija, "Two-step spectral clustering controlled islanding algorithm," *IEEE Transactions on Power Systems,* vol. 28, no. 1, pp. 75-84, 2013.

[34] Y. Morioka *et al.*, "System separation equipment to minimize power system instability using generator's angular-velocity measurements," *IEEE Transactions on Power delivery,* vol. 8, no. 3, pp. 941-947, 1993.

[35] M. Adibi, R. Kafka, S. Maram, and L. M. Mili, "On power system controlled separation," *IEEE Transactions on Power Systems,* vol. 21, no. 4, pp. 1894-1902, 2006.

[36] S. S. Ahmed, N. C. Sarker, A. B. Khairuddin, M. R. B. A. Ghani, and H. Ahmad, "A scheme for controlled islanding to prevent subsequent blackout," *IEEE transactions on power systems,* vol. 18, no. 1, pp. 136-143, 2003.

[37] A. Kyriacou, P. Demetriou, C. Panayiotou, and E. Kyriakides, "Controlled Islanding Solution for Large-Scale Power Systems," *IEEE Transactions on Power Systems,* vol. 33, no. 2, pp. 1591-1602, 2018.

[38] J. Quirós-Tortós, P. Demetriou, M. Panteli, E. Kyriakides, and V. Terzija, "Intentional Controlled Islanding and Risk Assessment: A Unified Framework," *IEEE Systems Journal,* 2017.

[39] F. Teymouri, T. Amraee, H. Saberi, and F. Capitanescu, "Towards Controlled Islanding for Enhancing Power Grid Resilience Considering Frequency Stability Constraints," *IEEE Transactions on Smart Grid,* 2017.

[40] A. Vahidnia, G. Ledwich, E. Palmer, and A. Ghosh, "Generator coherency and area detection in large power systems," *IET generation, transmission & distribution,* vol. 6, no. 9, pp. 874-883, 2012.

[41] M. Haque, "Equal-area criterion: an extension for multimachine power systems," *IEE Proceedings-Generation, Transmission and Distribution,* vol. 141, no. 3, pp. 191-197, 1994.

[42] Y. Xu, Z. Y. Dong, Z. Xu, R. Zhang, and K. P. Wong, "Power system transient stability-constrained optimal power flow: a comprehensive review," in *Power and Energy Society General Meeting, 2012 IEEE,* 2012: IEEE, pp. 1-7.

[43] D. Ruiz-Vega and M. Pavella, "A comprehensive approach to transient stability control. I. Near optimal preventive control," *IEEE Transactions on Power Systems,* vol. 18, no. 4, pp. 1446-1453, 2003.

[44] A. Pizano-Martianez, C. R. Fuerte-Esquivel, and D. Ruiz-Vega, "Global transient stability-constrained optimal power flow using an OMIB reference trajectory," *IEEE Transactions on Power Systems,* vol. 25, no. 1, pp. 392-403, 2010.

[45] R. Zárate-Miñano, T. Van Cutsem, F. Milano, and A. J. Conejo, "Securing transient stability using time-domain simulations within an optimal power flow," *IEEE Transactions on Power Systems,* vol. 25, no. 1, pp. 243-253, 2010.
[46] H.-D. Chiang, *Direct methods for stability analysis of electric power systems: theoretical foundation, BCU methodologies, and applications*. John Wiley & Sons, 2011.
[47] T. Amraee and H. Saberi, "Controlled islanding using transmission switching and load shedding for enhancing power grid resilience," *International Journal of Electrical Power & Energy Systems,* vol. 91, pp. 135-143, 2017.
[48] P. Aylett, "The energy-integral criterion of transient stability limits of power systems," *Proceedings of the IEE-Part C: Monographs,* vol. 105, no. 8, pp. 527-536, 1958.
[49] A. Fouad, V. Vittal, and T. K. Oh, "Critical energy for direct transient stability assessment of a multimachine power system," *IEEE transactions on power apparatus and systems,* no. 8, pp. 2199-2206, 1984.
[50] M. Jin, T. S. Sidhu, and K. Sun, "A new system splitting scheme based on the unified stability control framework," *IEEE Transactions on Power Systems,* vol. 22, no. 1, pp. 433-441, 2007.
[51] A. L. Da Silva, V. Arienti, and R. Allan, "Probabilistic load flow considering dependence between input nodal powers," *IEEE Transactions on Power Apparatus and Systems,* no. 6, pp. 1524-1530, 1984.
[52] E. Rosenblueth, "Point estimates for probability moments," *Proceedings of the National Academy of Sciences,* vol. 72, no. 10, pp. 3812-3814, 1975.
[53] H. S. Seo and B. M. Kwak, "Efficient statistical tolerance analysis for general distributions using three-point information," *International journal of production research,* vol. 40, no. 4, pp. 931-944, 2002.
[54] J. M. Morales and J. Perez-Ruiz, "Point estimate schemes to solve the probabilistic power flow," *IEEE Transactions on power systems,* vol. 22, no. 4, pp. 1594-1601, 2007.

تقدیر و تشکر

اکنون که به یاری پروردگار و کمک و راهنمایی اساتید بزرگ موفق به پایان این رساله شده‌ام وظیفه خود دانسته که نهایت سپاسگزاری را از تمامی عزیزانی که در این راه به من کمک کرده‌اند را به عمل آورم:

در آغاز از استاد بزرگ و دانشمند جناب آقای دکتر تورج امرایی که راهنمایی این پایانامه را به عهده داشته‌اند و هیچ لکی را از بنده دریغ نکردند و در تک تک مراحل این پایان نامه دلسوزانه کمک کردند، کمال تشکر را دارم.

از داوران گرامی که زحمت داوری و تصحیح این پایانامه را به عهده داشتند نکات ارزشمندی را در پیشنهاد رساله و در دیگر مراحل متذکر شدند کمال سپاس را دارم.

خالصانه از تمامی اساتید و معلمان و مدرسانی که در مقاطع مختلف تحصیلی به من علم آموخته و مرا از سرچشمه دانایی سیراب کرده‌اند متشکرم.

از کلیه هم دانشگاهیان و همراهان عزیز، دوستان خوبم در آزمایشگاه پایداری سیستم های قدرت نهایت سپاس را دارم.

و در پایان این پایان نامه را تقدیم می کنم به خدایی که آفرید و عزت همه از آن اوست.

تأییدیّه هیات داوران

(برای رساله دکتری)

اعضای هیئت داوران، نسخه نهائی رساله دکتری آقای: صادق کمالی

را با عنوان: **تعیین محدوده ی جزیره سازی کنترل شده سیستم های قدرت با هدف تامین پایداری در حضور عدم قطعیت ها**

از نظر فرم و محتوی بررسی نموده و پذیرش آن را برای تکمیل درجه دکتری تأیید می‌کند.

اعضای هیئت داوران	نام و نام خانوادگی	رتبه علمی	امضاء
استاد راهنما	دکتر تورج امرایی	دانشیار	
استاد ممتحن خارجی	دکتر مصطفی پرنیانی	استاد	
استاد ممتحن خارجی	دکتر محمود رضا حقی فام	استاد	
استاد ممتحن داخلی	دکتر سید محمد تقی بطحایی	استاد	
استاد ممتحن داخلی	دکتر مسعود علی اکبر گلکار	استاد	
نماینده تحصیلات تکمیلی	دکتر مهدی علیاری شوره دلی	استادیار	

بسمه تعالی

تاسیس ۱۳۰۷ دانشگاه صنعتی خواجه نصیرالدین طوسی	**اظهارنامه دانشجو**	**شماره :** **تاریخ :**

اینجانب **صادق کمالی** دانشجوی دکتری رشته **مهندسی برق** گرایش **قدرت** دانشکده برق و کامپیوتر دانشگاه صنعتی خواجه نصیرالدین طوسی گواهی می‌نمایم که تحقیقات ارائه شده در پایان نامه با عنوان **تعیین محدوده‌ی جزیره سازی کنترل شده سیستم های قدرت با هدف تامین پایداری در حضور عدم قطعیت‌ها** با راهنمایی استاد محترم جناب آقای دکتر تورج امرایی توسط شخص اینجانب انجام شده و صحت و اصالت مطالب نگارش شده در این پایان نامه مورد تأیید می‌باشد، و در مورد استفاده از کار دیگر محققان به مرجع مورد استفاده اشاره شده است. به علاوه گواهی می‌نمایم که مطالب مندرج در پایان نامه تا کنون برای دریافت هیچ نوع مدرک یا امتیازی توسط اینجانب یا فرد دیگری در هیچ جا ارائه نشده است و در تدوین متن پایان نامه چارچوب (فرمت) مصوب دانشگاه را بطور کامل رعایت کرده‌ام.

امضا دانشجو:

تاریخ:

تاسیس ۱۳۰۷ دانشگاه صنعتی خواجه نصیرالدین طوسی	**عنوان فرم** **حق طبع و نشر و مالکیت نتایج**	**شماره :** **تاریخ :**

اینجانب **صادق کمالی** دانشجوی دوره دکتری مهندسی **برق گرایش قدرت** دانشکده برق و کامپیوتر دانشگاه صنعتی خواجه نصیر الدین طوسی گواهی می‌نمایم که تحقیقات ارائه شده در این پایان نامه توسط شخص اینجانب انجام شده و صحت و اصالت نگارش شده مورد تایید می‌باشد و در موارد استفاده از کار دیگر محققان به مرجع مورد استفاده اشاره شده است. به علاوه گواهی می‌نمایم که مطالب مندرج در پایان نامه تاکنون برای دریافت هیچ نوع مدرک یا امتیازی توسط اینجانب یا فرد دیگری در هیچ جا ارائه نشده است و در تدوین متن پایان نامه چارچوب مصوب دانشگاه را بطور کامل رعایت کرده‌ام.

کلیه حقوق مادی و معنوی این اثر فقط متعلق به دانشگاه صنعتی خواجه نصیرالدین طوسی می‌باشد و بدون اجازه کتبی دانشگاه قابل واگذاری وبهره برداری نیست. همچنین استفاده از اطلاعات و نتایج موجود در پایان نامه بدون ذکر مرجع مجاز نمی باشد.

امضا دانشجو:

تاریخ:

چکیده

سیستم های قدرت به عنوان یک زیر ساخت حیاتی همواره در معرض انواع خطاهای الکتریکی هستند. برخی از این خطاهای الکتریکی می تواند در قالب خروج های آبشاری منجر به فروپاشی و خاموشی شبکه قدرت شوند. چنانچه خطوط انتقال الکتریکی میان نواحی مختلف، طولانی و دارای امپدانس بالایی باشد، آنگاه سنکرون ماندن نواحی الکتریکی مختلف تحت حوادث شدید همانندخروج های پی در پی، با چالش روبرو می شود. جزیره شدگی ناخواسته جدا شدن سیستم از مرزهای ناخواسته و به طور خودبه خودی است. وقوع جزیره شدگی ناخواسته ممکن است به علت نابرابری تولید و مصرف و عدم هماهنگی ژنراتورها در هر جزیره ایجاد گردد. برای مهار خروج های پی در پی نیاز به طرح های خاص حفاظت سیستمی است که بتواند یکپارچگی سیستم قدرت را در چنین شرایطی حفظ کند. جزیره سازی کنترل شده یک نوع طرح حفاظت سیستم است که به عنوان آخرین راهکار می تواند با تبدیل شبکه بهم پیوسته ولی در معرض خطر فروپاشی را به چندین ناحیه پایدار تبدیل کند. تعیین زمان و مکان بهینه جزیره سازی یک موضوع بسیار مهم در موفقیت هر طرح جزیره سازی است. طرح‌هایی که تاکنون برای کنترل جزیره شدگی سیستم قدرت ارائه شده‌اند به مدل سازی حالت ماندگار سیستم متمرکز بوده و انواع ناپایداری سیستم قدرت در مدل جزیره سازی دیده نشده است.

همچنین با پیدایش منابع انرژی نوین همانند مزارع بادی و نیز سایر تولیدات غیر سنکرون پارامترهایی مانند اینرسی سیستم، دچار عدم قطعیت‌های قابل‌توجهی شده اند. ازاین‌رو در این رساله جزیره سازی کنترل شده شبکه‌ی قدرت باهدف تعیین مرزهای جزیره سازی با رویکرد حفظ پایداری گذرا در حضور عدم قطعیت در پارامترهای سیستم مورد مطالعه قرار می گیرد. پایداری گذرا مهمترین نوع پایداری در تضمین موفقیت هر طرح جزیره سازی است.

در فصل اول رساله مبانی جزیره سازی کنترل شده ارائه می شود. سپس در فصل دوم ضمن تشریح مبانی تعیین زمان جزیره سازی کنترل شده، روش هایی که تاکنون برای تشخیص زمان جزیره سازی عرضه شده اند ارزیابی می شوند. در این رساله رویکردهای مختلفی برای تامین پایداری گذرا در جزیره سازی کنترل شده ارائه می شود. این رویکردها می تواند بر حسب نیاز مورد استفاده قرار گیرند. در این رساله در فصل سوم یک رویکرد تحلیل حالت ماندگار با هدف بهبود پایداری گذار پیشنهاد می گردد. در فصل چهارم جزیره شدگی کنترل شده به کمک داده های اندازه گیری فازوری با در نظر گرفتن معیار پایداری گذرا و جزیره های بحرانی مدل می شود. درنهایت در فصل پنجم و ششم پایداری گذرا به صورت یک قید در مساله جزیره سازی با و بدون نامعینی مورد مطالعه قرار می گیرد. مهمترین یافته های این پژوهش به همراه پیشنهاد برای کارهای آتی در فصل هفتم ارائه می شود.

کلیدواژه: دینامیک سیستم قدرت، جزیره سازی کنترل شده، پایداری گذرا، تابع انرژی ، ژنراتورهای هم پا، بهینه سازی.


بسم الله الرحمن الرحیم

دانشکده مهندسی برق و کامپیوتر

رساله دکتری

تعیین محدوده‌ی جزیره سازی کنترل شده سیستم های قدرت با هدف تامین پایداری در حضور عدم قطعیت‌ها

توسط:

صادق کمالی

استاد راهنما:

دکتر تورج امرایی

پاییز ۱۳۹۸